Monitoring Land Cover Change Using GEE and Multi-sources Remote Sensing Images -A Case Study in Vientiane, Lao PDR

VORLAJUCK KHANTIVONG

A THESIS SUBMITTED IN PARTIAL FULFILLMENT OF

THE REQUIREMENTS FOR MASTER OF SCIENCE

IN GEOINFORMATICS

FACULTY OF GEOINFORMATICS

BURAPHA UNIVERSITY

2020

COPYRIGHT OF BURAPHA UNIVERSITY

Monitoring Land Cover Change Using GEE and Multi-sources Remote Sensing Images -A Case Study in Vientiane, Lao PDR

VORLAJUCK KHANTIVONG

วิทยานิพนธ์นี้เป็นส่วนหนึ่งของการศึกษาตามหลักสูตรวิทยาศาสตรมหาบัณฑิต
สาขาวิชาภูมิสารสนเทศศาสตร์
คณะภูมิสารสนเทศศาสตร์ มหาวิทยาลัยบูรพา
2563

ลิขสิทธิ์เป็นของมหาวิทยาลัยบูรพา

Monitoring Land Cover Change Using GEE and Multi-sources Remote Sensing Images -A Case Study in Vientiane, Lao PDR

VORLAJUCK KHANTIVONG

A THESIS SUBMITTED IN PARTIAL FULFILLMENT OF

THE REQUIREMENTS FOR MASTER OF SCIENCE

IN GEOINFORMATICS

FACULTY OF GEOINFORMATICS

BURAPHA UNIVERSITY

2020

COPYRIGHT OF BURAPHA UNIVERSITY

The Thesis of Vorlajuck Khantivong has been approved by the examining committee to be partial fulfillment of the requirements for the Master of Science in Geoinformatics of Burapha University

Advisory Committee

Principal advisor

(Li Xi)

Co-advisor

(Chanika Sukawattanavijit)

Examining Committee

(Shu Hong) Principal examiner

(Jianguo Yan) Member

(Nengcheng Chen) Member

(Shu Hong) Member

(Hongxing Sun) Member

(Kitsanai Charoenjit) Dean of the Faculty of Geoinformatics

This Thesis has been approved by Graduate School Burapha University to be partial fulfillment of the requirements for the Master of Science in Geoinformatics of Burapha University

---

(Associate Professor Dr. Nujjaree Chaimongkol) Dean of Graduate School

---

61910097: MAJOR: GEOINFORMATICS; M.Sc. (GEOINFORMATICS)

KEYWORDS: Urban Expansion; Land Cover Changes; Machine Learning; Random Forest; Classification and Regression Trees; Multi-source Imagery; Google Earth Engine

VORLAJUCK KHANTIVONG : MONITORING LAND COVER CHANGE USING GEE AND MULTI-SOURCES REMOTE SENSING IMAGES -A CASE STUDY IN VIENTIANE, LAO PDR. ADVISORY COMMITTEE: LI XI, , CHANIKA SUKAWATTANAVIJIT 2020.

Increasing urbanization causes a variety of environmental changes, not only in regional but in the global context. Urban expansion is one part of the city growth process. Urbanization has a significant impact on the environment, which land cover change has created a new style of the development of the city. Land cover changes have become an essential element for the current strategy for natural management, resources, and environmental changes monitoring. Using the integration of geographic information system (GIS) and remote sensing provides us with an effective result in determining the land use/land cover pattern changes as well as providing valuable information needed for planning and researches. Thus, the information such as rate, pattern, and model of urban expansion is required by the city planners to accurately determine city planning direction and policies management for better urbanization.

Since its establishment in 1975 to the Lao people's Democratic Republic (hereinafter, referred to as Lao PDR or Laos), Laos is attempting to prioritize relations between states, people, land, and the natural environment in a manner that is conducive to achieve state goals in making political security, economic development, and environmental protection and conservation. Therefore, this research will be targeting on the study of the urban expansion and land cover changes in Vientiane. The research focuses on its dynamic pattern changing of urban development for three decades between 1989 and 2019. To quantitatively and assess the rate of the changes in land cover and measure the direction of the urban expansion over the period time in the study area, an innovation and modernization technology must be utilized.

A new approach has been introduced for detecting and monitoring urban expansion. The changes in land cover patterns by using the Big Data platform via the Google Earth Engine (GEE) cloud computing. The machine learning algorithms have been recommended for this research, such as Random Forest (RF), Classification and Regression Tree (CART), Continuous Naïve Bayes (CNB), GMO Max Entropy (GMO Maxent), and Minimum Distance (MD). The different classifiers will be used to compare the performance of those machine learning algorithms and determine the adequate performance of the classifiers. Analyzing and monitoring urban areas is an essential factor for town or city planning. Many kinds of research tried to understand and explain the expansion of nature for the increasing and growth direction of the city. In this research, I conducted GEE combining with multiple sources of satellite optical images time-series from three main satellites, Landsat 5 and Landsat 8 from the partnership of the National Aeronautics and Space Administration (NASA) and the U.S. Geological Survey (USGS), and Sentinel-2, Which has been developed and is being operated by European Space Agency (ESA), These three satellites will be used for assessments and feature extraction for urban expansion and land cover changes during the 30-year in Vientiane Capital, Lao PDR.

This research is the first attempt, using the GEE platform for detecting and monitoring the urban growth and land cover changes in Laos. It takes advantage of machine learning classifiers by using satellite image analysis for 30 years. The findings of this study include:

The GEE can provide a significant role with highly competent and precisely for land cover changes detection and used for city administration and policymaking of the Lao government in the future.

GEE platforms are quick and freely provides simple tools for users. Therefore, the combination of machine learning algorithms and high-resolution images (Sentinel-2 satellite image) has a high effect. This study found that CART can achieve overall accuracy of 96.34% and a Kappa coefficient of 0.95. Moreover, RF can achieve overall accuracy of 95.08% and a kappa coefficient of 0.93. At the same time, CNB, GMO Max Entropy, and MD made overall accuracies of 90.59%, 81.49%, and 73.95%, respectively, and the Kappa coefficients are 0.88, 0.74 and 0.66, respectively.

After evaluation and classification, it was found that the urban is increased from 9.11 Sq.km in 1989 to 13.52 Sq.km in 1994 and increased to 26.70, 43.50, 47.514, 83.11, 105.06 Sq.km in 1999, 2004, 2009, 2014, 2019 respectively. This is about 0.25% of the total area in 1989 to 2.90% in 2019 with the direction of expansion generated into three main routes, such as to 13th North, 13th South Road, and along Thadeua Road, connected and shared border to Thailand via Mekong River Friendship Bridge No. I.

This research could be beneficial for the Lao government and the policymaker for performing urban development and planning that would accelerate green growth and sustainable infrastructure management. This research will be led to socio-economic, ecological, prosperity development, and for the betterment of city sustainable development plans in the future

ACKNOWLEDGEMENTS

Throughout my research journey in my Double Master program that gathering full collaboration between Geographical Informatics and Space Technology Development Agency (GISTDA) Public, Wuhan University (China), and Burapha University (Thailand). I have made great learning based on a variety of observations and analysis of my research. I am thankful to many people who have kindly helped and guided me throughout this period.

Firstly, I am highly indebted to my kindly Supervisors Assoc Prof. Dr Li Xi, Dr Chanika Sukawattanavijit, Dr Tanita Suepa, Dr Haoran Zhang, for their timely guidance and support. Assoc Prof Dr Li Xi has been a constant support throughout the research period, guiding and patience guided doing me towards, He always encouraged me new ideas and instilled confidence in me by his calm nature. He made me great success in this research. Dr Chanika Sukawattanavijit, Dr Tanita Suepa, Dr Haoran Zhang had always kindly given me a proper consultation and discussion whenever facing issues and helping me develop the research skills with an open mind. Assoc Prof. Dr Li Xi guided and steered me in the right direction when required to provide valuable suggestions on my research work. I thank all my supervisors for pushing me towards the right goal and encouraging me never to give up. That was an honour for me to be your student.

I would very much like to extend my heartful gratitude to Teachers who always had our back during the whole Double Master Degree program, making sure that everything is in place to ensure the research smooths progress. I would like to thank all the facilities of LIESMARS, GISTDA, and Burapha University for showering us with your extensive knowledge and for helping us in learning new skills and ideas. I am much thankful to the GEE team and developers group for their inputs and provide great GEE tools.

The acknowledgment will not be completed without extending my gratitude to my family and friends. My sincere thanks to parents, brother, and especially my wife Chanthepha HOUNGSAVANG for standing by me always, the one who supported me fund and encouraged me throughout the Double Master Course, once thanks Maung Chitmyowin for being my back, helping me in technical issues, and keep me and my research going well.

Vorlajuck KHANTIVONG

Vorlajuck Khantivong

TABLE OF CONTENTS

Page

ABSTRACT ..... D

ACKNOWLEDGEMENTS ..... F

TABLE OF CONTENTS ..... G

LIST OF TABLES ..... J

LIST OF FIGURES ..... M

CHAPTER 1 1

INTRODUCTION 1

1.1 Motivation and Problems Statement 2

1.2 Research Questions and Objective 5

1.3 Contribution of Thesis 6

1.4 Research Structure 6

CHAPTER 2 7

THEORETICAL REVIEW 7

2.1 General Urban and Land Cover Changes Definition 7

2.2 Urban in South East Asia 8

2.3 Dynamics Changes of Urban in Laos 10

2.3.1 Urban Expansion 12

2.3.2 Population Growth 13

2.3.3 Economic Activity 14

2.4 Google Earth Engine (GEE) 15

2.5 Machine Learning Classifiers 16

2.5.1 Random Forest (RF) 16
2.5.2 Classification and Regression Trees (CART) 17
2.5.3 Continuous Naive Bayes (CNB) 17
2.5.4 GMO Max Entropy (GMO Max Ext) 18
2.5.5 Minimum Distance (MD) 18
2.6 Supervised Learning 19
2.7 Spectral Indices 20
2.7.1 Normalized Difference Vegetation Index (NDVI) 20
2.7.2 Normalized Difference Built-Up Index (NDBI) 21
2.8 Satellite Image Feature Extraction 22
CHAPTER 3 25
METHODS AND DATA 25
3.1 Study Area: 25
3.2 Data 26
3.2.1 Landsat 5 27
3.2.2 Landsat 8 28
3.2.3 Sentinel-2 29
3.3 Data Combination 29
3.4 Methods and Data Used 30
3.5 Classification Accuracy Assessment 33
CHAPTER 4 35
EXPERIMENTS AND RESULTS 35
4.1 Urban and Land Cover Extraction Applied with Difference Satellite 35

4.2 Experiment by Automatic Machine Learning Classifiers...35
4.2.1 Classification Using Random Forest 37
4.2.2 Classification Using Classification and Regression Trees....39
4.2.3 Classification Using Continuous Naïve Bayes 40
4.2.4 Classification Using GMO Max Entropy 41
4.2.5 Classification Using Minimum Distance 43
4.3 Comparison of Machine Learning Classifiers 44
4.4 Post-Classification of Land Cover Changes Detection....49
4.4.1 Classification Using Different ML Classifiers 49
4.4.2 Classification Change Detection Using Time-series Data 54
4.5 Summary 63
CHAPTER 5 66
DISCUSSION....66
5.1 Implementation of GEE Machine Learning 66
5.2 Comparison of Difference Machine Learning 67
CHAPTER 6 69
CONCLUSION AND FUTURE STUDIES 69
6.1 Conclusion 69
6.2 Future Recommendation....71
REFERENCES 2
APPENDIX....13
BIOGRAPHY 24

LIST OF TABLES

Page

Table 1 Population growth in Lao PDR 13

Table 2 Description of spectral bands and a ground resolution of Landsat 5 TM 28

Table 3 Landsat 8, Operational Land Imager (OLI) & Thermal Infrared Sensor (TIRS) 28

Table 4 Description of spectral bands and resolution of Sentinel-2 29

Table 5 Confusion Matrix of Reference Points for Random Forest in 1989 37

Table 6 Percentage of LC Accuracies and Kappa Performed by RF in 1989(L5) 37

Table 7 Percentage of LC Accuracies and Kappa Performed by RF in 1999(L5) 38

Table 8 Percentage of LC Accuracies and Kappa Performed by RF in 2009(L5) 38

Table 9 Percentage of LC Accuracies and Kappa Performed by RF in 2019(L8) 38

Table 10 Percentage of LC Accuracies and Kappa Performed by RF in 2019(S2) 38

Table 11 Confusion Matrix of Reference Points for CART in 1989 39

Table 12 Percentage of LC Accuracies and Kappa Performed by CART in 1989(L5) 39

Table 13 Percentage of LC Accuracies and Kappa Performed by CART in 2019(L8) 39

Table 14 Percentage of LC Accuracies and Kappa Performed by CART in 2019(S2) 40

Table 15 Confusion Matrix of Reference Points for CNB in 1989 40

Table 16 Percentage of LC Accuracies and Kappa Performed by CNB in 1989(L5) 40

Table 17 Percentage of LC Accuracies and Kappa Performed by CNB in 2019(L8) 41

Table 18 Percentage of LC Accuracies and Kappa Performed by CNB in 2019(S2) 41

Table 19 Confusion Matrix of Reference Points for GMO in 1989 41

Table 20 Percentage of LC Accuracies and Kappa Performed by GMO in 1989(L5) 42

Table 21 Percentage of LC Accuracies and Kappa Performed by GMO in 2019(L8) 42

Table 22 Percentage of LC Accuracies and Kappa Performed by GMO in 2019(S2) 42

Table 23 Confusion Matrix of Reference Points for Minimum Distance in 1989 43

Table 24 Percentage of LC Accuracies and Kappa Performed by MD in 1989(L5) 43

Table 25 Percentage of LC Accuracies and Kappa Performed by MD in 2019(L8) 43

Table 26 Percentage of LC Accuracies and Kappa Performed by MD in 2019(S2) 44

Table 27 Overall Accuracy and Kappa for each Machine Learning by Landsat5 in 1989 44

Table 28 Overall Accuracy and Kappa for each Machine Learning by Landsat8 in 2019 45

Table 29 Overall Accuracy and Kappa for each Machine Learning by Sentinel-2 in 2019 46

Table 30 Overall Accuracy performed by Random Forest for 1989-2019 46

Table 31Overall Accuracy performed by Landsat-8 and Sentinel-2 in 2019 47

Table 32 Kappa coefficient performed by Landsat-8 and Sentinel-2 in 2019 48

Table 33 Overall Acc and Kappa performed by All ML Classifiers with Landsat 5, Landsat 8, and Sentinel-2 during 1989-2019 48

Table 34 Coverage area changing on each class in sq.km 1989-2019 62

Table 35 Coverage area changed on each class in Percentage (%) 1989-2019 62

LIST OF FIGURES

Page

Figure 1 White areas: Nighttime light emission in 2012, Pink areas: Increase of nighttime light emission between 2012 and 2016, Source: NASA 2013 & 2017[32]. 10

Figure 2 Urban growth in Laos from 2007-2016 (Source: World Bank) 11

Figure 3 Laos-Urban population growth 2008-2018 (annual%). 12

Figure 4 Per Capita GDP Growth Rate: Lao People's Democratic Republic 15

Figure 5GEE performed by Machine Learning of Random Forest in 1989, Vientiane, Laos 16

Figure 6 Concept of Minimum Distance Classifier 19

Figure 7 Normalized Difference Vegetation Index (NDVI) during the Year 2019 21

Figure 8 Normalized Difference Built-Up Index (NDBI) during 2019 22

Figure 9 RGB image Bands 12:8:5 from Sentinel-2 in 2019 23

Figure 10 Feature Extraction of LC Classification from Sentinel-2 in 2019 24

Figure 11 Study Area (Vientiane Capital, Laos) 26

Figure 12 Sampling and Classification structure by ML 27

Figure 13 Overall Steps of the proposed method for Land Use Changes and urban extraction 32

Figure 14 Land Cover Map of Vientiane in 1989- 2019 performed by ML Classifier of Random Forest with Landsat 5, Landsat 8 and Sentinel-2 36

Figure 15 Accuracy and Kappa with different ML Classifiers in 1989 (L5) 45

Figure 16 Overall Accuracy and Kappa of different ML Classifiers in 2019 (L8) 45

Figure 17 Overall Accuracy and Kappa of different ML Classifiers in 2019 (S2) 46

Figure 18 Overall Accuracy and Kappa of primary classifier RF from 1989- 2019 47

Figure 19 Overall Accuracy of Different ML Classifiers by Landsat-8 and Sentinel-2 in 2019 47

Figure 20 Kappa coefficient of Different ML Classifiers by Landsat-8 and Sentinel-2 in 2019 48

Figure 21 LC Classified by different Classifiers RF, CART, CNB, GMO and MD with Sentinel-2 in only 2019 53

Figure 22 Thematic map of Land Cover Changes from 1989-1994 in Vientiane, Lao PDR 55

Figure 23 Thematic map of Land Cover Changes from 1994-1999 in Vientiane, Lao PDR 56

Figure 24 Thematic map of Land Cover Changes from 1999-2004 in Vientiane, Lao PDR 57

Figure 25 Thematic map of Land Cover Changes from 2004-2009 in Vientiane, Lao PDR 58

Figure 26 Thematic map of Land Cover Changes from 2009-2014 in Vientiane, Lao PDR 59

Figure 27 Thematic map of Land Cover Changes from 2014-2019 in Vientiane, Lao PDR 60

Figure 28 Thematic map of Land Cover Changes from 1989-2019 in Vientiane, Lao PDR 61

Figure 29 Legend of Thematic map of LCCD from 1989-2019 61

Figure 30 Bar Chart of the coverage area of each land classes by sq.km from 1989-2018 62

Figure 31 Chart of the average area on each changed class by Percentages (%) 1989-2018 63

CHAPTER 1
INTRODUCTION

Remote Sensing satellite imagery is one of the primary data sources of remote sensing information that can provide us with assistance to access the enormous volumes of data and information for earth observation and monitoring. Using remote sensing techniques analysis, and study the urban expansion and the changes in the land coverage area are widely used. With various sensors, resolution imageries, differences collection methods, and spatial-temporal characteristics provided by the satellites aimed to study earth's surface to space for earth observation. Increasing urbanization causes a variety of natural resources and environmental changes, both in regional and global scale, including expansion processes and forms, and it is only part of the growth process of the city [1][2]. Factors such as infrastructure, density, and facilities enhancement, built-up area play an essential role in urban development and its growth [3][4]. Urbanization has a significant effect on changes in the nature and environment status and [5] and caused people to live in various cities [6]. Land cover changes generate a new style of town expansion. This research will provide technical assistance in urban development planning and in line with planning for sustainable development, natural ecology, and the impact of land use planning management. Long-term satellite imagery is needed to help us understand past and present ground coverage for patterns and changes and is useful for detecting vegetation changes and views and mapping. The best Have studied land use and land cover changes in the form of land classification, extension, direction, and distribution of urban areas. Excessive urbanization leads to many problems, including the loss of agricultural land, ecological degradation, regional inequality, and food security issues [7].

Research on urban space separation allows us to understand the process of urbanization and is a guideline for the development of infrastructure plans. According to the economies and societies' development in the last few decades both in a regional and global scale, Humans on Earth have significantly increased in changing the surface of the earth, and the extent and intensity of changes in land coverings have changed dramatically[8]. However, Remote Sensing data alone only is not able to capture the properties well enough; similarly, the study using remote sensing features may result in

differentiation between urban and non-urban areas. Present-day, the development of a spatial positioning system reveals high technology. Open-source data of Geographical Information System (GIS) has attracted the researchers in the study of urban extraction, as well as city expansion[9][10], by using a combination of Geographical Information System and Remote Sensing data, gives us an outstanding result of accuracy and features. The classification method based on the classifiers of machine learning via a cloud computing of GEE platform is now giving us very highly active. The machine learning algorithms of the classifiers to be used like Random Forest (*RF*). The standard classifier used for urban study with simple construction and high accuracy [11]. This study ‘s purpose has proposed the combination of machine learning algorithms and multi-optical images by implementing via the cloud computing platform of GEE. This study is targeted to extract urban expansion. It changes land coverage over a while and a large scale by using the primary classifier as Random Forest. Other classifiers such as Classification and Regression Trees (*CART*), Continuous Naïve Bayes (*CNB*), GMO Max Entropy (*GMO Max Ext*), Minimum Distance (*MD*) are also used in classification. Predictive evaluation is also the focus of this study. This research will be a part of defining enough space to support the projected expansion for urban development, investment in the basics of trunk infrastructure to support the development and protect the sensitive area from encroachment by developing city of urban in the future.

1.1 Motivation and Problems Statement

Land cover changes give us detailed on expansion direction and the features land coverage area on the earth’s surface such those features like agriculture, bare land, urban expansion, forest, and water bodies. The person needed to understand its physical land cover types. One feasible way to extract the land cover information is some kind of using the classification method obtaining by remote sensing[12]. Utilizing machine learning algorithms classifiers became popular in the past years. Nowadays, classifiers such as non-parametric machine learning classifier is a comprehensive approach in Earth Observation study, especially for land Classification. The classifiers include Random Forest, Classification And Regression Trees, and Continuous Naïve Bayes [13]. Random Forest is an assemble classifier formed by using the combining of varied CART-like trees. Each tree classifies without dependently the data and votes for the most popular class[14].

In addition, Random Forest follows a bagging approach where the samples of each tree subset feature and training data with replacement. High computation and precision calculation results made Random Forest as the one of the favorite classifier for land cover[15]. GEE provides a large scale of data processing, especially for many petabytes of images for land cover classification. Besides, GEE also provides assistance access to the Big Data platforms, and assistance in computation problems in recent years. Particularly GEE is a powerful tool that many people have been used in several studies on a specific classification for land cover applications related to crop and city expansion in level of regional and global [16]. GEE has also help to collaborate and work with the same preprocessed dataset. Thus, it is also paving the way for various users to re-use or validate the concepts. This research focuses basically classification the most appropiate machine learning classifiers for large size land cover maps in terms of method and design for training data with high accuracy as well as sampling on a cloud computing of GEE platform.

Vientiane, the capital city of Lao PDR, one of the most densely populated cities, central management, and it has high potential for economic and population growth. There is a tendency that urban areas will rapidly expanding to the suburbs along the main road without sufficient and readiness of infrastructure systems. Therefore, creating problems for urban expansion with poor living conditions and inappropriate social services, and suffering from lack of insufficient drainage and sewer systems. Then, the charm and attraction of the city's view may be lost forever.

Vientiane Capital needs to strengthen the city and functions base of economic. Especially in today's digital world of business and commercial industries as well as logistics and increasing livability at the same time. So, working for improving the urban sector became essential for national development as well as increasing urbanization. It leads to calls for urban enhancement management through decentralization. Vientiane, the country's capital and premier of the city Centre, has grown in many different areas. The infrastructure and services network are partly relevant to establish with efficiency, effectiveness, and sustainable trends.

Vientiane Capital needs to set up a strategic objective to upgrade life quality, increase urban productivity, and economic growth. On the other hand, economic conditions and social problems remain at the top of households. The local authorities of Vientiane have created the idea and proposed to consider the size and location of the functions needed to support them with three points, such as a factor that must be taken into account as a central or distributed model. Location power necessary for jobs in the city and conservation of the natural environment and the effective maintenance of agricultural land. These concepts aimed to control the expansion of the existing city center by creating sub-centers and city to avoid excessive clutter and extension of the current city Centre. Urban development should be limited to properly design areas. The areas should well-managed and suitable whether agricultural land, conservation areas must be maintained primarily by land use or existing conserved. To counter and solve this problem. The proper and appropriate measures must be taken immediately under the comprehensive urban development plan.

The increasing numbers of construction are more and more in urban expansion. Those problems have been happened a long time and still not solve; well-planned urban development is needed. The issues facing are massive-scale like project development, housing, and road construction. Unplanned city development caused the problem later. Waste management, overflow of a drainage system, city flooding are issues right now. Because of these problems, the government sector authority needs to competently plan and encounter these obstacles by analyzing correctly land cover changes because this issue is crucial for urban planning and city management.

These essential tasks here will help and proceed with the decentralization process to upgrade the quality of urban planning and establish for capacity building of urban development and sustainable management. With properly planning will help improve the urban environments, the overall health of the population, and increasing access to essential services (through improving the quality of urban infrastructure and services, especially with the environment of the poor people), develop urban management in Vientiane and take appropriate policy reform measures (resulting in a well-functioning, and sufficient financial city administration in Vientiane). Recommended to local government and involved agencies, especially for Vientiane Urban Development

Administration Authority (VUDAA), the central authority responsible for urban development and management as well as other related organizations carefully, and examine the problem faced. Think carefully about the best solution to develop and establish the critical task for sustainable development in the future to be an attractive place and beloved capital city of Laos and foreign tourists.

These factors are the most vital part of finding a solution and solving the problems. But besides issues faced, accessing data and the capacity of the utilization of new technology is also essential. With entire facilities will help us more understand the urban pattern with high competent. Otherwise, Digitals processing remote sensing data information is enabled to retrieve and enhance the built-up area features covered more than four decades. These new technologies will allow us to access, such as Landsat and Sentinel images. And the imagery from Landsat and Sentinel is being used in this research also to reach the reality of ground features of land cover information structure to more effective in land cover and urban planning extraction.

1.2 Research Questions and Objective

- What is the land cover changes and Spatial-temporal variations that have taken place in the areas of Vientiane Capital during 1989-2019?
- What are the determinants of these changes of land cover?
- Could the GEE platform provide us with a highly accurate and compelling interpretation of the land-classification by using multi-sources optical satellite imagery?

Objectives: This research intends to examine the pattern and direction extension of the urban in the study area. To understand its features and land cover changes mapping and monitoring during the past three decades, the location of studying is focusing on the capital city of the Lao PDR between the year 1989 to 2019 and their determinants through the application of spatial models.

- To reach the precise and high effectiveness of the land cover map, the enable to use of technology such as GIS and remote sensing metadata for expansion monitoring.
- Cloud computing platforms such as Big data, GEE can perform very fast and effective for land cover classification.

- To evaluate the Machine learning algorithms and find out the one performed the best result and give us high accuracy.
- Determine the trend of the changes in land coverage in the study area from 1989 to 2019 with every 5-year intervals

1.3 Contribution of Thesis

Overall, the participation of this research is summarized as follow:

- To check the deviations in land use/land cover
- To monitor the changes of urban and land cover and to take appropriate action
- To maintain the green cover and support sustainable development

Land use/land cover patterns of the research area will help a lot in the policies formulation and programs required for developmental planning, and it would subsequently help the corporation authorities to extend services and amenities.

Normalized Difference Built-Up Index (NDBI), Normalized Difference Vegetation Index (NDVI) are used as additional bands in an input image.

1.4 Research Structure

In the aim of developing the proposed Monitoring Urban and Land Cover Changes methods and achieving the objective of this research, the thesis is organized as follow:

This thesis will have a structure to present the main work, as stated above. Firstly, by a brief discussion about the selected topic and the explanation of the problem, Chapter 2 will give a Theoretical Review and background of the research study, a brief introduction, and the history of extraction in the study area. Followed by thoroughly literature review of urban extraction techniques using such GEE machine learning Classifiers, quality measurement, and available data fusion methods. Finally, different data types and color spaces will be briefly discussed. Chapter 3 describes the methodology used in this study and steps in more detail, and detailed implementation and analysis of the experiment, along with the discussion of the results, are provided in Chapter (4). In contrast, Chapter (5) and Chapter (6) will mention the discussion and conclusion of the research as well as recommendations for studying in the future.

CHAPTER 2
THEORETICAL REVIEW

This part is about the conceptual scope of this work. It begins with a review of the performance.

GEE cloud computing platform applications and machine learning algorithms to be used in this research. The Application Platforms Interfaces (APIs) of GEE will be the primary tool for implementation. Machine Learning Classifiers and Multi-source optical images from Satellites will be used as the parts under the ML Classifiers for classifying and extract the land cover features information follows by definition of urban, population, and economic growth in Laos.

2.1 General Urban and Land Cover Changes Definition

The study focused on the built-up areas as well as urban expansion during the study period of 1989-2019; it is like the identity of the metropolitan region. The constructed areas cover all Public utilities and facilities, including all built material structures such as roads, buildings, and parks with plants and water[17]. The study defined the difference according to the current physical boundary of the built-up area by using remote sensing imageries covered for three decades to comply with GEE. Land cover information retrieved from satellite image is playing a crucial role for human beings due to the earth's surface existed many types of natural that intervened and being used by humans. The high effectiveness of utilizing and analyzing with timely, accurately, and precisely of land cover is an essential factor in developing the human being's life and society. The fast growth of urbanization and the construction of human's activities led to changes in the land cover surface. Earth ground in regional and global scale is threatening and impact on the ecological system, natural transformations, aesthetical, and socio-economic. In this case, it required to in-depth study and well plan for sustainable development and brought us a better result for future urban planning.

Covered space refers to all physical environments on the Earth's surface. The situation means everything around us, such as forests, cities, lakes, mountains, and others. Generally, there is two majors' method for land cover detecting such using the Global Positioning System (GPS) by field surveying, extracting, and retrieving information from satellite image using processing techniques such as classification. The surveying method is high cost and time consuming and cannot perform with a large scale of the

area. By using remote sensing, retrieving and deriving information from the satellite sensors are widely used, especially for studying land coverage patterns, disaster, air quality, forest management, urban expansion, weather prediction, etc. Technically, the methods that most of the researchers being used for urban development is that extract information from satellite remote sensing images.

Probably the most prominent feature of urbanization in such developing countries is the daunting step of the rural change. Such high urban growth rates are often caused by migration in rural areas and urbanization, which leads to the integration of nearby settlements [18][19]. In general, the capital city is where most of the wealth, resources, and intensive employment opportunities [19][20]. Environmental degradation [19][21][22][23]. And the uneven distribution of wealth and advantages in urban areas is the result of this swift and uneven city expansion[24]. Another issue is the domination of urban expansion and suburban growth [21][25]. Through the invasion of forests, farmlands, wetlands, and other natural ecosystems and habitats [26]. The utilization of land in the urban area leads to ecological sustainability, but forest resource values are in the risk resulting in deforestation and the uncertainty of the environment.

2.2 Urban in South East Asia

The growth rate of the cities in Southeast Asia is still relatively high at 2.38 per cent (the price is below 1 per cent for many developed countries)[27][28]. The high rate of city growth caused a significant threat to the environment and is putting pressure on the areas as well as urban management [29][30]. Town and cities, the significant place with densely populated, high utilizing of labour, technological innovation, and economic growth. Many issues led to disposal and crime large population concentration, and they can cause problems such as congestion, pollution, and disturbance. So, well managed urban planning needs to perform with positive development promoted and negative one mitigated. This problem is hardly possible because of the cities in the central of people living, technological innovation, trading, socio-economic activities; it is subject to formal control mechanisms rather than convention and traditions.

Southeast Asia is continuously growing. Today, approximately 41.8 per cent of the total regional population, nearly 245 million live in urban areas. In the 1950s, only 15.4 per cent of the region's urban population, and it would increase to 49.7 per cent of the total

population by the year 2025. Style levels vary widely. Most advanced economy countries (Brunei, Malaysia, and Singapore) have a high urbanization level of more than 65 per cent. The states with the least economic development (Cambodia, Laos, Myanmar, Timor-Leste, and Vietnam) have low urbanization below 34 per cent. The growth rate of the country with the least growth is much higher. In essence, 5.0% in Timor-Leste, 4.8% in Lao PDR, 3.2% in Cambodia, almost all countries will have a more significant number of the total population living in cities center by 2050. The majority of the people of Southeast Asian cities (67 per cent or nearly 165 million people) live in small towns and cities with a population of fewer than 500,000 people. These cities and small towns are often struggling to develop the local economy and develop infrastructure because they cannot manage the city[31].

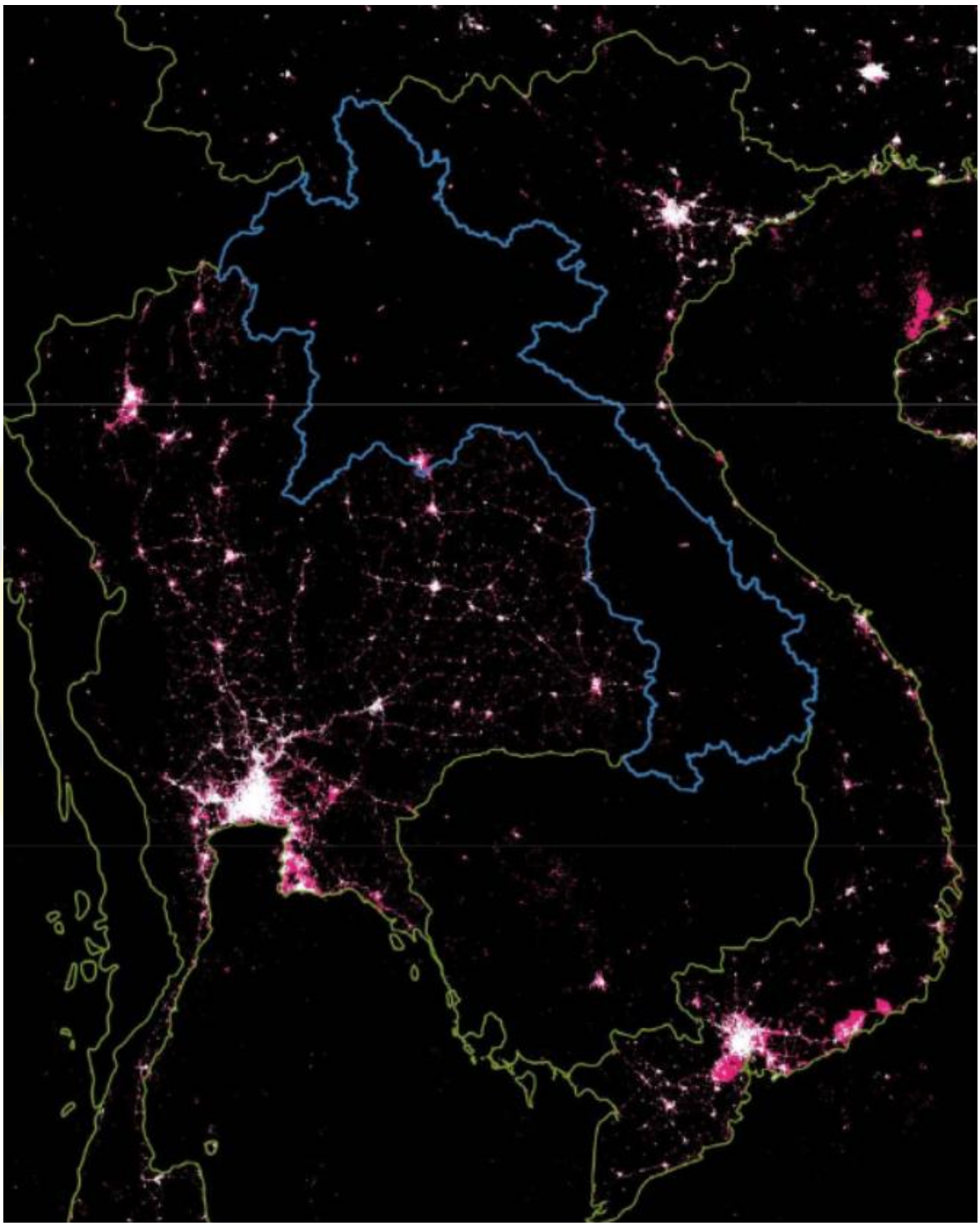

*Figure 1 White areas: Nighttime light emission in 2012, Pink areas: Increase of nighttime light emission between 2012 and 2016, Source: NASA 2013 & 2017[32]***.**

2.3 Dynamics Changes of Urban in Laos

Lao PDR is a mostly rural country in the Southeast Asian region with a low number of populations; about half of the country's land is full of forests. three decades later, the leader of Laos introduced a new economic mechanism (NEM) by the fourth congress

of the Lao People ‘s Revolutionary Party (LPRP) in November 1986, it aimed at the rapid change of the controlled socialist economy and the transition from an dictatorship to a market economy. The country has changed gradually from socialism to a market economy [33][34][35]. Since then, the infrastructure sector from foreign investment has been expanded; pressure on cultural and environmental assets are increasing, and rural migration is becoming more intense [36]. Urban Population growth (Percentage of total) in Lao PDR was reported at 35% in the year 2018. Accordance with the World Bank Group (WBG) collection of indicators on development, compiled from officially known sources that Lao-Urban population growth (% of total)- actual values, historical data, forecasts, and projections were sourced from World Bank on March of 2020 [37].

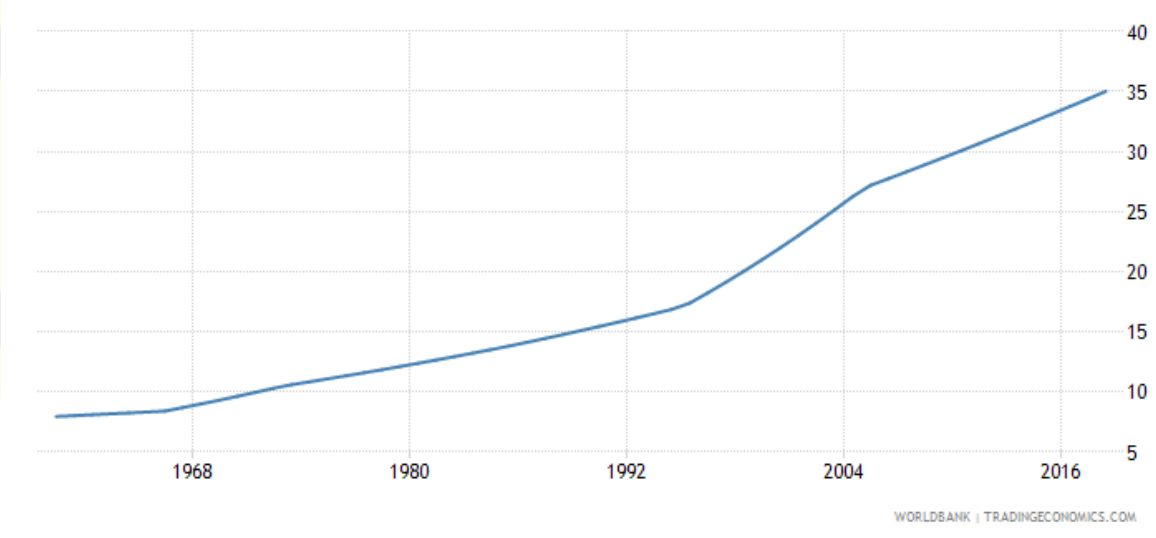

Figure 2 Urban growth in Laos from 2007-2016 (Source: World Bank)

Urban population growth (annual %) in Lao PDR was reported are 3.38% in 2018; this report was given by the World Bank collection of development indicators, compiled from officially recognized sources. Lao-Urban population growth (annual %) – current values, historical data, forecasts, and projections were sourced from the World Bank in April of 2020 [38].

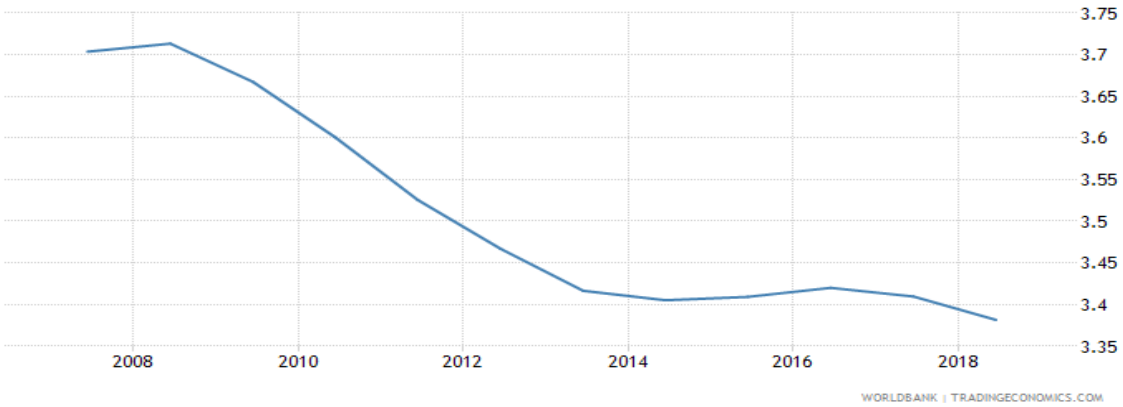

Figure 3 Laos-Urban population growth 2008-2018 (annual%).

2.3.1 Urban Expansion

For Lao PDR, the country with urban expansion is new compared to the developed countries. The population growth rate in urban areas is more than the average of national. It shows the migration of rural town urban areas are associated with several issues such as increased inequality, moving of the workers, child rights and protection, disease, malnourished children in families in the city, pollution, and poor sanitation. Urban sanitation in Vientiane Capital is generally poor; they are suffering from the lack of insufficient drainage and waste system and the bad design of sewage disposal that exists for the septic tank from a small household to the number of industries as well as from central to the edge of the city. Untreated and overflowing water flows into the lowland area, which poses a threat to public health, destroys the environment, and impacts to surrounded areas. To achieve national planning goals by 2020, the World Bank calculates that each year Laos will have to invest the US $ 19 million for city water supply and the US $ 12 million for city sanitation[39].

According to Vientiane has high potential of economic and population growth. There is a tendency that urban areas will be will rapidly expanded rapidly x to the suburbs along the main roads without sufficient infrastructure. Therefore, it will also create problems for urbanization through poor conditions living and improper social services. From then on, the charm of the city may be lost forever if no appropriate action in urban planning. To distinct these problems, the immediate measures need to be taken following a comprehensive urban development plan in this situation. It is recommended

that the local government of Vientiane Capital and all citizens pay attention catch up on eyes to the problems found and consider the appropriate procedure to develop Vientiane Capital to be an attractive and beloved capital of Laos and foreign tourists as well. In response to the request of the Government of the Lao PDR, The Government of Japan decided to proceed with the "Urban Development Master Plan in Vientiane Capital Project" (UDMP). Therefore, the Japan International Cooperation Agency (JICA) conducted a study in close collaboration with relevant agencies of the Lao Government[40].

2.3.2 Population Growth

Since 1955, during World war II, the Lao population throughout the country is only 1,890,854 with density at eight people/ sq.km. Then after took over to Lao People's Democratic Republic (Lao PDR) in 1975, the Lao population is increased to 3,051,577. Over the last four decades, the growth rate is at 1.48%, with a total population in 2020 at 7,275,560 due to the increased fertility rate at 2.70, and about 35.7 % of the total population is living in the urban (see more Figure 3. This statistic shows the city level and urbanization in Laos from 2008 to 2018). Most of the population generated along the Mekong River, the branch of the main river, and the flat area along the riverside. According to a report from Worlddometers found the Lao population is projected to grow at 8,226,273 in 2030, with a growth rate of 1.14%. It will be reached 9,479,747 in 2050 by living in the urban increased to 53.8% (see Table 1. Population growth in Lao PDR) below for Laos population recorded and future forecast, Source from Worlddometers[41].

Table 1 Population growth in Lao PDR

Year	Population	Yearly Change	Fertility Rate	Density (P/Km²)	Urban-Pop %	Urban Population
1955	**1,890,854**	41,588	5.94	8	7.60%	143,427
1960	**2,120,898**	46,009	5.96	9	7.90%	168,533
1965	**2,382,594**	52,339	5.97	10	8.30%	198,298
1970	**2,688,428**	61,167	5.98	12	9.60%	258,749
1975	**3,051,577**	72,630	5.99	13	11.10%	338,147
1980	**3,258,144**	41,313	6.15	14	12.40%	403,247
1985	**3,687,898**	85,951	6.36	16	13.80%	509,071
1990	**4,258,472**	114,115	6.27	18	15.40%	657,373
1995	**4,846,483**	117,602	5.88	21	17.40%	843,190
2000	**5,323,700**	95,443	4.81	23	22.00%	1,171,236

2005	**5,751,676**	85,595	3.9	25	27.20%	1,564,297
2010	**6,249,165**	99,498	3.4	27	30.10%	1,877,890
2015	**6,741,164**	98,400	2.93	29	32.70%	2,206,330
2016	**6,845,846**	104,682	2.88	30	33.30%	2,279,990
2017	**6,953,035**	107,189	2.88	30	33.90%	2,356,986
2018	**7,061,507**	108,472	2.88	31	34.50%	2,436,711
2019	**7,169,455**	107,948	2.88	31	35.10%	2,518,056
2020	**7,275,560**	106,105	2.7	32	35.70%	2,600,131

2.3.3 Economic Activity

Despite continued economic growth, driven by large mining industries and hydropower, limited private investment and obsolete trade regulations affect the long-term economic trends. To ensure and support diversity as well as comprehensive economic growth. The organization of the United States Agency for International Development (USAID) collaborates with the public and private sectors to improve current policies that can help strengthen Laos in economic development on the stage of the Association of Southeast Asian Nations (ASEAN) and the World Trade Organization. (WTO) Gateway to foreign investment. In 2018, the Gross Domestic Product (GDP) growth at an average of 6.3% over the past ten years while 5.2% in 2019 with income per capita reached at US$ 2,670 (nominal, 2019 est.) while GDP growth per capita is expected at 5.0% in 2019 and 6.5% in 2020. The Lao government is trying to sustain macroeconomic stability by decreasing the fiscal deficits and strengthen public debt management with a fiscal balance that is expected to decrease to 4.3% of GDP in 2019 from 4.4% in 2018 and 5.5% in 2017, Source from ADB[42].

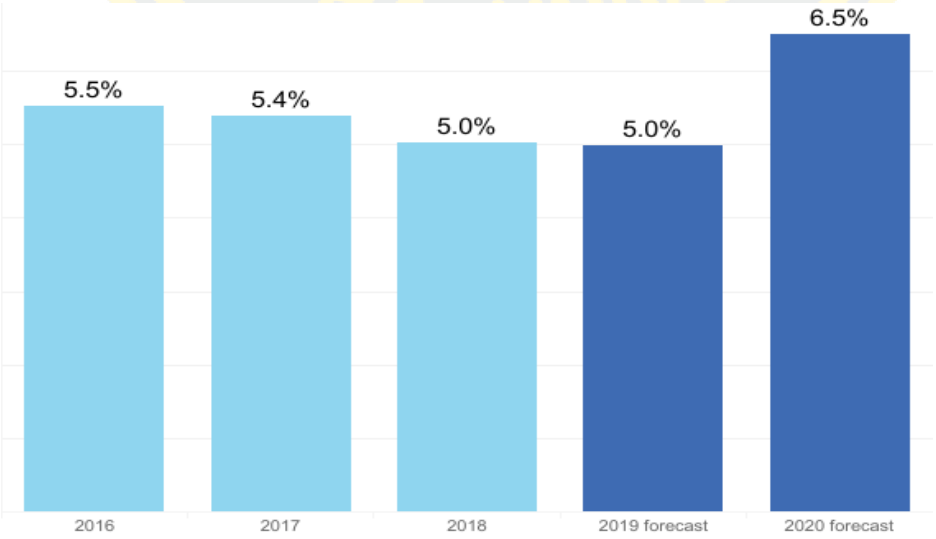

Source: Asian Development Bank. *Asian Development Outlook 2019* (April 2019)

Figure 4 Per Capita GDP Growth Rate: Lao People's Democratic Republic

2.4 Google Earth Engine (GEE)

The GEE, a cloud platform of computing for geospatial analysis, can access over forty years of satellite imagery. Provide accessibility of scientific investigation, visualization, and implementation of geospatial datasets by using advanced algorithms of machine learning with simple bands combinations such as NDVI, NDBI, masking bands using existing bands, classifying satellite data, sub setting data spatially using vector data. It is free to access the extensive catalogues of satellite imagery and other geospatial datasets for the utilization of academic researches, non-profit aids organizations, and the state government organization. Moreover, it can be used in monitoring a commercial use if that commercial organization is under license by the earth engine products. An extensive collection of large satellite imageries can be restored directly, and Advanced processing of imageries can be rigorously tested and implemented according to machine learning algorithms in GEE [43][44]. Since then, GEE has worked with large volume capacity in petabytes scale. It has reduced processing time and steps, including increasing the efficiency of a global analysis[45]. You can apply to be free users and explore the GEE with these web addresses for more details on GEE APIs, and please see these links for more information: (https://earthengine.google.com/, https://explorer.earthengine.google.com/#workspace).

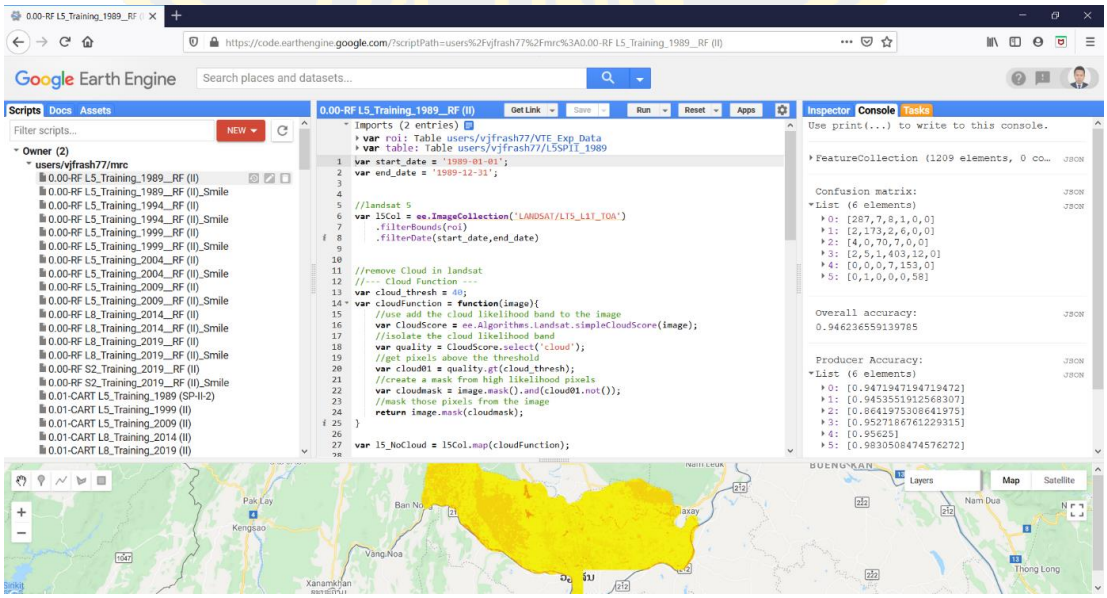

Figure 5GEE performed by Machine Learning of Random Forest in 1989, Vientiane, Laos

2.5 Machine Learning Classifiers

2.5.1 Random Forest (RF)

Kagan TUMER and JOY DEEP GHOSH substantiated that output combination from multiple classifiers for outcome prediction offers very high accuracies of classification [46]. This method is the basis for RF classifier, combined production from numerous decision trees to identify the label for a new input data based on the highest information.

RF were selected randomly to select a sub-sets samples of training through replacement to create a single tree, i.e., it uses a bagging technique where for every tree, data sampled from the original complete training set [47]. The examples that not used for training (out-of-bag samples) Used internally for evaluating the efficiency of the classifier and providing general error evaluation. Also, at each RF node, the selection for a random of variables from the training samples to define the best separation to create a tree. Though this would reduce the strength of individual trees, it reduces the correlation between the trees, resulting in lower generalization error [14]. Separations are performed in a way that decreases entropy and increases the data received after the separation. But the efficiency of tree-based classifiers is more affected by choice of pruning methods than the best split selection measure[48]. RF is immune to such effects as it builds trees without the need to employ pruning techniques [49].

One of the parameters that the user-defined for RF is the number of trees. Nathan A and Scobell A suggested that generalization errors tend to converge as the number of trees increases [50]. Therefore, there is no problem of overfitting, which can also be attributed to the Strong Law of Large Numbers [51]. Thus, for RF, the number of trees possible to be significant, but aside from a certain point. Additional, trees will not help in improving the classifier's performance [52]. [53] suggests in their review that most papers use 500 trees for the number of trees for RF classification, while a few other studies use 5000,1000 or 100 trees for RF. And among this 500 is considered the most suitable value and acceptable for the number of trees.

A single tree may not accept the essential of all the input features. Still, a combination of trees takes into account all the features which randomly chosen from the training

sample. Hence, from the perspective of remote sensing research, RF helps to understand the relative importance of various variables derived from bands of satellite imagery. RF evaluates each variable by deleting one variable from the randomly selected input variables while maintaining other variables constant. It evaluates the accuracy according to out-of-bag error, and the Gini Index decreases [54]. Besides, RF also measures the distance of two samples selected according to the number of times the pair end in the same terminal node [55][56].

RF has received essential due to its robustness to noise and outliers. Furthermore, RF performs better than other classifiers that use ensemble methods such as bagging and boosting [15]. RF has been proven to give good results when used in various applications such as classification for urban landscape [57], classification for land cover on multi-temporal, and multi-frequency SAR data [58]. And so, on.

2.5.2 Classification and Regression Trees (CART)

CART is a binary decision tree classifier that takes the time to make a logical question for simple decisions. The classifier checks the input variables and selects the variable with the highest data acquisition according to the nodes at all level separation [59]. This processing, the entered data will be randomly divided into several groups, and trees were created, using all the groups leaving out one. The left out the group is used to check the correctness of the tree, and trimmed trees that provide the least deviation. In this research, Classification using CART was performed via GEE. CART method available in the library of Earth Engine. The best choice of cross-validation factor is 5 or 10, according to studies [60], and it is so considered as an input value.

2.5.3 Continuous Naive Bayes (CNB)

The simple model of Naïve Bayes with exceptional powerful according to Bayes theory declared on equation (1) below and the assumption of independence between input variables. The classifier of CNB is formulated to meet binary and multiclass classification issues. This model, the target value is calculated according to the independent assumptions condition instead of trying to calculate the cost for each attribute value. Due to the optimization step that is not necessary to suit the coefficient, the learning of the Naïve Bayes model from data training. Furthermore, it can reduce the average risk of classification errors in procedure’s learning.

$$\left(\frac{h}{d}\right) = \frac{p\left(\frac{d}{h}\right) * P(h)}{P(d)} \quad (1)$$

Where P(h/d) be the posterior probability, P(d/h) can be the probability of data d given that the hypothesis h was real, P(h) is the prior probability of h, and P(d) is the probability of the data [61][62].

2.5.4 GMO Max Entropy (GMO Max Ext)

Multinomial logistic regression is a common characteristic of linear regression using softmax conversion function, and the main task is to reduce the error function to minimize by removing the logarithm of the probability, which means cross-entropy. The main difference between models and other algorithms is the result scores that may be considered a probability value [62][63].

2.5.5 Minimum Distance (MD)

One of the simplest classifiers that are overseen is a parallel method. But some better approach in terms of greater accuracy called as minimum distance classifier. This classifier sets up a group in multi-dimensional space, each defining a distinct (named) class. Any of the pixel sizes are then assigned to that class if the shortest vector distance is close. Begin with the simplest example of supervised classification by creating using the minimum distance routine. The software programming will act on the DNS number in kind of multi-dimensional band space to recognize the pixel into the selected classes. Each of the unknown pixels is placed in types that are close to the average vector in this band space, which can choose to combine the classes to have one color theme (similar colors for related classes) and set apart spatially adjacent categories by using different colors. Minimum distance requires that the user provides the mean vectors for each class in each hand µck from the training data. To perform a minimum distance classification. A program must calculate the distance to each mean vector, $U_{cK,}$ from each unknown pixel (BV_{ijK}). BV_{ijK} is the brightness value at the same location in-band k, at row i, column j. BV_{ijK} is the brightness value in band 1. It is possible to calculate this distance using Euclidean distance based on the Pythagorean Theorem. The computation of the Euclidean distance from the point to means of Class-1 measured in the band relies on the equation[64].

$$d_k^2 = (x - \mu_k)^t (x = \mu_k) \qquad (2)$$

where **X** : vector of image data (n bands)
X = [x_1, x_2, ... x_n]
μ_k : mean of the kth class
μ_k = [m_1, m_2, ... m_n]

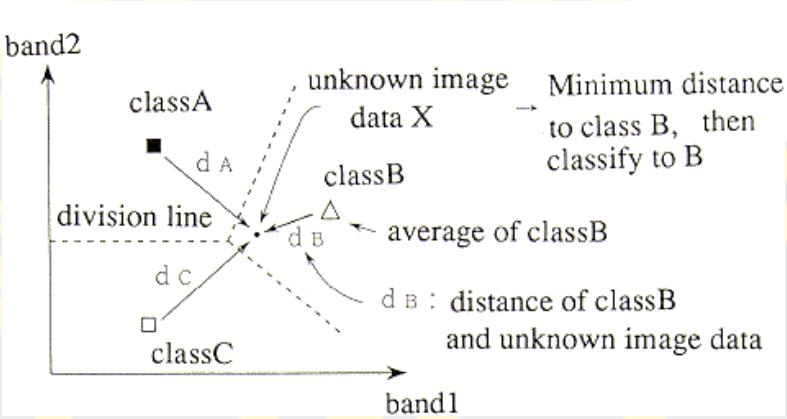

Figure 6 Concept of Minimum Distance Classifier

2.6 Supervised Learning

Nowadays, supervised learning is one of the sub-branches that commonly used in machine learning algorithms. Usually, the new learners of machine learning will start their studies with supervised learning. Consequently, supervised learning can be divided into two sub-categories, such as Classification and Regression.

The algorithms of supervised machine learning are designed to learn by using an example. The name "supervised" learning innovates from the idea that this type of algorithm training is like having a teacher supervising the whole process.

While training implementation with the instructional of a supervised learning algorithm, the training data consists of inputs matched with the correct outputs. During the practice of training, the algorithm searches for patterns in the relevant data to the desired outputs. After the training process, an algorithm supervised learning will receive new invisible input and will consider which labels of unique contributions will be classified according to training data first. The purpose of a supervised learning model is the correct label prediction for newly proposed input data. In the most basic form, an algorithm of supervised learning can be written simply as:

$$Y=f(x) \qquad (3)$$

Where Y is the predicted output that is determined by a mapping function that assigns a class to an input value x, the function used to connect input features to a predicted output is created by the machine learning model during training [65].

2.7 Spectral Indices

Spectral indices are the combinations between the two or more spectral wavelengths that indicate an abundance of interesting features. The vegetation index is the most popular type, but other indices are available for burned areas, human-made (built-up) features, water, and geologic features [66]. It is used to emphasize specific properties or phenomena in an images processing that are perceived from a distance. There are many types of spectrum indexes that can be used in scientific work. And the capability of the spectrum index is especially vital in surveying and evaluating land cover classes. In this classification guidelines, I firstly calculate NDVI and NDBI values. Due to the study area is a modern city, our study only focused on the calculation of NDVI value to detect vegetation changes of the forest, and agriculture, as well as the NDBI value to detect changes in the built-up area index.

2.7.1 Normalized Difference Vegetation Index (NDVI)

NDVI defines us to know the density of vegetation and greenness on the land; Most researchers are interested in observing different visible colors (Wavelengths) and bands near-infrared in which the light from the sun is reflected from plants. The various wavelengths make up the spectrum of sunlight during it strikes objects so that a few wavelengths of this spectrum are absorbed, and some wavelengths are reflected. Plants leave contained pigment such as strongly chlorophyll absorbs visible light with wavelength about 0.400-0.700 μm was used for photosynthesis. The structure of the cell in leaves strongly reflects in the wavelength of near-infrared light between 0.700-1.100 μm, the more these wavelengths of light are affected, respectively. The measurement of NDVI uses two bands between near-infrared (NIR) and the RED band as the following equation. On the other hand, Satellite maps for vegetation monitoring demonstrate plant growth's density around the world. The most common measurement used is called the Normalized Difference Vegetation Index (NDVI). With low values of NDVI is range from 0.1 and below correspond to barren areas of rock, sand, or snow. Moderate values represent shrub and grassland ranging from 0.2 to 0.3, while high

values represent for temperate and tropical rainforests with values between 0.6 to 0.8 [67].

$$NDVI = \frac{(\mathrm{NIR}-\mathrm{RED})}{\mathrm{NIR}+\mathrm{RED})} \qquad (4)$$

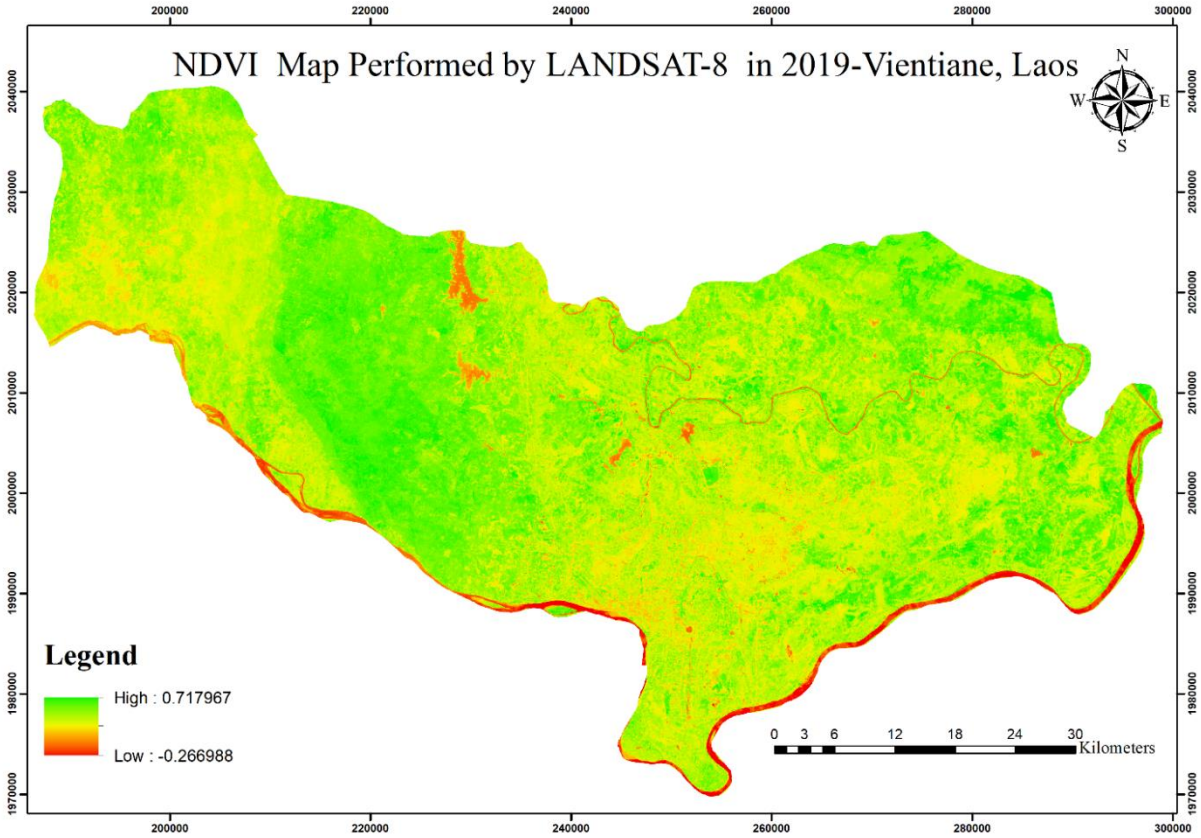

Figure 7 Normalized Difference Vegetation Index (NDVI) during the Year 2019

2.7.2 Normalized Difference Built-Up Index (NDBI)

Most of the professionals and scientists working in the urban planning sectors are emphasized studying and examining spatial distribution and differences of the urban areas. A common index used for mapping cities, urban and built areas is the normalized difference built-up index (NDBI). Nowadays, due to the increase of urbanization around the world, play an essential role in urban studying so that the NDBI becomes more widely used as one of the crucial spectral indices in satellite image mapping and processing. The NDBI can be calculated as the following equation below:

$$NDBI = \frac{(\mathrm{SWIR}-\mathrm{NIR})}{(\mathrm{SWIR}+\mathrm{NIR})} \qquad (5)$$

Where NDBI refers as Normalized Difference Build-up Index, SWIR is the shortwave Infrared band and the NIR is a near-infrared band of the associated satellite sensors [68].

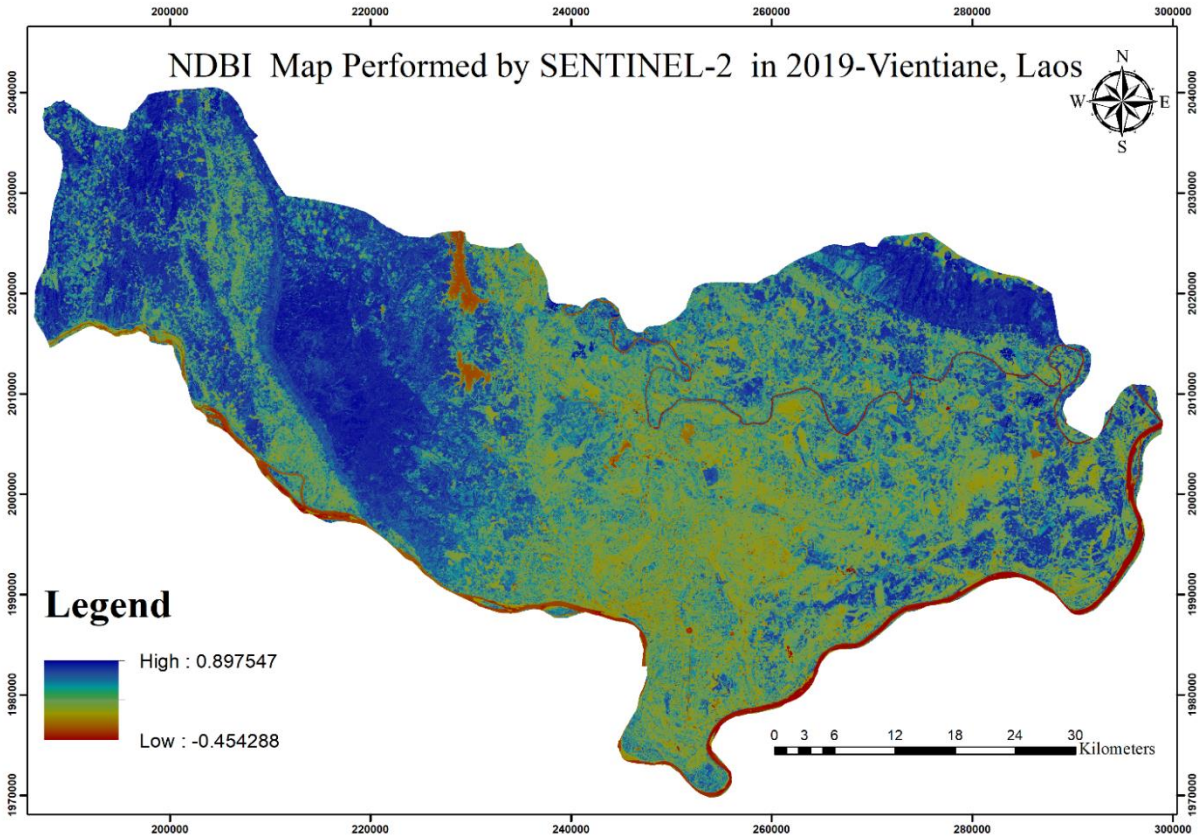

Figure 8 Normalized Difference Built-Up Index (NDBI) during 2019

2.8 Satellite Image Feature Extraction

Regarding the satellite image processing, the feature extraction will be processed via GEE using machine learning classifiers and sample data collected from Arc GIS software (sample training collection). Laos has no access database to provide accurate datasets. So, I have to extract features by using Geographic information system techniques and machine learning algorithms instead in some point, line, and polygon, and then operating the experiment covered the study areas by the approach of Object-based such as Random Forest (RF), Classification and Regression Trees (CART). In the sample feature extraction below, I proposed an image from Sentinel-2 in 2019 and shown the raw image in the RGB band (12-8-5). The collected sample has been uploading via GEE assets and applied with the Random Forest classifier to extract land

cover in the study area (see the image shown feature extraction in Figure 10. Feature Extraction of LC Classification from Sentinel-2 in 2019).

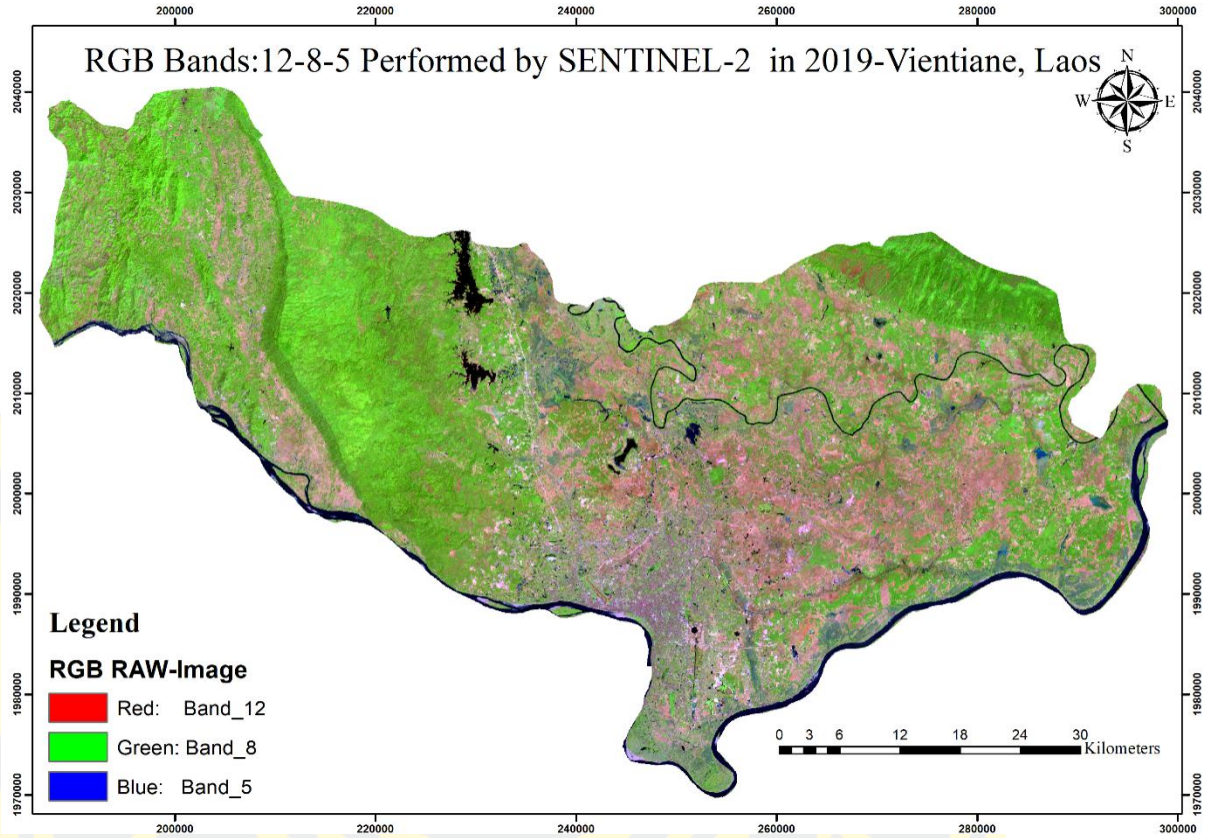

Figure 9 RGB image Bands 12:8:5 from Sentinel-2 in 2019

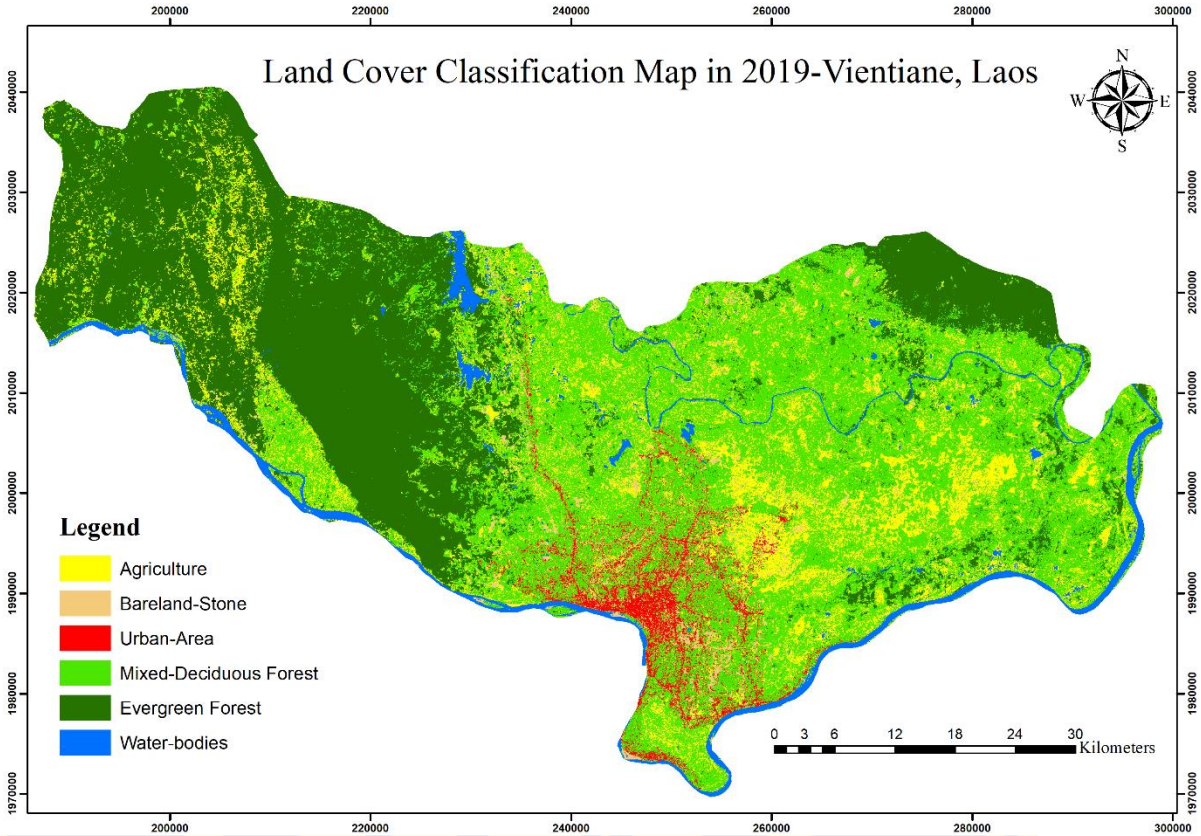

Figure 10 Feature Extraction of LC Classification from Sentinel-2 in 2019

CHAPTER 3
METHODS AND DATA

This section will provide details of the study area and explain the data used and the data collection methods used in this research. Analysis methods will be covered in Chapter 4. As it been shown in detail. The satellite images from Landsat 5, Landsat 8, and Sentinel-2 data to be used in this study were the main dataset. Then after the machine learning algorithms will be used as classifiers to classify and extract the features from satellite images. And I am proposed to use five classifiers of machine learning such as Random Forest, Classification and Regression Trees, Continuous Naive Bayes, GMO Max Entropy, and Minimum Distance, Additional. Normalized Difference Vegetation Index (NDVI) was also used for plant health measurement and the Normalized Difference Built-Up Index (NDBI) used for automatic mapping of city areas. GEE will extract both of these indices and used to realize the role of urban expansion and land cover changes in Vientiane, Laos.

3.1 Study Area:

This research study focuses on Vientiane, of Lao PDR''s capital city with a total area of about 3,920 sq.km, which selected as a study area for many reasons. Earlier, Vientiane is the central economic, administration, and management of Lao PDR. Secondly, Vientiane is the increasing population exceeding reach three-quarters of million in Vientiane urban area, Thirdly potential impacts of population density, transportation, high utilization of water, wastewater, liquid and solid waste management, and inappropriate environment of urban expansion, etc. the study area located in the north-west of the country shared border with the Kingdom of Thailand on coordinate of latitude and longitude between 17° 58' 29.4780" N and 102° 37' 51.1212" E.

Vientiane population growth steadily since 1950 during World War II (In the era of France governance), the population in Vientiane is below 100,000 people. Then after took over to Lao People Democratic Republic under the conduction of the Lao People's Revolutionary Party (LPRP), the population is about 187,000, and in 2020 Vientiane population is reaching 683,000. And projected to grow at 756,000 in 2025, 8,226,273 in 2030, 8,971,946 in 2040 and 9,479,747 in 2050 respectively [41].

Vientiane Capital has a high potential for economic growth and population. There is a tendency that urban areas will expand rapidly to the suburbs along the main roads without sufficient infrastructure, causing urban expansion problems with poor conditions of living and inappropriate social services. From then on, the charm of the city may be lost forever. By solving this problem, appropriate and properly measures must be taken immediately in the cities covered for the Development Plan. In this predicament, it is recommended that the local government of Vientiane Capital and all citizens must carefully examine the problems faced and determine the proper output to develop the capital city with the modernization of Vientiane Capital in 2030, and is a highly attractive and well-known capital. The love of Laos and foreign tourists as well this year is a wonderful opportunity for the master plan as the capital city of Vientiane celebrates the 450th anniversary of the transfer of money to the city.

Figure 11 Study Area (Vientiane Capital, Laos)

3.2 Data

in Data collection, the primary material used for this study is the satellite dataset, and it will be utilized in the research are introduced. The satellite image will be used as training data in Arc GIS and will be added as an archive as a zip file then uploads to the machine learning classifiers in GEE. The classification based on a time-series dataset and will be used for three satellites such as Landsat 5, Landsat 8, and Sentinel-2, for the study period is covered for three decades as from 1989-2019.

Firstly, I download the images with full bands by using GEE. Then after the sampling collection is started by using Arc GIS software. For sample collection, I collect for

every five years, beginning with 1989, 1994, 1999, 2004, 2009, 2014 and 2019. After completing samples collection, then zipped all samples collected upload to GEE 's assets again and applied the created machine learning interface, then running the classification.

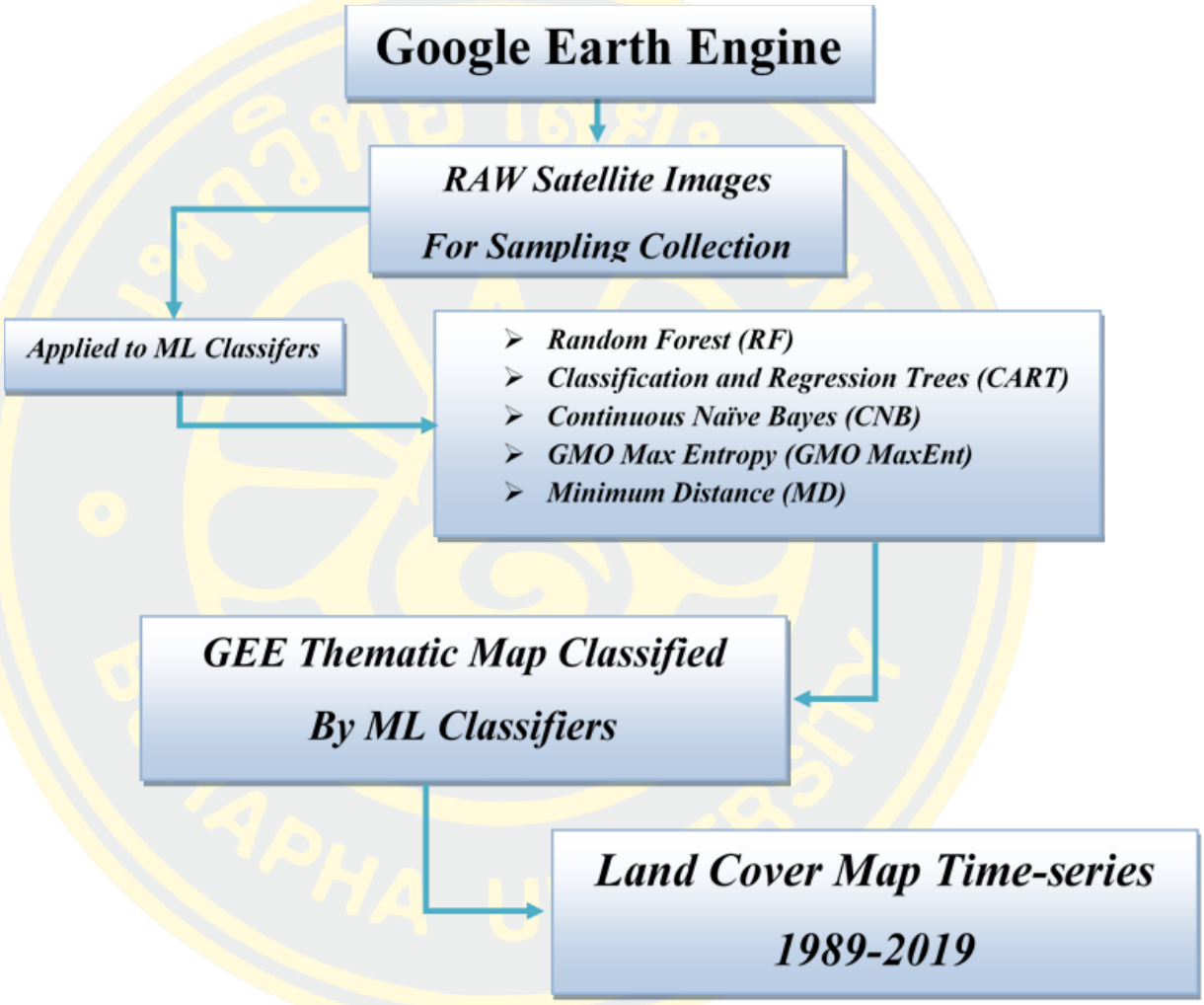

Figure 12 Sampling and Classification structure by ML

3.2.1 Landsat 5

The Landsat 5 has delivered nearly 29 years of the Earth-imaging data and was set a Guinness World Record for "longest Operating Earth Observation Satellite" on Earth orbit. It was launched on March 1, 1984. The purpose of this Satellite was to collect the images for Earth's surface. This Satellite was jointly managed by the two organizations, such as the United States Geological Survey (USGS), an organization of the National Aeronautics and Space Administration (NASA). The orbit height is 438 miles

(705Km), and it was a low Earth orbit with speed on an orbit about 3.999miles/s (6.421283Km/s) and repeat interval every 16 days [69].

Table 2 Description of spectral bands and a ground resolution of Landsat 5 TM

Landsat 5	**Wavelength (μm)**	**Resolution (m)**	**Description**
Band 1	0.450-0.520	30	Blue
Band 2	0.520-0.600	30	Green
Band 3	0.630-0.690	30	Red
Band 4	0.760-0.900	30	Near Infrared (NIR)
Band 5	0.1.550-1.750	30	Mid Infrared
Band 6	10.400-12.500	30*	Thermal Infrared
Band 7	2.080-2.350	30	Mid Infrared

3.2.2 Landsat 8

Landsat 8, at first, was known as the "Landsat Data Continuity Mission." it was launch on February 11, 2013. This kind of Satellite carried two primary Sensors as Operational Land Imager (OLI) and the Thermal Infrared Sensor (TIRS). Its orbit is in a Sun-Synchronous, near-polar realm, the attitude is 438 miles (705Km), inclined at 98.2degree, and circles the Earth every 99 minutes. The Satellite has a 16-day repeat circle with an equatorial crossing time 10:00 a.m (+/- 15minutes). It was designed on a Worldwide Reference System-2 (WRS-2) path/row system with scene size 106x115miles (170x185Km) [70].

Table 3 Landsat 8, Operational Land Imager (OLI) & Thermal Infrared Sensor (TIRS)

Landsat 8	**Wavelength (μm)**	**Resolution (m)**	**Description**
Band 1	0.433-0.453	30	Coastal/Aerosol
Band 2	0.450-0.515	30	Blue
Band 3	0.525-0.600	30	Green
Band 4	0.630-0.680	30	Red
Band 5	0.845-0.885	30	Near Infrared (NIR)
Band 6	1.560-1.660	30	Short Wave Infrared (SWIR-1)
Band 7	2.100-2.300	30	Short Wave Infrared (SWIR-2)
Band 8	0.500-0.680	15	Panchromatic
Band 9	1.360-1.390	30	Cirrus
Band 10	10.30-11.30	100	Long Wave Infrared
Band 11	11.50-12.50	100	Long Wave Infrared

3.2.3 Sentinel-2

The mission of Copernicus Sentinel-2 from the European Space Agency (ESA) consists of a group of two satellites orbiting the poles, which are in orbit around the same sun, which are at 180 ° each other. Its objective is to examining and monitoring the variability in the surface conditions of the Earth's ground. This Satellite has a full swath-width at 290km. The returning time is ten days at the equator of one each Satellite, which means that five days for two satellites and operating under no cloudy condition in two to three days at the middle latitudes. This Satellite will be used for assisting and supporting the monitoring mission of the Earth's surface changes. The coverage limit is from latitudes between 56 ° south and 84 ° North [71].

Bands	**Spectral Resolution (µm)**	**Spatial Resolution (m)**	**Description**
B1	0.433 – 0.453	60	Coastal aerosol
B2	0.458 – 0.523	10	Blue
B3	0.543 – 0.578	10	Green
B4	0.650 – 0.680	10	Red
B5	0.698 – 0.713	20	Red-edge 1
B6	0.733 – 0.748	20	Red-edge 2
B7	0.773 – 0.793	20	Red-edge
B8	0.785 – 0.900	10	Near Infrared (NIR)
B8A	0.855 – 0.875	20	Near Infrared narrow (NIRN)
B9	0.935 – 0.955	60	Water vapor
B10	1.360 – 1.390	60	Cirrus
B11	1.565 – 1.655	20	Shortwave Infrared (SWIR) 1
B12	2.100 – 2.280	20	Shortwave Infrared (SWIR) 2

Table 4 Description of spectral bands and resolution of Sentinel-2

3.3 Data Combination

Data processing and combining a multi-source of data can provide us with more accurate measurement than the one source, the target of connecting is to enlarge the accuracy level of the datasets. On the other hand, increasing size of data collection by combining various data source have been widely utinlized in remote sensing study such

as remote sensing of land cover change for large areas has become common in many types of landscapes (21,22), like the previous research as Forms of Urban Expansion of Chinese Municipalities and Provincial Capitals, the 1970s–2013 [17], A national dataset of 30-m annual urban extent dynamics in the conterminous United States [72], Urban sprawl assessment and modelling using Landsat images and GIS [73], etc.

"Combining the spatial and temporal indices data provided by two or more different instruments and sources able to improve the processing, interpretation, and visualization."

3.4 Methods and Data Used

In this test site, in this section, we have introduced each classifier. Since our focus is on how to use these classifiers instead of in the theory of design, I only provide conceptual explanations for each classifier, focusing on issues that are important when using classify. I am proposed to use the Supervised Classification with two datasets; the first one is satellite image (RGB colour) with a resolution 30m Landsat from NASA/USGS Satellite and another 10m resolution of sentinel-2 from European Space Agency (ESA) Copernicus. Two primary sources of satellite image downloaded and implemented with machine learning via GEE in the Year 1989, 1994, 1999, 2004, and 2009 from Landsat 5, the Year 2014, and 2019 from Landsat 8 and Year 2019 from Sentinel-2. Data collection will be used Arc GIS software and collect the sampling in study areas; the prepared samples upload to GEE web interfaces (APIs) to process by the primary classifier as Random Forest (RF) and other classifiers such as Classification and Regression Trees (CART), Continuous Naïve Bayes (CNB), GMO Max Entropy (GMO Max Ent), and Minimum Distance (MD). These classifiers will be used to compare the results of Land Cover Classification and extract the needed features. The study focuses on the time-series dataset and open-source such as Google Earth, Satellite Images, Arc GIS software will also be used as well for Post-Processing. The procedure steps are implemented as below:

1. Filtering based on the date (annual image average), cloud cover clear less than 20%, atmospheric and geometric correction, subset, and mosaic within the study area boundary by uploading the shapefile of the study area into GEE assets.

2. Download the image in targeted such in 1989, 1994, 1999, 2004, 2009 from Landsat 5, 2014, and 2019 from Landsat 8, and 2019 from Sentinel-2. All downloaded images are combined bands (full band composite).
3. Open the images on Arc GIS to undertake sample training collection in the targeted years. The samples training collection designed into six classes, and the method of sample training taking are used the polygon tool with pixel size about +/-5. Every class contained the samples of about 75-80. And the total samples approximately 480-500 per annual.
4. The training samples have been collected. That sample is Zipped to upload to the GEE's assets using Upload a new shapefile asset tool and import it to the entry of GEE's APIs.
5. Filtering the date and machine learning classifiers selected, hit Run (Ctrl+Enter) to find classification results see in figure 5 **(**GEE performed by Machine Learning of Random Forest in 1989, Vientiane, Laos)

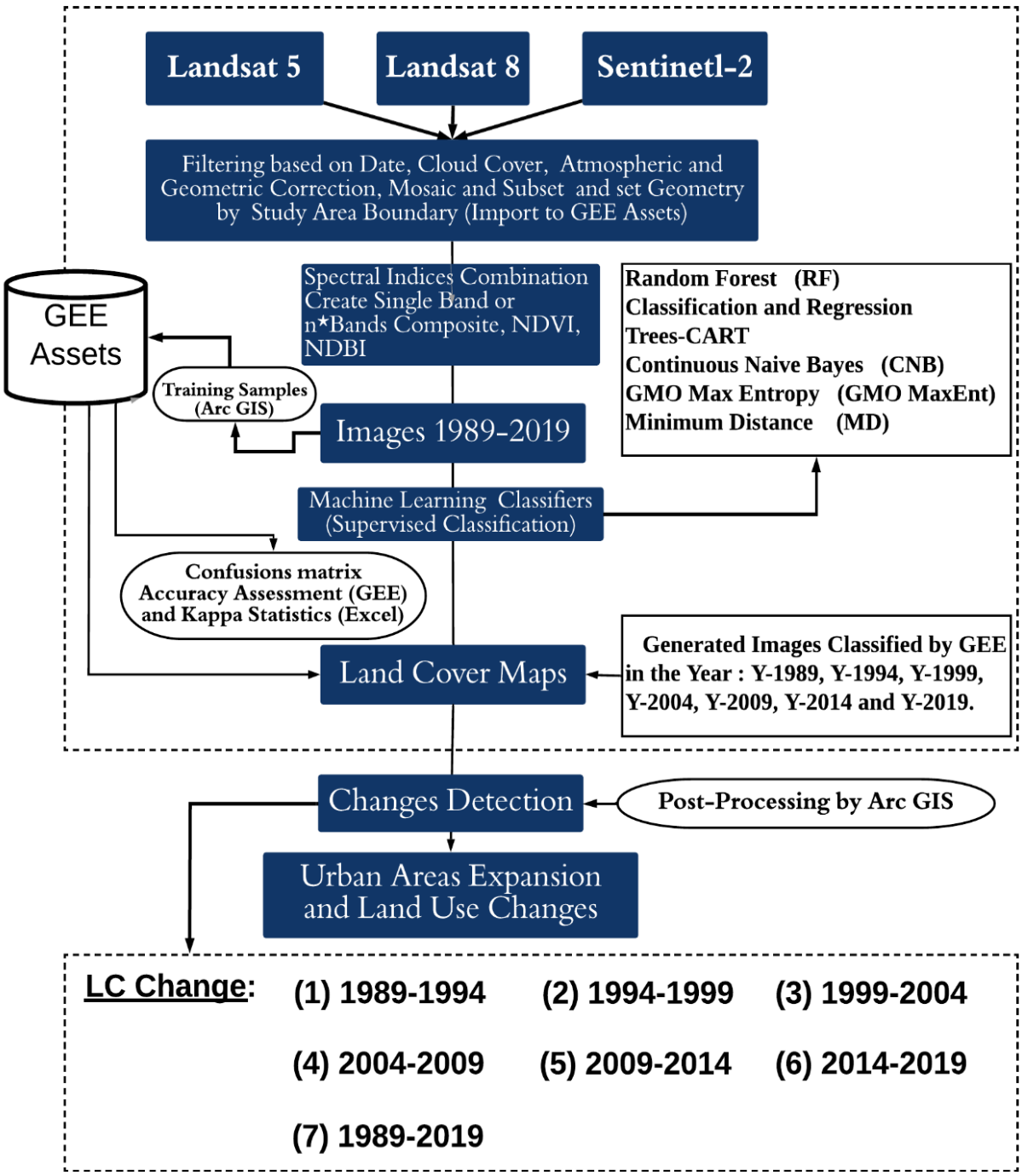

Figure 13 Overall Steps of the proposed method for Land Use Changes and urban extraction

3.5 Classification Accuracy Assessment

The assessment of accuracy is a general terminology for comparing classification levels with real-world geographic data. It is assumed that it is correct to determine the classification process of an accuracy. Usually, the assumed-true data are derived from ground truth data. Evaluation quality of the experimental results is achieved by automatically extracted on GEE that obtained urban classification. Once the manual accuracy assessment is performed in Post-processing Overall Accuracy and Kappa coefficient, the classification feature classes and amount of number changing with six categories will be calculated to find the land cover is increased or decreased during the study period. Then Accuracies such as Producer Accuracy, User Accuracy, and Overall Accuracy is calculated respectively following by the number of Kappa coefficient.

$$Overal\ Accuracy\ (\mathrm{OA}) = \frac{\text{Number of correctly classified site}}{total\ number\ of\ reference\ sites} * 100 \ldots\ldots\ldots\ldots (6)$$

$$Producer\ Accuracy = \frac{Number\ of\ reference\ from\ feature\ class}{Total\ number\ of\ All\ Class} * 100 \ldots\ldots (7)$$

$$User\ Accuracy = \frac{Number\ of\ reference\ from\ feature\ class}{Total\ number\ of\ feature\ class} * 100 \ldots\ldots\ldots\ldots (8)$$

$$Kappa = \frac{N \sum_{i=1}^{r} * x_{ii} - \sum_{i=1}^{r} (x_{i+} * x_{+i})}{N^2 - \sum_{i=1}^{r} (x_{i+} * x_{+i})} \ldots\ldots\ldots\ldots\ldots\ldots\ldots\ldots\ldots\ldots\ldots\ldots\ldots\ldots\ldots\ldots\ldots\ldots (9)$$

$$Kap = \frac{Total * Sum\ of\ Correct - Sum\ of\ the\ All\ the\ (Row\ total * Column\ total)}{total\ squared - Sum\ of\ the\ All\ the\ (Row\ total * Column\ total)}$$

where:
r = number of rows in matrix error
xii = number of observations in row I and column i
xi+ = total number of observations in row i
x+i = total number of observations in column i
N = total number of observations included in matrix

มหาวิทยาลัยบูรพา
BURAPHA UNIVERSITY

CHAPTER 4
EXPERIMENTS AND RESULTS

The analysis of the results is divided into three parts to answer three research questions. The first one is to reach the precise and high effectiveness of land cover map extraction and enable it to use for urban planning. The second one is using cloud computing platforms such as Big data and GEE to perform with fast and useful tools, and the third one is evaluating the machine learning algorithms and find out the one performed the best with high accuracy.

4.1 Urban and Land Cover Extraction Applied with Difference Satellite

The classification experiment of land cover in this research is based on the data training and performed by using GEE. This approach is aimed to detect urban expansion changes and land cover using time-series satellite imageries from 1989-2019. Since the Image from Landsat 5 is available from 1984-2013, Landsat 8 is available from 2013-Present, and Sentinel-2 is available from 2015 to present as well; this study is no ground-truth observation. Thus, the images covered for 30-Year of the study period has calculated the accuracy via thematic map classified by GEE. The research using Automatic Machine Learning Classifiers, and they are categorized into 6 Classes such as Agriculture, Bareland, Built-Up Area (Urban), Mixed Deciduous Forest, Evergreen Forest, and Water Bodies. All experiments implemented via GEE cloud-based platform since 1989, 1994, 1999, 2004, 2009 (Landsat 5), the Year 2014, 2019 (Landsat8), and only for Sentinel-2 study only in 2019 due to the Sentinel-2 is available only from 2017.

4.2 Experiment by Automatic Machine Learning Classifiers

the Machine Learning are included for 5 Machine Classifiers such as Random Forest (RF-1), Classification and Regression Trees (CART-2), Continuous Naïve Bayes (CNB-3), GMO Max Entropy (GMO-4), Minimum Distance (MD-5) to be used for extracting the land cover changes and its features as in the following analysis results given by Random Forest from 1989-2019 (every 5-year interval) as following:

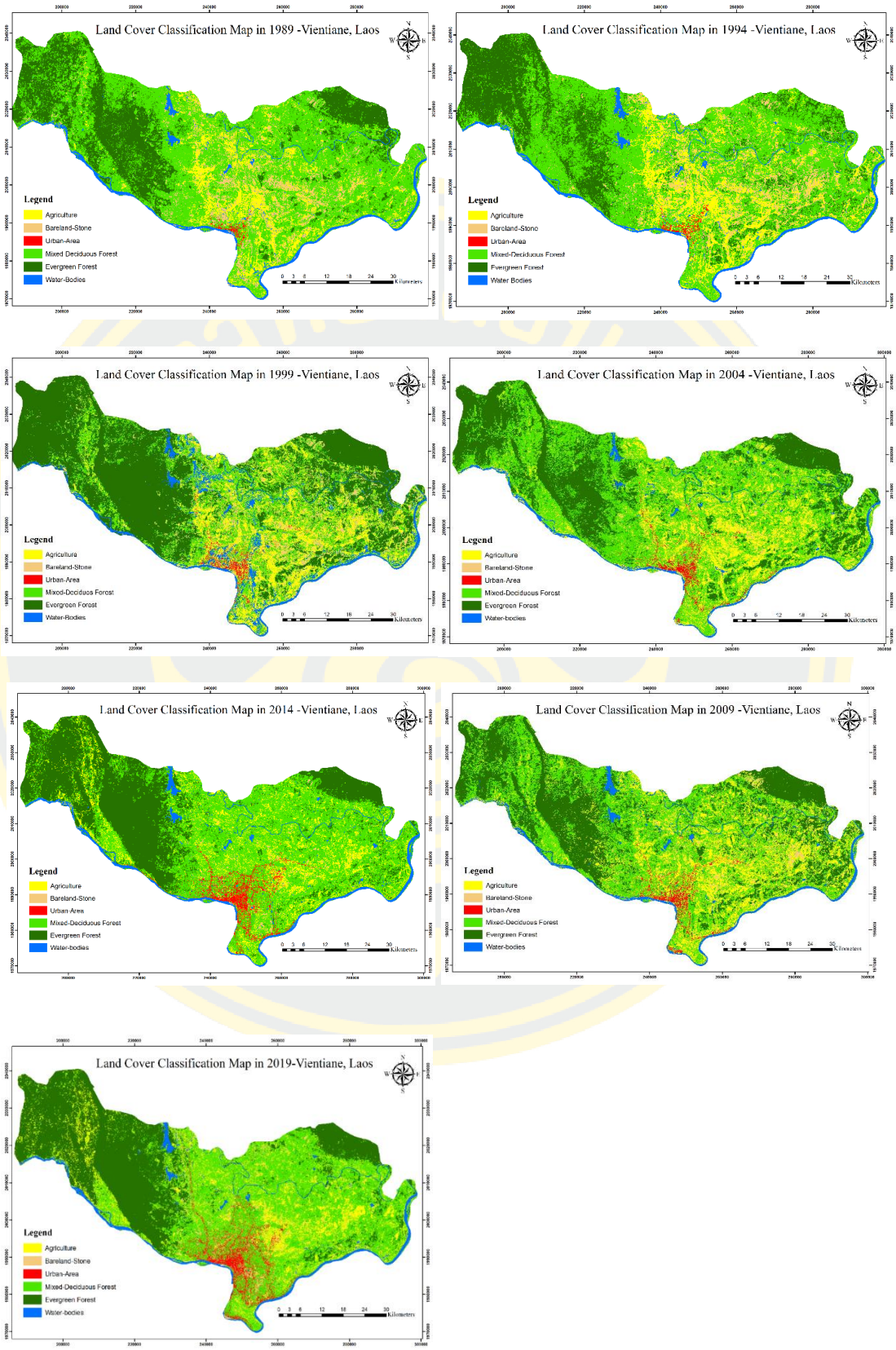

Figure 14 Land Cover Map of Vientiane in 1989- 2019 performed by ML Classifier of Random Forest with Landsat 5, Landsat 8 and Sentinel-2

4.2.1 Classification Using Random Forest

Random Forest ‘s Result performed under Machine Learning, which operated in every ten years such in 1889,1999, 2009, 2019 and for 2019 is produced within two kinds of Satellite such as Landsat8 and Sentinel-2 with details of Confusion Matrix and Percentage of performance in each class (see table below):

Table 5 Confusion Matrix of Reference Points for Random Forest in 1989

LC-Classification Classes	**Agr**	**Bare L**	**Urb**	**MDF**	**EVGF**	**WB**	**Gr-Total**
Agriculture	**287**	7	8	1	0	0	**303**
Bare Land	2	**173**	2	26	0	0	**203**
Urban (Built-Up Area)	4	0	**70**	7	0	0	**81**
Mixed Deciduous Forest	2	5	1	**403**	12	0	**423**
Evergreen Forest	0	0	0	7	**153**	0	**160**
Water Bodies	0	1	0	0	0	**58**	**59**
Total	**295**	**186**	**81**	**444**	**165**	**58**	**1229/1144**

$$Overall\ Accuracy\ (OA) = \frac{Number\ of\ correctly\ classified\ site}{total\ number\ of\ reference\ sites} * 100$$

Overall Accuracy = 93.08 %

$$Kap = \frac{Total * Sum\ of\ Correct - Sum\ of\ the\ All\ the\ (Row\ total * Column\ total)}{total\ squared - Sum\ of\ the\ All\ the\ (Row\ total * Column\ total)}$$

Kappa coefficient = 0.90

Table 6 Percentage of LC Accuracies and Kappa Performed by RF in 1989(L5)

Land Cover Classes	**Producer Accuracy (%)**	**User Accuracy (%)**
Agriculture	94.71	97.28
Bare Land	85.22	93.01
Urban-Built-Up Area	86.41	86.41
Mixed Deciduous Forest	95.27	90.76
Evergreen Forest	95.62	92.72
Water Bodies	98.30	100
Overall Accuracy (%)		**93.08**
Kappa coefficient		**0.90**

Table 7 Percentage of LC Accuracies and Kappa Performed by RF in 1999(L5)

Land Cover Classes	Producer Accuracy (%)	User Accuracy (%)
Agriculture	83.98	83.98
Bare Land	84.94	86.81
Urban-Built-Up	77.31	77.31
Mixed Deciduous Forest	87.79	87.79
Evergreen Forest	99.45	99.45
Water Bodies	98.59	98.59
Overall Accuracy (%)		**90.67**
Kappa coefficient		**0.88**

Table 8 Percentage of LC Accuracies and Kappa Performed by RF in 2009(L5)

Land Cover Classes	Producer Accuracy (%)	User Accuracy (%)
Agriculture	84.56	86.89
Bare Land	86.99	80.45
Urban-Built-Up	88.95	90.06
Mixed Deciduous Forest	89.08	89.31
Evergreen Forest	97.09	96.04
Water Bodies	99.34	100
Overall Accuracy (%)		**90.44**
Kappa coefficient		**0.90**

Table 9 Percentage of LC Accuracies and Kappa Performed by RF in 2019(L8)

Land Cover Classes	Producer Accuracy (%)	User Accuracy (%)
Agriculture	81.72	83.97
Bare Land	79.24	81.55
Urban-Built-Up	86.09	86.66
Mixed Deciduous Forest	91.34	90.72
Evergreen Forest	93.53	91.44
Water Bodies	98.61	100
Overall Accuracy (%)		**89.31**
Kappa coefficient		**0.89**

Table 10 Percentage of LC Accuracies and Kappa Performed by RF in 2019(S2)

Land Cover Classes	Producer Accuracy (%)	User Accuracy (%)
Agriculture	94.43	94.21
Bare Land	96.52	96.72
Urban-Built-Up	95.36	91.13
Mixed Deciduous Forest	95.96	94.00
Evergreen Forest	90.11	97.09
Water Bodies	99.18	100
Overall Accuracy (%)		**95.08**
Kappa coefficient		**0.67**

4.2.2 Classification Using Classification and Regression Trees

Table 11 Confusion Matrix of Reference Points for CART in 1989

LC-Classification Classes	Agr	Bare L	Urb	MDF	EVGF	WB	Gr-Total
Agriculture	**410**	0	1	6	1	0	**418**
Bare Land	3	**130**	0	9	6	0	**148**
Urban (Built-Up Area)	1	0	**115**	1	0	0	**117**
Mixed Deciduous Forest	4	0	0	**456**	46	0	**506**
Evergreen Forest	0	0	0	25	**363**	0	**388**
Water Bodies	0	0	0	0	0	**184**	**184**
Total	**418**	**130**	**116**	**497**	**416**	**184**	**1761/1658**

$$Overall\ Accuracy\ (OA) = \frac{Number\ of\ correctly\ classified\ site}{total\ number\ of\ reference\ sites} * 100$$

Overall Accuracy = 94.15 %

$$Kap = \frac{Total * Sum\ of\ Correct - Sum\ of\ the\ All\ the\ (Row\ total * Column\ total)}{total\ squared - Sum\ of\ the\ All\ the\ (Row\ total * Column\ total)}$$

Kappa coefficient = 0.87

Table 12 Percentage of LC Accuracies and Kappa Performed by CART in 1989(L5)

Land Cover Classes	Producer Accuracy (%)	User Accuracy (%)
Agriculture	98.08	98.08
Bare Land	87.83	100
Urban-Built-Up	98.29	99.13
Mixed Deciduous Forest	90.11	91.75
Evergreen Forest	93.55	87.25
Water Bodies	100	100
Overall Accuracy (%)		**94.15**
Kappa coefficient		**0.87**

Table 13 Percentage of LC Accuracies and Kappa Performed by CART in 2019(L8)

Land Cover Classes	Producer Accuracy (%)	User Accuracy (%)
Agriculture	78.49	100
Bare Land	98.11	100
Urban-Built-Up	94.03	95.94
Mixed Deciduous Forest	99.32	91.54
Evergreen Forest	98.09	100
Water Bodies	100	100

Overall Accuracy (%)	**95.61**
Kappa coefficient	**0.89**

Table 14 Percentage of LC Accuracies and Kappa Performed by CART in 2019(S2)

Land Cover Classes	**Producer Accuracy (%)**	**User Accuracy (%)**
Agriculture	87.09	95.85
Bare Land	98.11	99.04
Urban-Built-Up	98.01	96.73
Mixed Deciduous Forest	98.13	93.98
Evergreen Forest	96.19	100
Water Bodies	100	100
Overall Accuracy (%)		**96.34**
Kappa coefficient		**0.89**

4.2.3 Classification Using Continuous Naïve Bayes

Table 15 Confusion Matrix of Reference Points for CNB in 1989

LC-Classification Classes	**Agr**	**Bare L**	**Urb**	**MDF**	**EVGF**	**WB**	**Gr-Total**
Agriculture	**275**	25	2	1	0	0	**303**
Bare Land	22	**146**	0	15	0	0	**183**
Urban (Built-Up Area)	14	18	**48**	1	0	0	**81**
Mixed Deciduous Forest	1	21	4	**374**	23	0	**423**
Evergreen Forest	0	0	0	6	**154**	0	**160**
Water Bodies	0	0	1	0	0	**58**	**59**
Total	**312**	**210**	**55**	**397**	**177**	**58**	**1209/1055**

$$Overall\ Accuracy\ (OA) = \frac{Number\ of\ correctly\ classified\ site}{total\ number\ of\ reference\ sites} * 100$$

Overall Accuracy = 87.26 %

$$Kap = \frac{Total * Sum\ of\ Correct - Sum\ of\ the\ All\ the\ (Row\ total * Column\ total)}{total\ squared - Sum\ of\ the\ All\ the\ (Row\ total * Column\ total)}$$

Kappa coefficient = 0.91

Table 16 Percentage of LC Accuracies and Kappa Performed by CNB in 1989(L5)

Land Cover Classes	**Producer Accuracy (%)**	**User Accuracy (%)**
Agriculture	90.75	88.14
Bare Land	79.78	69.52
Urban-Built-Up	59.25	87.27
Mixed Deciduous Forest	88.41	94.20
Evergreen Forest	96.25	87.00

Water Bodies	98.30	100
Overall Accuracy (%)		**87.26**
Kappa coefficient		**0.91**

Table 17 Percentage of LC Accuracies and Kappa Performed by CNB in 2019(L8)

Land Cover Classes	**Producer Accuracy (%)**	**User Accuracy (%)**
Agriculture	76.34	55.25
Bare Land	61.32	65.00
Urban-Built-Up	69.53	78.35
Mixed Deciduous Forest	74.87	85.13
Evergreen Forest	95.43	87.45
Water Bodies	98.61	100
Overall Accuracy (%)		**78.63**
Kappa coefficient		**0.90**

Table 18 Percentage of LC Accuracies and Kappa Performed by CNB in 2019(S2)

Land Cover Classes	**Producer Accuracy (%)**	**User Accuracy (%)**
Agriculture	91.87	81.14
Bare Land	90.59	93.85
Urban-Built-Up	85.56	90.21
Mixed Deciduous Forest	86.32	96.50
Evergreen Forest	98.50	85.23
Water Bodies	99.18	100
Overall Accuracy (%)		**90.59**
Kappa coefficient		**0.71**

4.2.4 Classification Using GMO Max Entropy

Table 19 Confusion Matrix of Reference Points for GMO in 1989

LC-Classification Classes	**Agr**	**Bare L**	**Urb**	**MDF**	**EVGF**	**WB**	**Gr-Total**
Agriculture	**258**	35	0	10	0	0	**303**
Bare Land	46	**125**	0	12	0	0	**183**
Urban (Built-Up Area)	18	45	**0**	18	0	0	**81**
Mixed Deciduous Forest	1	4	0	**400**	18	0	**423**
Evergreen Forest	0	0	0	89	**71**	0	**160**
Water Bodies	0	0	1	0	0	**58**	**59**
Total	**323**	**209**	**1**	**529**	**89**	**58**	**1209/912**

$$Overall\ Accuracy\ (OA) = \frac{Number\ of\ correctly\ classified\ site}{total\ number\ of\ reference\ sites} * 100$$

Overall Accuracy = 75.43 %

$$Kap = \frac{Total * Sum\ of\ Correct - Sum\ of\ the\ All\ the\ (Row\ total * Column\ total)}{total\ squared - Sum\ of\ the\ All\ the\ (Row\ total * Column\ total)}$$

Kappa coefficient = 0.66

Table 20 Percentage of LC Accuracies and Kappa Performed by GMO in 1989(L5)

Land Cover Classes	**Producer Accuracy (%)**	**User Accuracy (%)**
Agriculture	85.14	79.87
Bare Land	68.30	59.80
Urban-Built-Up	0	0
Mixed Deciduous Forest	94.56	75.61
Evergreen Forest	44.37	79.77
Water Bodies	98.30	100
Overall Accuracy (%)		**75.43**
Kappa coefficient		**0.66**

Table 21 Percentage of LC Accuracies and Kappa Performed by GMO in 2019(L8)

Land Cover Classes	**Producer Accuracy (%)**	**User Accuracy (%)**
Agriculture	0	NA
Bare Land	0	NA
Urban-Built-Up	43.04	40.12
Mixed Deciduous Forest	98.81	63.74
Evergreen Forest	77.94	70.20
Water Bodies	0	0
Overall Accuracy (%)		**62.32**
Kappa coefficient		**0.42**

Table 22 Percentage of LC Accuracies and Kappa Performed by GMO in 2019(S2)

Land Cover Classes	**Producer Accuracy (%)**	**User Accuracy (%)**
Agriculture	70.96	78.57
Bare Land	41.50	59.45
Urban-Built-Up	80.13	74.23
Mixed Deciduous Forest	87.94	80.43
Evergreen Forest	87.07	92.33
Water Bodies	97.22	100
Overall Accuracy (%)		**81.49**
Kappa coefficient		**0.74**

4.2.5 Classification Using Minimum Distance

Table 23 Confusion Matrix of Reference Points for Minimum Distance in 1989

LC-Classification Classes	Agr	Bare L	Urb	MDF	EVGF	WB	Gr-Total
Agriculture	**101**	5	7	0	0	0	**113**
Bare Land	19	**50**	16	1	0	0	**86**
Urban (Built-Up Area)	1	3	**22**	4	0	0	**30**
Mixed Deciduous Forest	0	4	14	**118**	39	0	**175**
Evergreen Forest	0	0	0	0	**64**	0	**64**
Water Bodies	0	0	1	0	0	**26**	**27**
Total	**121**	**62**	**60**	**123**	**103**	**26**	**495/381**

$$Overall\ Accuracy\ (OA) = \frac{Number\ of\ correctly\ classified\ site}{total\ number\ of\ reference\ sites} * 100$$

Overall Accuracy = 76.96 %

$$Kap = \frac{Total * Sum\ of\ Correct - Sum\ of\ the\ All\ the\ (Row\ total * Column\ total)}{total\ squared - Sum\ of\ the\ All\ the\ (Row\ total * Column\ total)}$$

Kappa coefficient = 0.71

Table 24 Percentage of LC Accuracies and Kappa Performed by MD in 1989(L5)

Land Cover Classes	Producer Accuracy (%)	User Accuracy (%)
Agriculture	89.38	83.47
Bare Land	58.13	80.64
Urban-Built-Up	73.33	36.66
Mixed Deciduous Forest	67.42	95.93
Evergreen Forest	100	62.13
Water Bodies	96.29	100
Overall Accuracy (%)		**76.96**
Kappa coefficient		**0.71**

Table 25 Percentage of LC Accuracies and Kappa Performed by MD in 2019(L8)

Land Cover Classes	Producer Accuracy (%)	User Accuracy (%)
Agriculture	20.43	19.09
Bare Land	11.32	11.53
Urban-Built-Up	69.53	41.66
Mixed Deciduous Forest	58.06	76.00
Evergreen Forest	44.48	61.25
Water Bodies	66.66	28.07
Overall Accuracy (%)		**48.42**
Kappa coefficient		**0.33**

Table 26 Percentage of LC Accuracies and Kappa Performed by MD in 2019(S2)

Land Cover Classes	Producer Accuracy (%)	User Accuracy (%)
Agriculture	27.14 %	43.65 %
Bare Land	84.04 %	67.15 %
Urban-Built-Up	80.92 %	88.70 %
Mixed Deciduous Forest	77.21 %	82.01 %
Evergreen Forest	98.80 %	75.51 %
Water Bodies	99.18 %	100 %
Overall Accuracy		73.95 %
Kappa coefficient		0.66

4.3 Comparison of Machine Learning Classifiers

The classifiers performed by GEE is an achievement on a different scale. The best classifier with the highest accuracy performed in 2019 with an image from Sentinel-2 is CART) with an overall accuracy of 96.34% (Kappa coefficient 0.95), While the other classifiers performed a bit low. RF's overall accuracy of 95.08% (Kappa coefficient 0.93), CNB's 90.59% (Kappa coefficient 0.88), GMO's 81.49% (Kappa coefficient 0.74), MD's 73.95% (Kappa coefficient 0.66).

Theoretically, RF receives higher accuracy than CART. When we use this classifier through software, due to the developers from Google Earth Engine, they developed the machine's learning algorithm via the cloud computing platform. Fighting The top things that give us high accuracy are CART, which has higher accuracy than RF, CNB, GMO, and MD. We have used five types of machine classification tools with three satellites, such as Landsat 5, Landsat 8, and Sentinel-2. After the experiment. CART is higher than the others. See below table took the experiment in detail.

Table 27 Overall Accuracy and Kappa for each Machine Learning by Landsat5 in 1989

Classifiers Operating (Landsat5, 1989)	**Overall Accuracy (%)**	**Kappa coefficient**
Random Forest (RF)	93.08	0.90
Classification and Regression Trees	94.15	0.87
Continuous Naïve Bayes (CNB)	87.26	0.91
GMO Max Entropy (GMO)	75.43	0.66
Minimum Distance (MD)	76.96	0.71

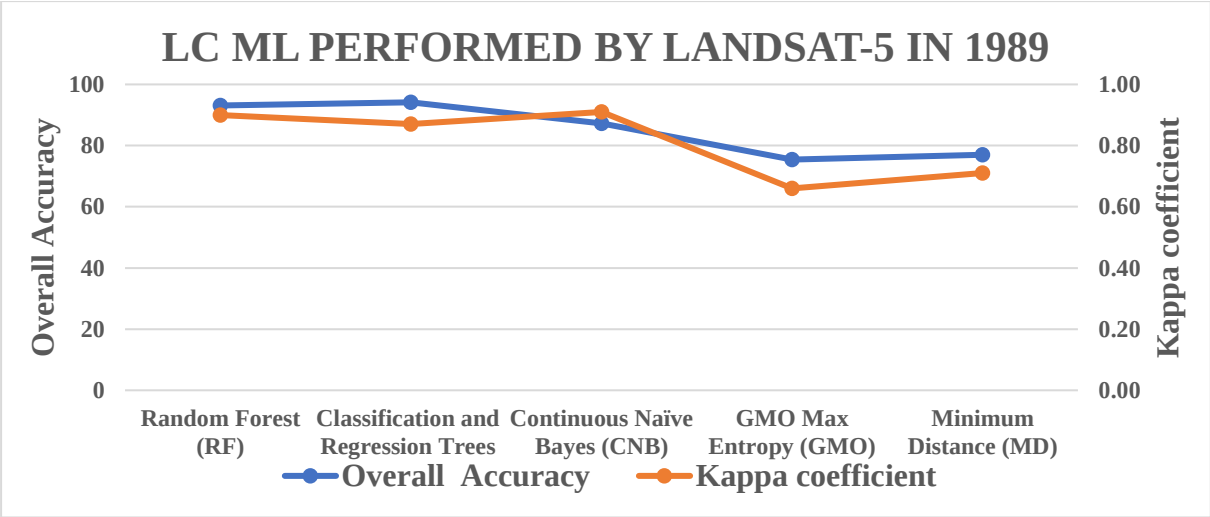

Figure 15 Accuracy and Kappa with different ML Classifiers in 1989 (L5)

Table 28 Overall Accuracy and Kappa for each Machine Learning by Landsat8 in 2019

Classifiers Operating (Landsat8, 2019)	**Overall Accuracy (%)**	**Kappa coefficient**
Random Forest (RF)	89.31	0.85
Classification and Regression Trees	95.61	0.93
Continuous Naïve Bayes (CNB)	78.63	0.71
GMO Max Entropy (GMO)	62.32	0.42
Minimum Distance (MD)	48.42	0.33

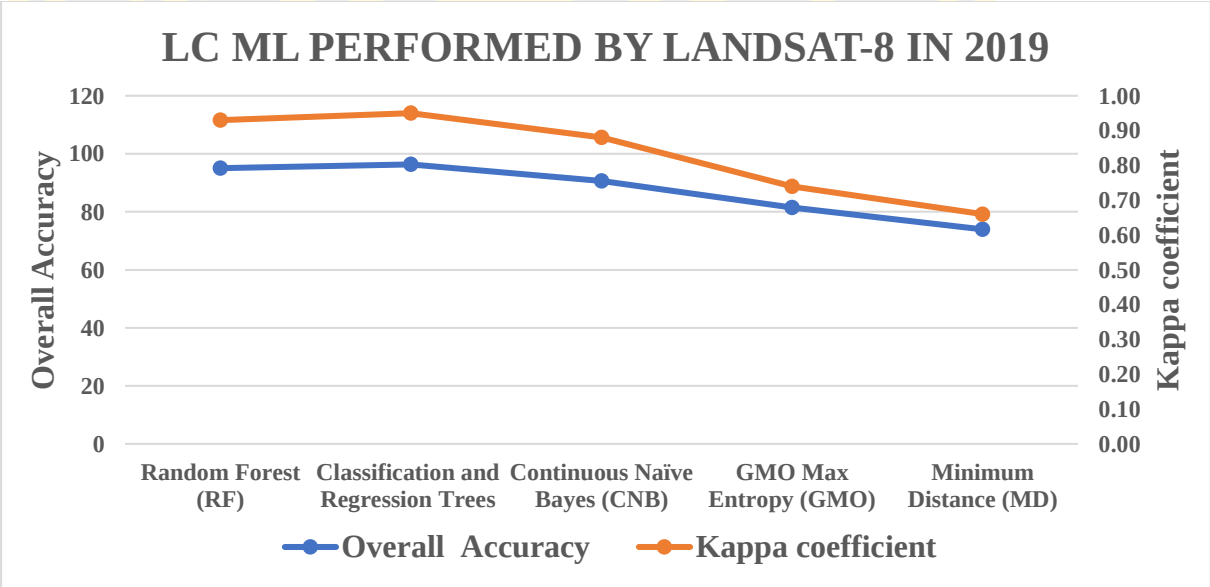

Figure 16 Overall Accuracy and Kappa of different ML Classifiers in 2019 (L8)

Table 29 Overall Accuracy and Kappa for each Machine Learning by Sentinel-2 in 2019

Classifiers Operating (Sentinel-2, 2019)	**Overall Accuracy-%**	**Kappa coefficient**
Random Forest (RF)	95.08	0.93
Classification and Regression Trees	96.34	0.95
Continuous Naïve Bayes (CNB)	90.59	0.88
GMO Max Entropy (GMO)	81.49	0.74
Minimum Distance (MD)	73.95	0.66

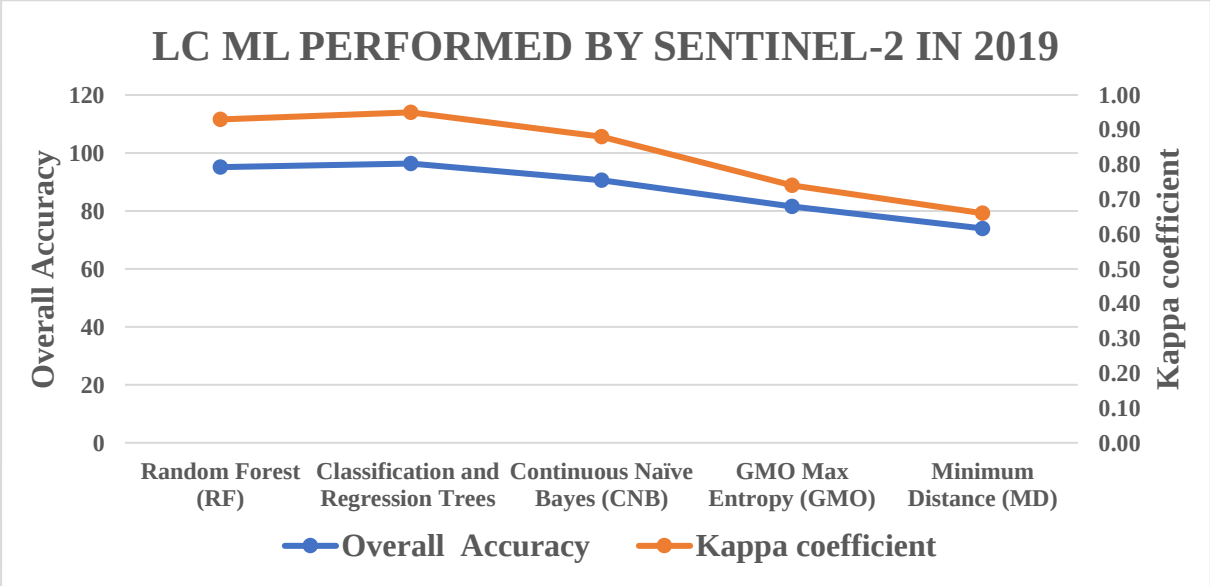

Figure 17 Overall Accuracy and Kappa of different ML Classifiers in 2019 (S2)

Table 30 Overall Accuracy performed by Random Forest for 1989-2019

ML-Random Forest performed from the Year 1989-2019	**Year Operation**	**Overall Accuracy (%)**	**Kappa coefficient**
	1989-Landsat-5	93.08	0.90
	1994-Landsat-5	94.10	0.88
	1999-Landsat-5	90.67	0.88
	2004-Landsat-5	92.20	0.90
	2009-Landsat-5	90.44	0.90
	2014-Landsat-8	91.66	0.89
	2019-Landsat-8	89.31	0.89
	2019-Sentinel-2	95.08	0.93

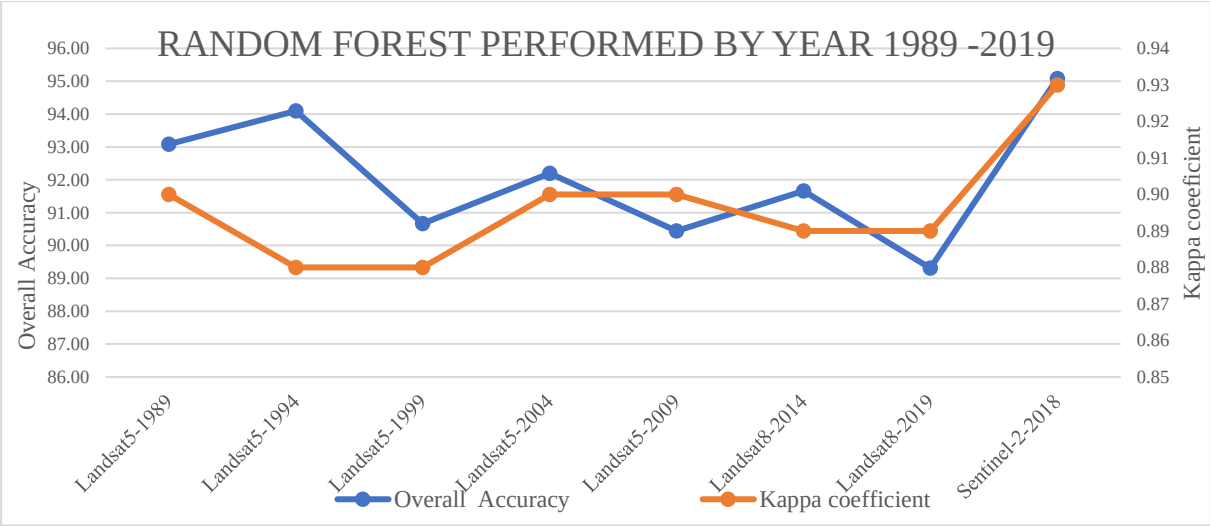

Figure 18 Overall Accuracy and Kappa of primary classifier RF from 1989- 2019

Table 31Overall Accuracy performed by Landsat-8 and Sentinel-2 in 2019

Machine Learning Classifiers	**OA for Landsat-8**	**OA for Sentinel-2**
Random Forest (RF)	89.31	95.08
Classification and Regression Trees (CART)	95.61	96.34
Continuous Naïve Bayes (CNB)	78.63	90.59
GMO Max Entropy (GMO)	62.32	81.49
Minimum Distance (MD)	48.42	73.95

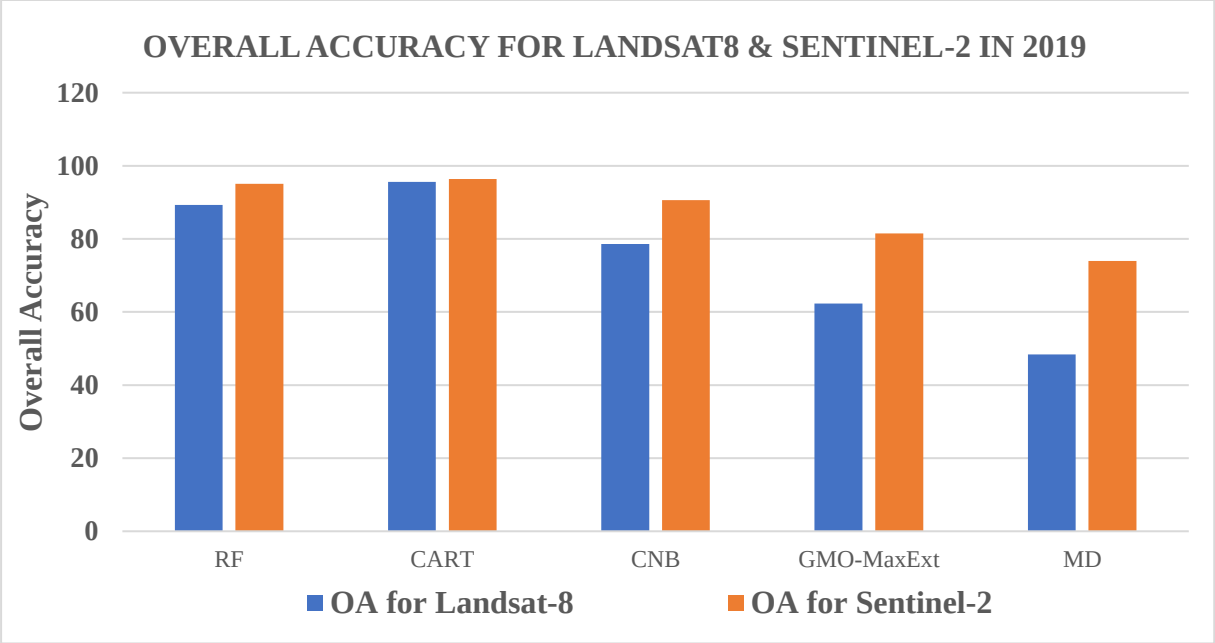

Figure 19 Overall Accuracy of Different ML Classifiers by Landsat-8 and Sentinel-2 in 2019

Table 32 Kappa coefficient performed by Landsat-8 and Sentinel-2 in 2019

Machine Learning Classifiers	Kappa for Landsat-8	Kappa for Sentinel-2
Random Forest (RF)	0.85	0.93
Classification and Regression Trees	0.93	0.95
Continuous Naïve Bayes (CNB)	0.71	0.88
GMO Max Entropy (GMO)	0.42	0.74
Minimum Distance (MD)	0.33	0.66

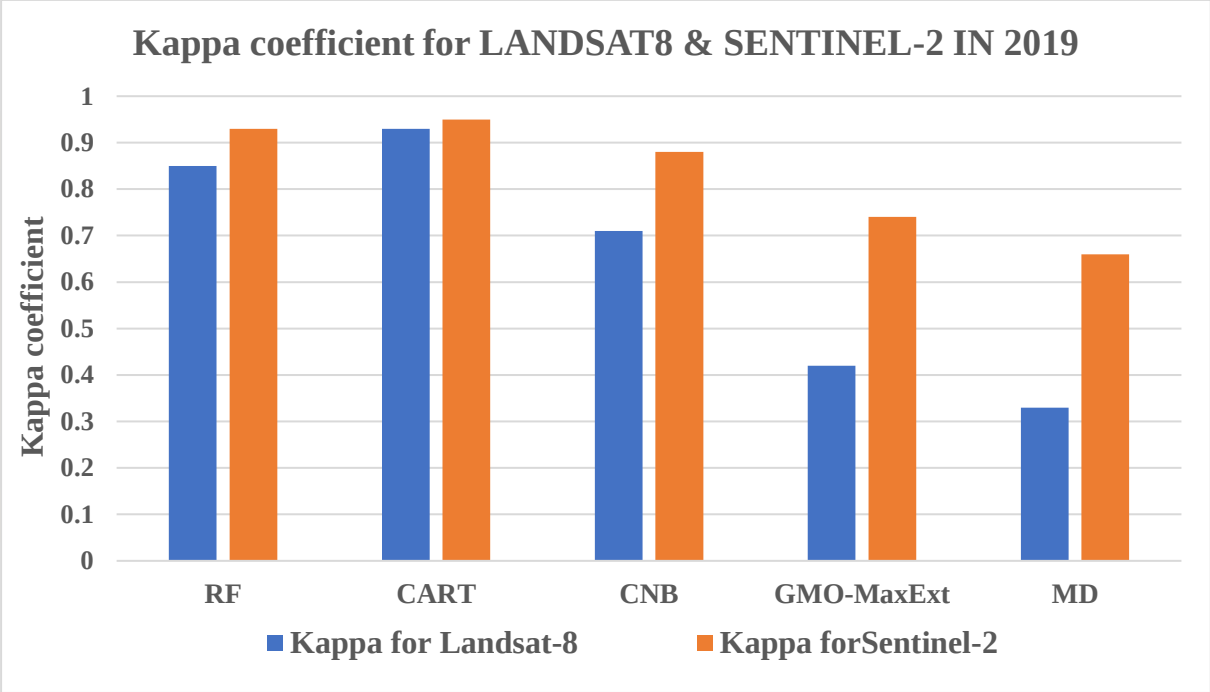

Figure 20 Kappa coefficient of Different ML Classifiers by Landsat-8 and Sentinel-2 in 2019

Table 33 Overall Acc and Kappa performed by All ML Classifiers with Landsat 5, Landsat 8, and Sentinel-2 during 1989-2019

Satellites	ML Classifiers Name	Year	Overall ACC	Kappa
Landsat 5	Random Forest	1989	93.08	0.90
Landsat 5	Smile Random Forest	1989	94.12	0.92
Landsat 5	Random Forest	1994	94.10	0.88
Landsat 5	Smile Random Forest	1994	93.92	0.88
Landsat 5	Random Forest	1999	90.67	0.88
Landsat 5	Smile Random Forest	1999	89.54	0.86
Landsat 5	Random Forest	2004	92.20	0.90
Landsat 5	Smile Random Forest	2004	90.18	0.90
Landsat 5	Random Forest	2009	90.44	0.88
Landsat 5	Smile Random Forest	2009	90.86	0.88
Landsat 8	Random Forest	2014	91.66	0.89

Landsat 8	Smile Random Forest	2014	92.09	0.89
Landsat 8	Random Forest	2019	89.31	0.85
Landsat 8	Smile Random Forest	2019	88.22	0.83
Sentinel-2	Random Forest	2019	95.08	0.93
Sentinel-2	Smile Random Forest	2019	94.18	0.92
Landsat 5	CART	1989	94.15	0.87
Landsat 5	CART	1999	94.41	0.92
Landsat 5	CART	2009	94.49	0.93
Landsat 8	CART	2019	95.61	0.93
Sentinel-2	CART	2019	96.34	0.95
Landsat 5	Continuous Naïve Bayes	1989	87.26	0.91
Landsat 5	Continuous Naïve Bayes	1999	82.29	0.77
Landsat 5	Continuous Naïve Bayes	2009	79.86	0.74
Landsat 8	Continuous Naïve Bayes	2019	78.63	0.71
Sentinel-2	Continuous Naïve Bayes	2019	90.59	0.88
Landsat 5	GMO Max Entropy	1989	75.43	0.66
Landsat 5	GMO Max Entropy	1999	70.09	0.60
Landsat 5	GMO Max Entropy	2009	80.13	0.74
Landsat 8	GMO Max Entropy	2019	62.32	0.42
Sentinel-2	GMO Max Entropy	2019	81.49	0.74
Landsat 5	Minimum Distance	1989	76.96	0.71
Landsat 5	Minimum Distance	1999	72.96	0.65
Landsat 5	Minimum Distance	2009	74.04	0.68
Landsat 8	Minimum Distance	2019	48.42	0.33
Sentinel-2	Minimum Distance	2019	73.95	0.66

4.4 Post-Classification of Land Cover Changes Detection

4.4.1 Classification Using Different ML Classifiers

They were using the selected sample training and automatic machine learning with classifiers proposed to provide us a different perspective. The classification of land cover has used the images from both Landsat 5 and Landsat 8, and Sentinel-2. The classification results for each classifier, such as RF, CART, CNB, GMO MaxEnt, and MD, shown in figure Figure 21, respectively. From a visual comparison, spatial patterns of land cover types are similar to the results in the whole classifiers set. The number of training sample and classification validation (including the Overall Accuracy and Kappa coefficient performed with Sentinel-2) for each classifier is given in Table 1. Accuracy measurements are adjusted according to the area of each layer (Classes), presented for CART came with the rank of the overall accuracy of 96.34% (Kappa coefficient 0.95). In contrast, other classifiers such as RF, CNB, GMO, and MD came second, third, fourth, and fifth rank with an overall accuracy of 95.08%, 90.59%,

81.49%, and 73.95% while Kappa coefficient values are 0.93, 0.88, 0.74 and 0.66. respectively.

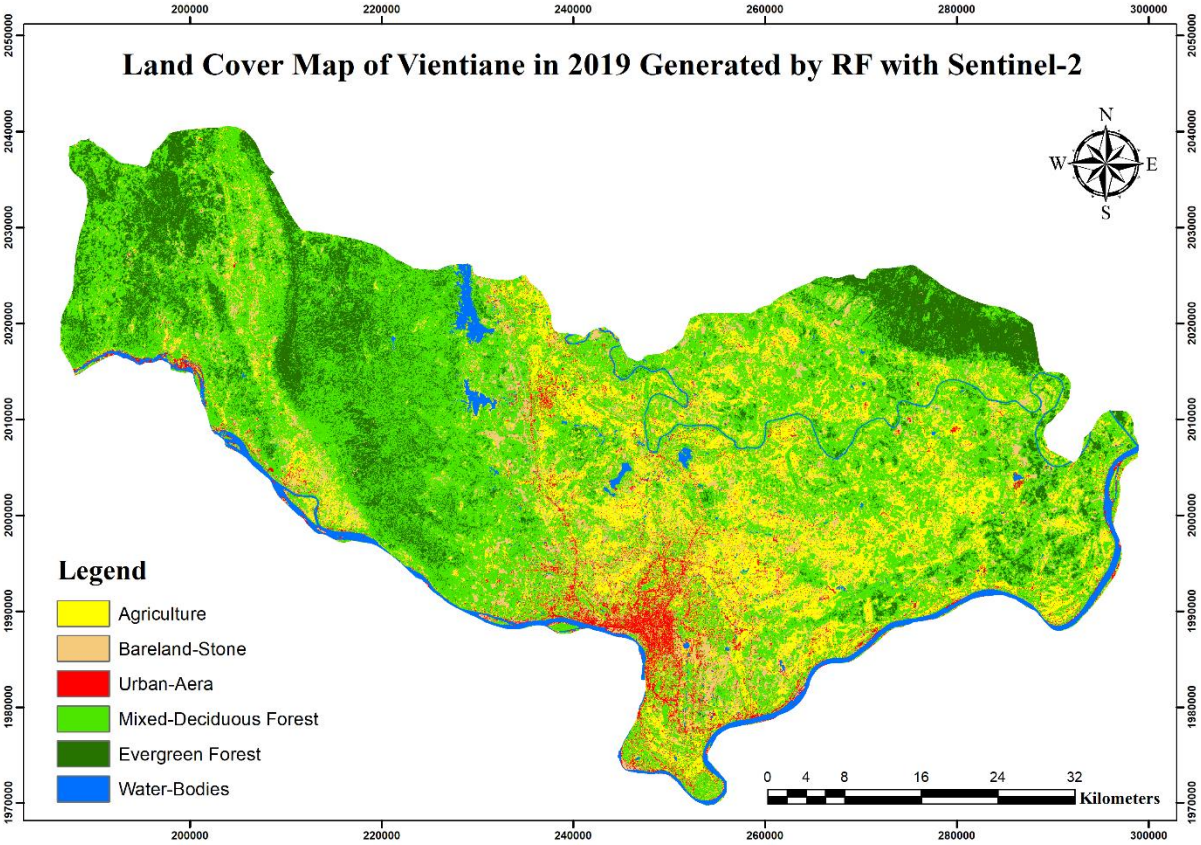

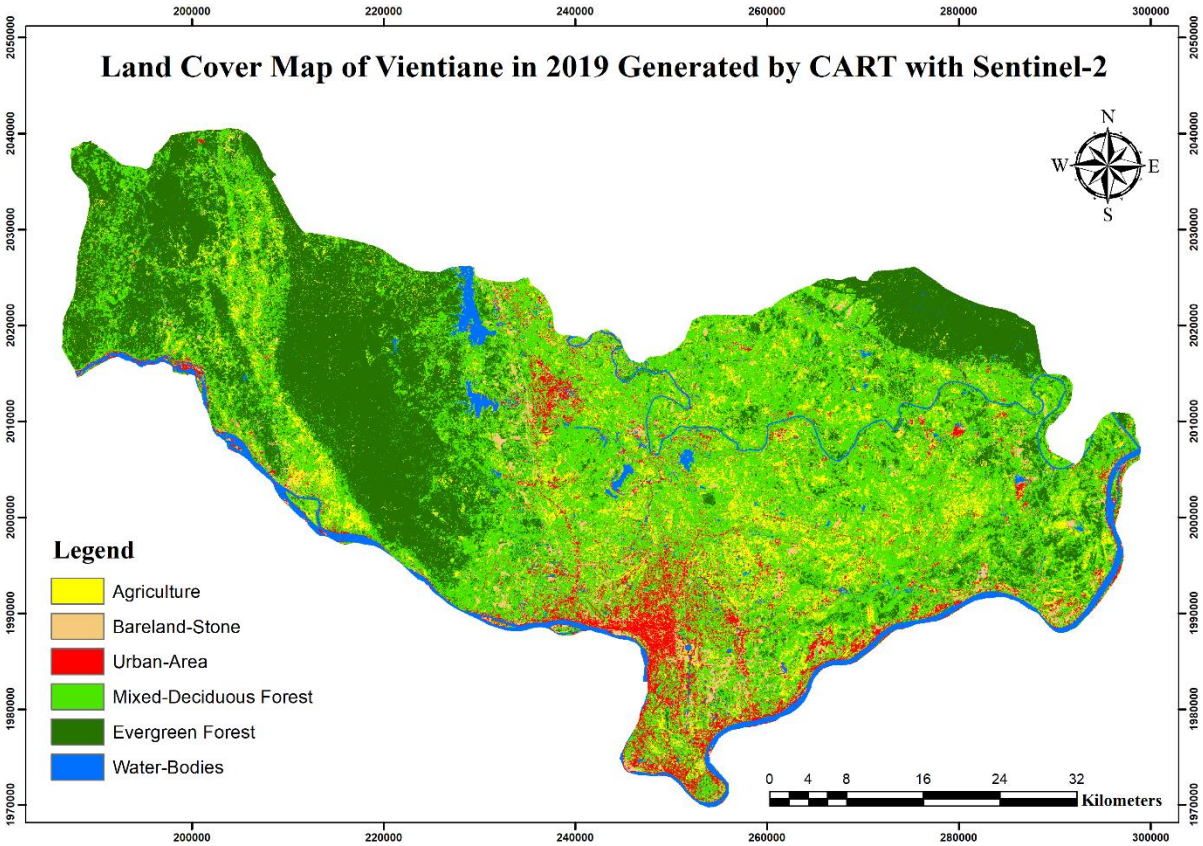
Land Cover Map of Vientiane in 2019 Generated by CART with Sentinel-2
N
W
E
S
Legend
Agriculture
Bareland-Stone
Urban-Area
Mixed-Deciduous Forest
Evergreen Forest
Water-Bodies
0 4 8 16 24 32
Kilometers
200000
220000
240000
260000
280000
300000
2050000
2040000
2030000
2020000
2010000
2000000
1990000
1980000
1970000

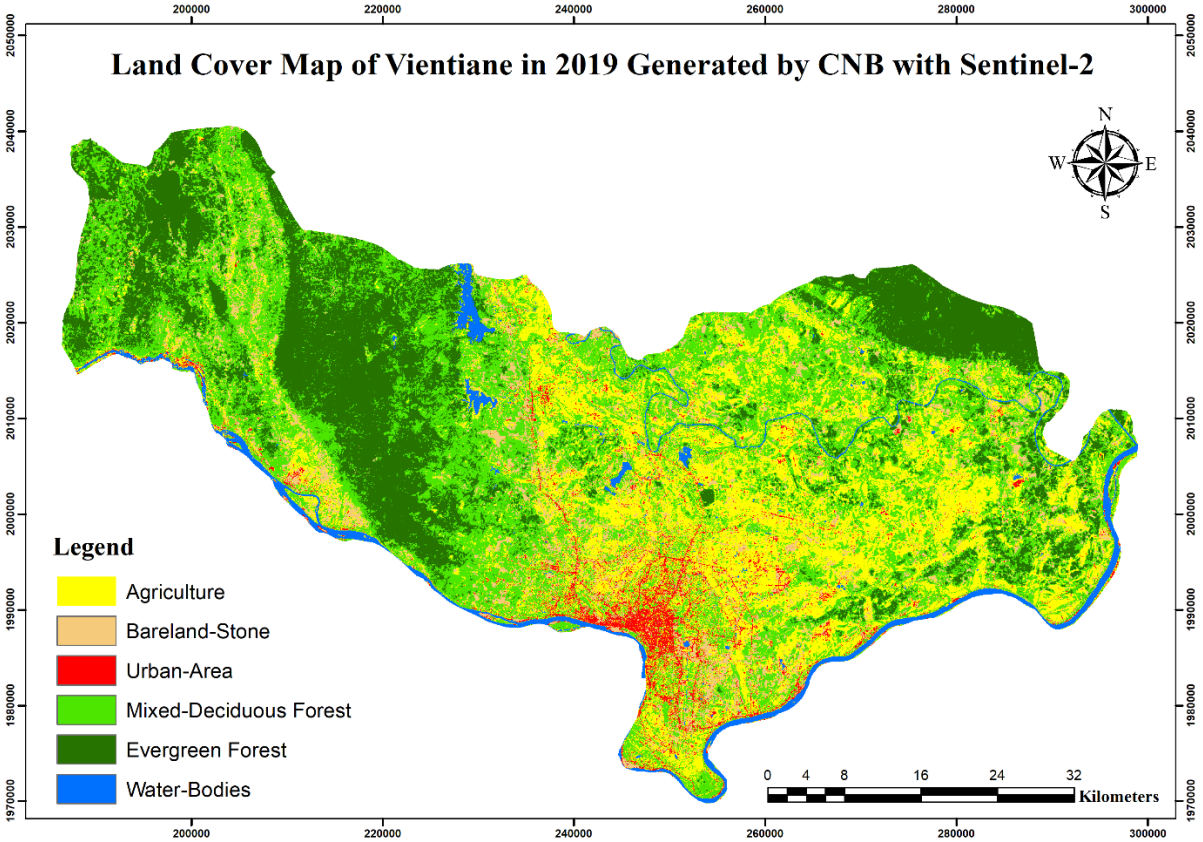
Land Cover Map of Vientiane in 2019 Generated by CNB with Sentinel-2
N
W
E
S
Legend
Agriculture
Bareland-Stone
Urban-Area
Mixed-Deciduous Forest
Evergreen Forest
Water-Bodies
0 4 8 16 24 32
Kilometers
200000
220000
240000
260000
280000
300000
2050000
2040000
2030000
2020000
2010000
2000000
1990000
1980000
1970000

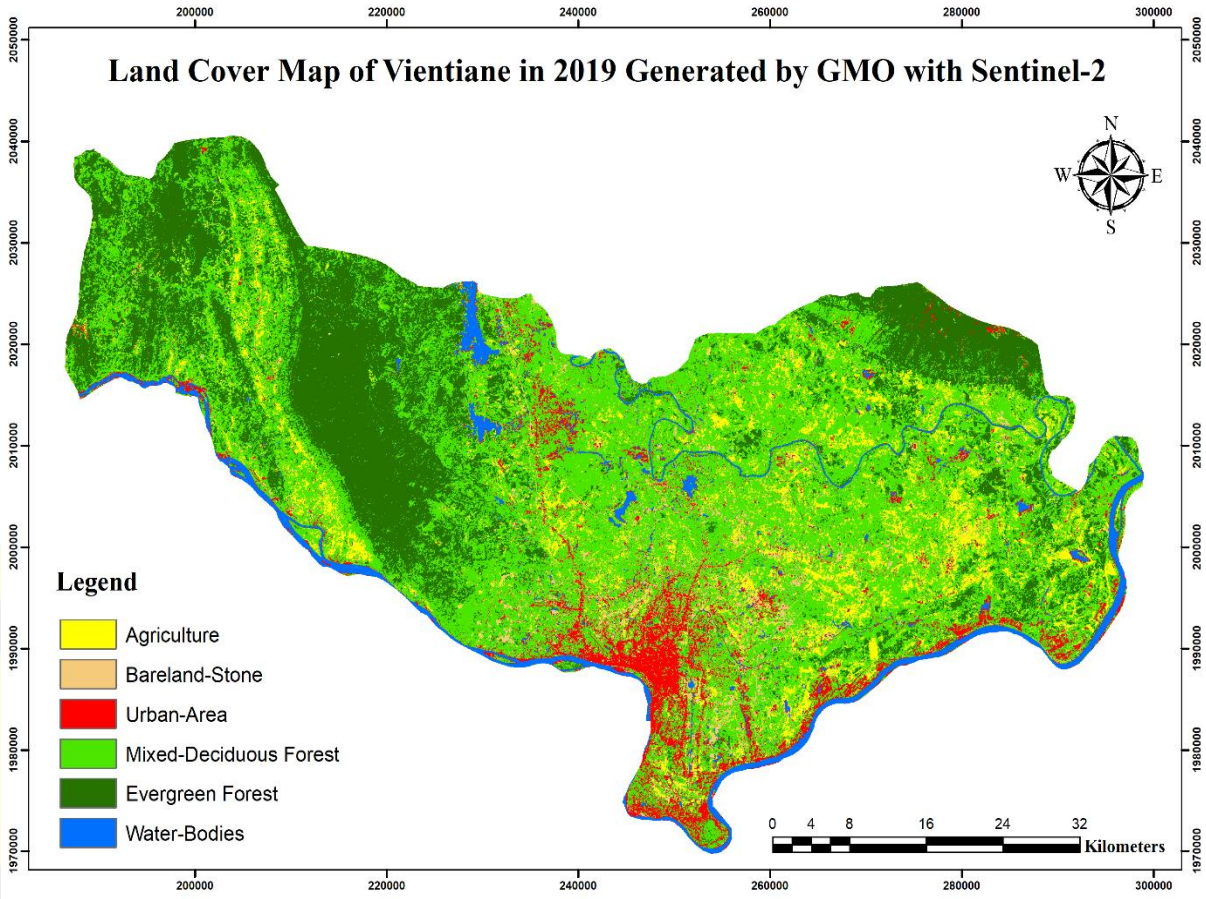
Land Cover Map of Vientiane in 2019 Generated by GMO with Sentinel-2
N
W
E
S
Legend
Agriculture
Bareland-Stone
Urban-Area
Mixed-Deciduous Forest
Evergreen Forest
Water-Bodies
0 4 8 16 24 32
Kilometers
200000
220000
240000
260000
280000
300000
2050000
2040000
2030000
2020000
2010000
2000000
1990000
1980000
1970000

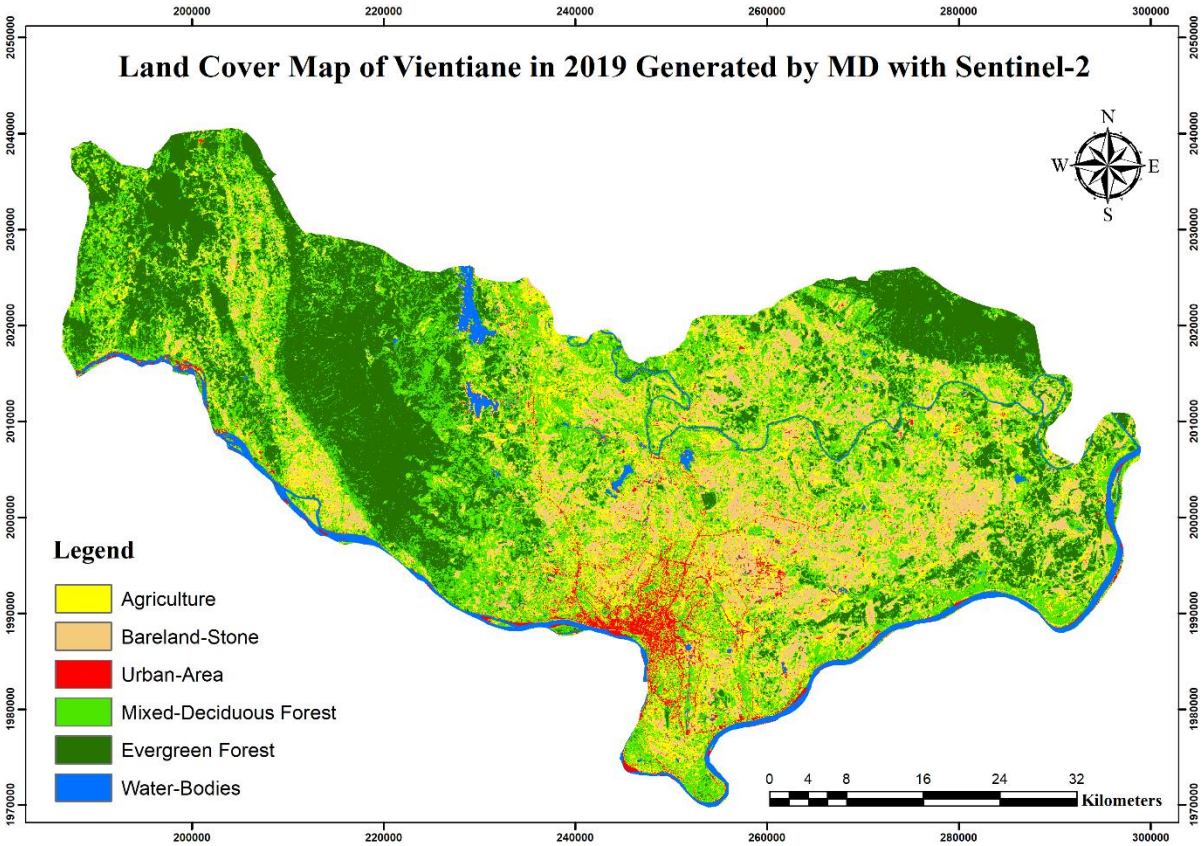

Figure 21 LC Classified by different Classifiers RF, CART, CNB, GMO and MD with Sentinel-2 in only 2019

The selected sample training and automatic machine learning with proposed classifiers provide us a different perspective. The classification of land cover has used the images from both Landsat 5 and Landsat 8, and Sentinel-2. The classification results for each classifier, such as RF, CART, CNB, GMO Maxent, and MD has shown in figure 21, respectively. From a visual comparison, spatial patterns of land cover types are similar to the results in the whole classifiers set. The number of training sample and classification validation (including the Overall Accuracy and Kappa coefficient performed with Sentinel-2) for each classifier is given in Table 29. Accuracy measurements are adjusted according to the area of each layer (Classes) presented for CART came with the rank of the overall accuracy of 96.34% (Kappa coefficient 0.95). In contrast, other classifiers such as RF, CNB, GMO, and MD came second, third, fourth, and fifth rank with an overall accuracy of 95.08%, 90.59%, 81.49%, and 73.95% while Kappa coefficient values are 0.93, 0.88, 0.74 and 0.66. respectively

4.4.2 Classification Change Detection Using Time-series Data

The urban expansion and land cover changes are performed, calculated, and classified via GEE using machine learning Classifiers in implementation. We began with exporting the land cover classified from GEE APIs and imported to Arc GIS software to perform a calculation to find changing numbers in study areas in terms of Square Kilometers. Comparative characteristics of land coverage for the study area is separated into the six classes for 30 years with bar charts are also shown. (See more in Table 2)

In this section, the changes detection of Vientiane for 30-year implemented using the Arc GIS software tool. The changes detection is carried out according to previous of time-series data classification results. The results of change detection are demonstrated in the thematic, and legend map was out of the main map (Figure 22). For more details in visualization of changes detection, a land cover map for each 5-year interval is executed, and Overall changed detection map started from 1989 to 2019 with different Satellite images. The thematic maps generated, calculated the changing area to find how much of area changing such from 1989-1994, 1994-1999, 1999-2004, 2004-2009, 2009-2014 and 2014-2019 and 1989-2019 with following Thematic maps as shown in Figure 22 to Figure 28 below:

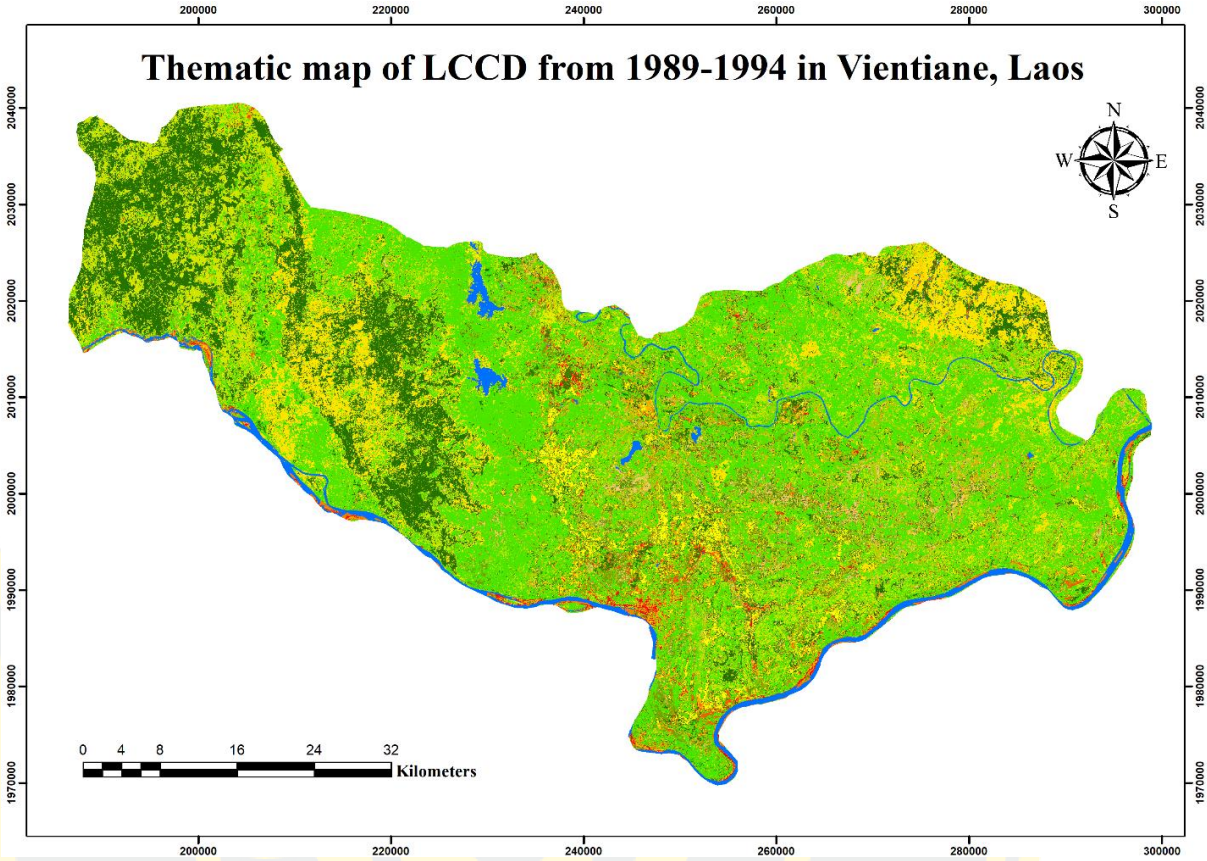

Figure 22 Thematic map of Land Cover Changes from 1989-1994 in Vientiane, Lao PDR

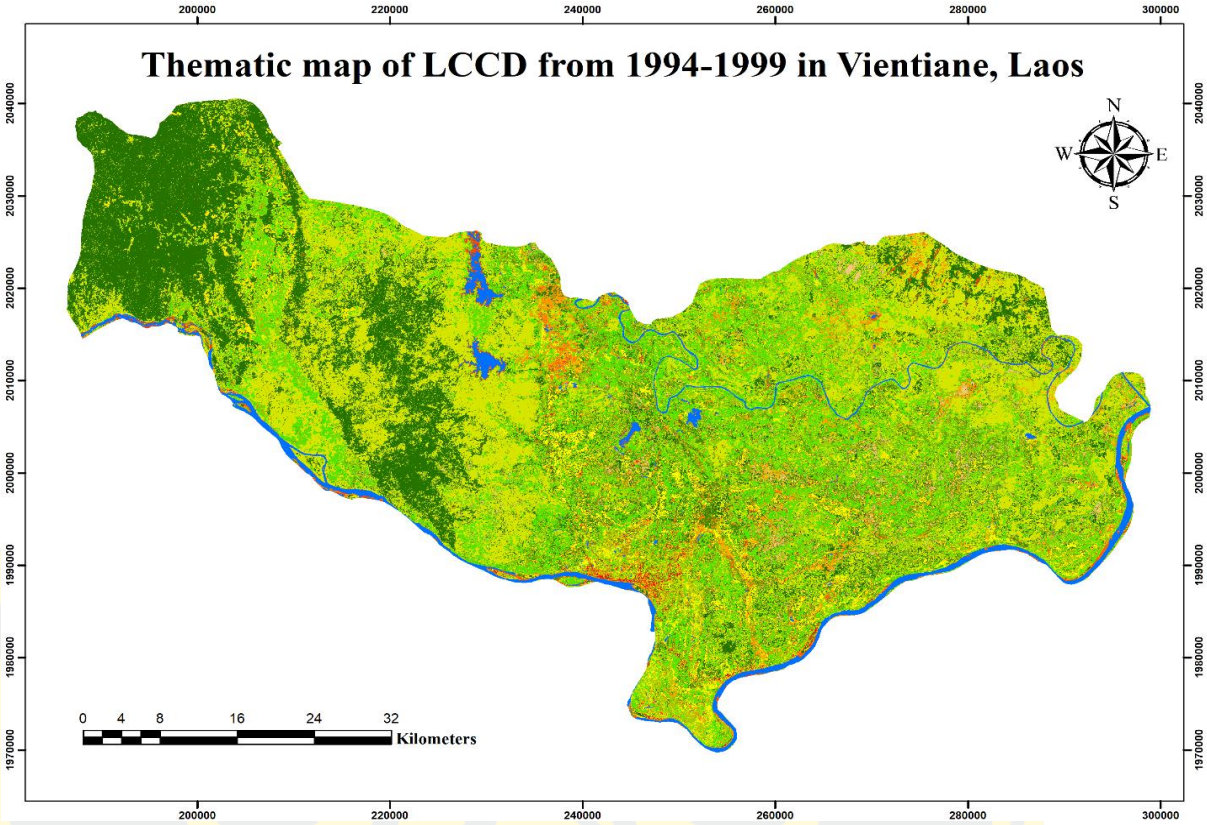

Figure 23 Thematic map of Land Cover Changes from 1994-1999 in Vientiane, Lao PDR

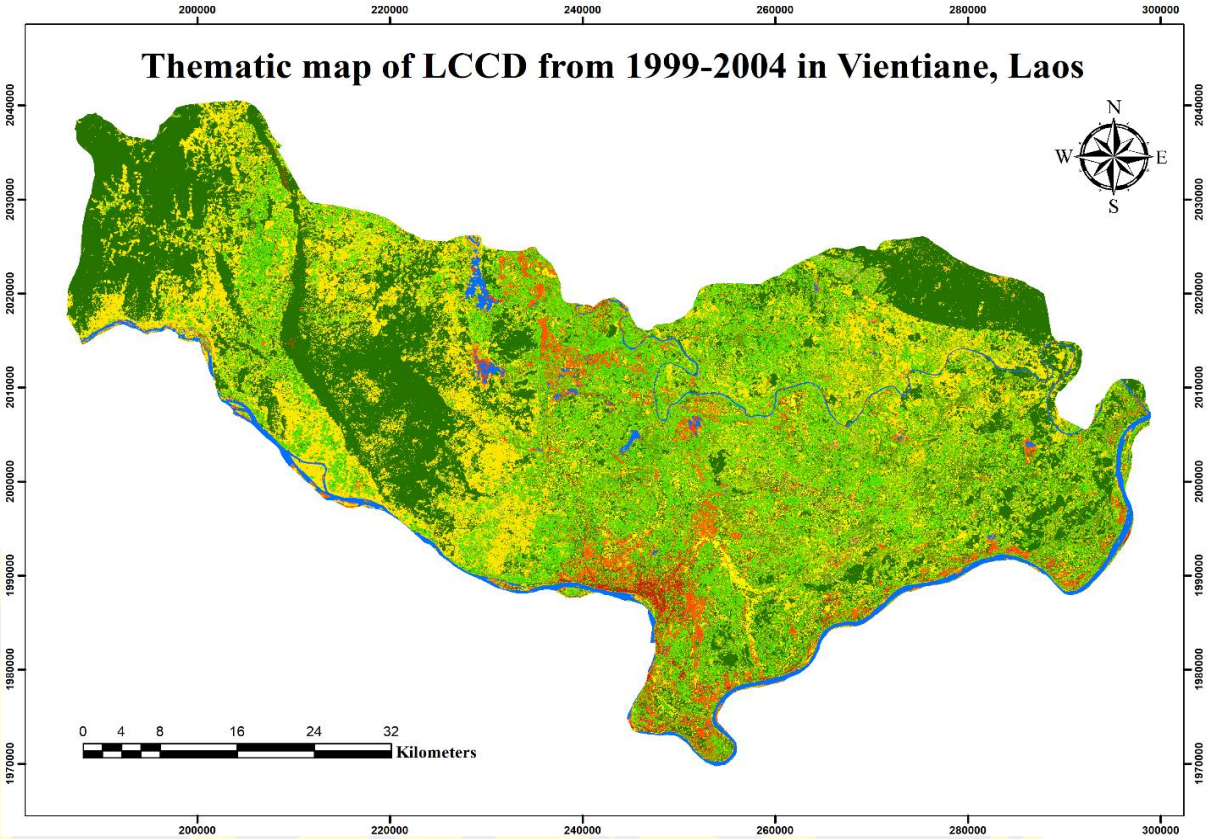

Figure 24 Thematic map of Land Cover Changes from 1999-2004 in Vientiane, Lao PDR

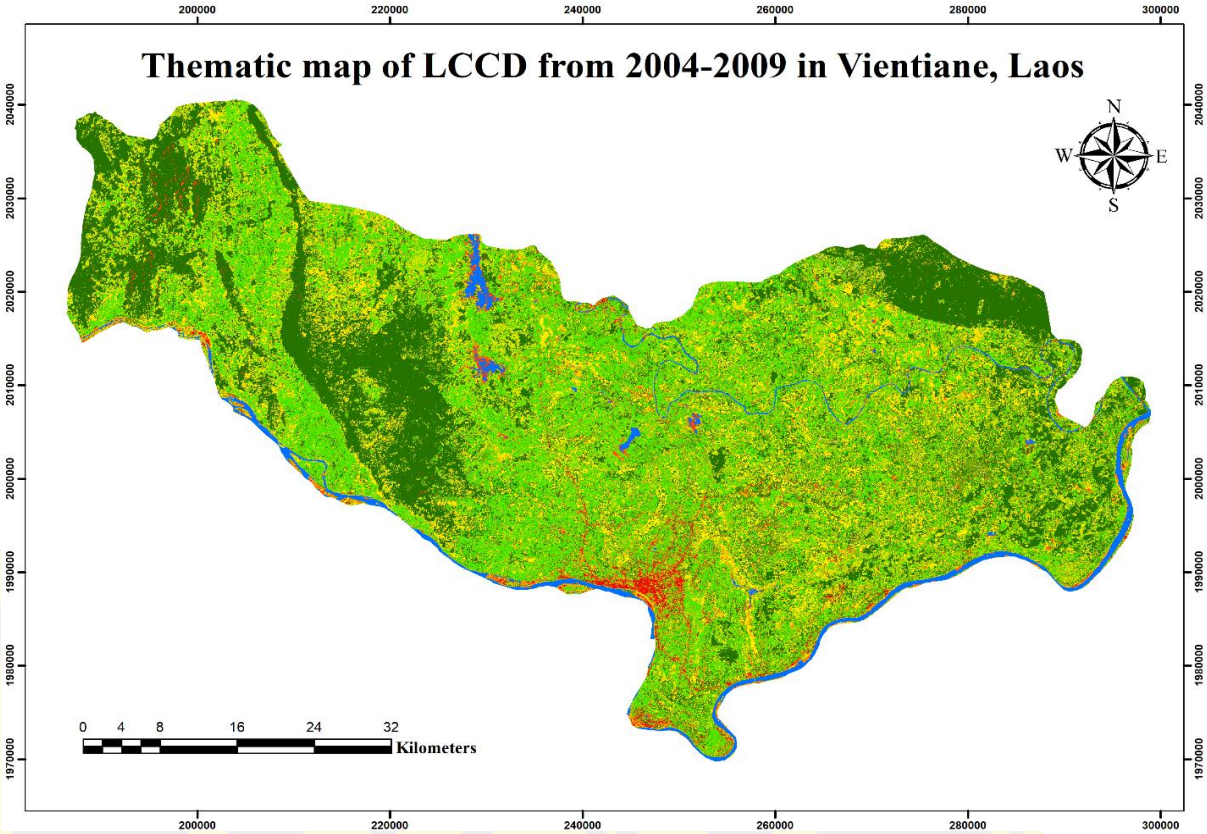

Figure 25 Thematic map of Land Cover Changes from 2004-2009 in Vientiane, Lao PDR

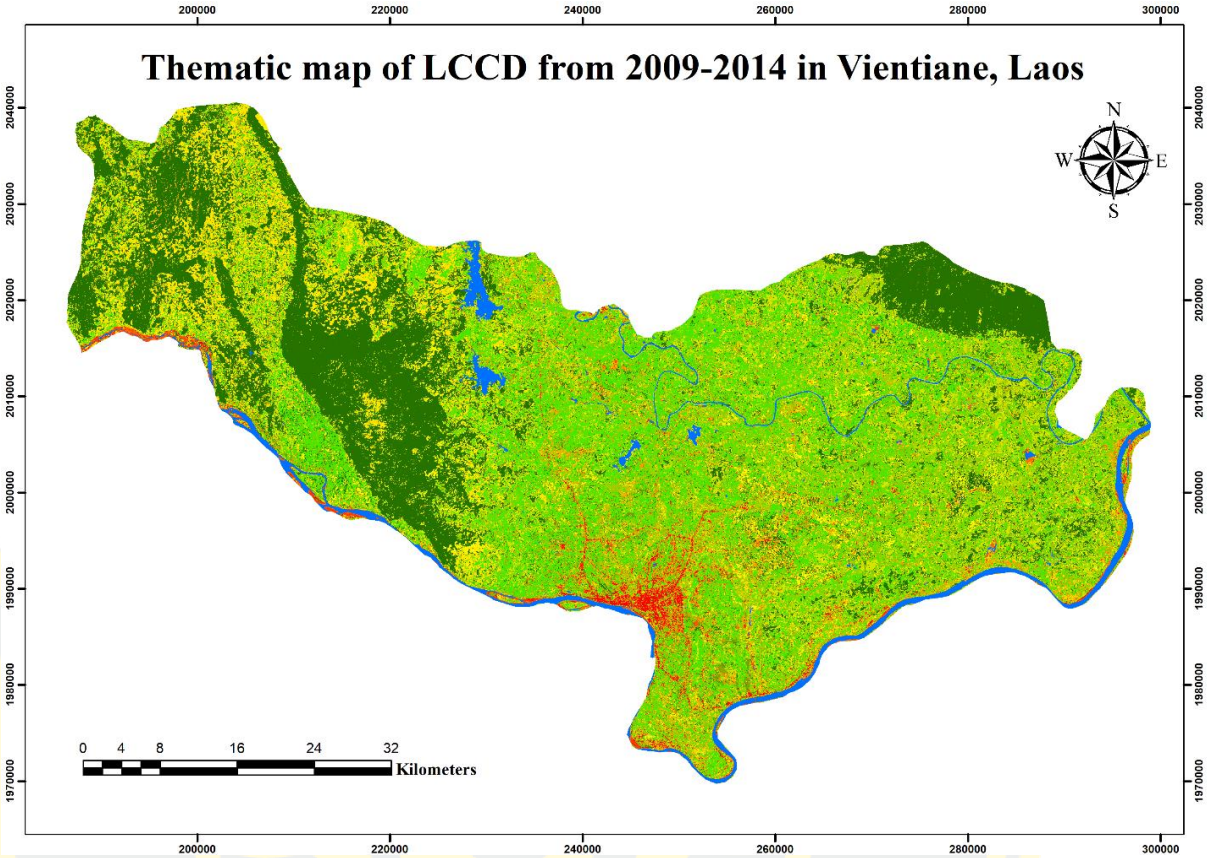

Figure 26 Thematic map of Land Cover Changes from 2009-2014 in Vientiane, Lao PDR

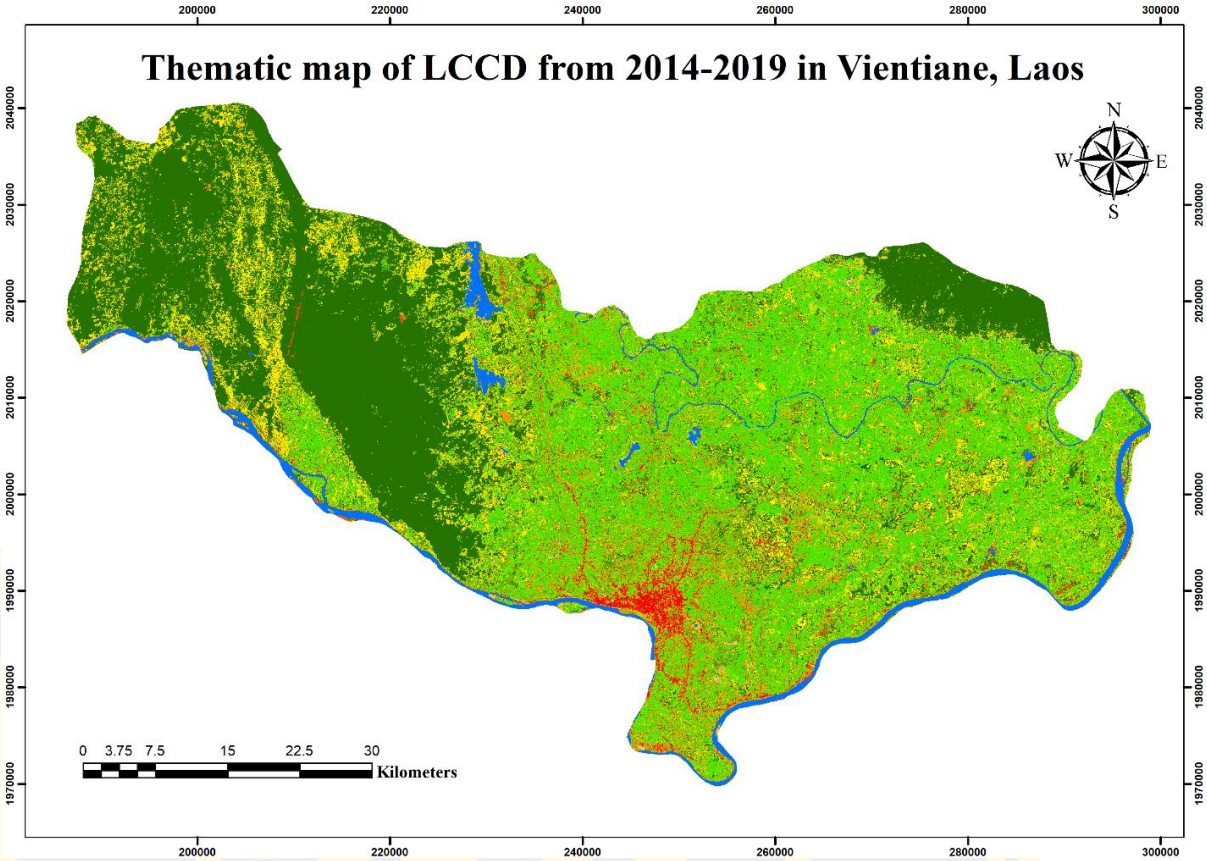

Figure 27 Thematic map of Land Cover Changes from 2014-2019 in Vientiane, Lao PDR

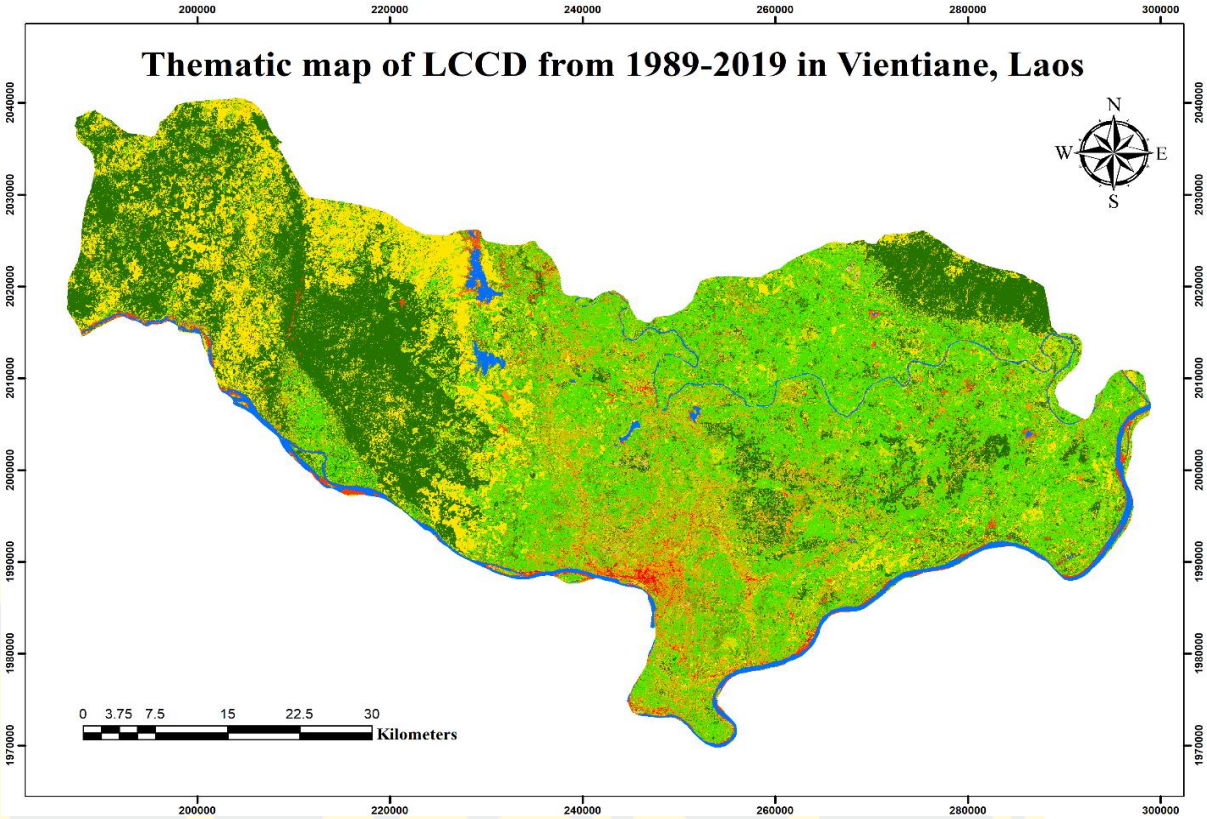

Figure 28 Thematic map of Land Cover Changes from 1989-2019 in Vientiane, Lao PDR

Legend

- Agriculute- Agriculute
- Agriculute- Bareland-Stone
- Agriculute- Deciduous Forest
- Agriculute- Evergreen Forest
- Agriculute- Urban-Area
- Agriculute- Water-Bodies
- Bareland-Stone- Agriculute
- Bareland-Stone- Bareland-Stone
- Bareland-Stone- Deciduous Forest
- Bareland-Stone- Evergreen Forest
- Bareland-Stone- Urban-Area
- Bareland-Stone- Water-Bodies
- Deciduous Forest - Agriculute
- Deciduous Forest- Bareland-Stone
- Deciduous Forest- Deciduous Forest
- Deciduous Forest- Evergreen Forest
- Deciduous Forest- Urban-Area
- Deciduous Forest- Water-Bodies
- Evergreen Forest- Agriculute
- Evergreen Forest- Bareland-Stone
- Evergreen Forest- Deciduous Forest
- Evergreen Forest- Evergreen Forest
- Evergreen Forest- Urban-Area
- Evergreen Forest- Water-Bodies
- Urban-Area- Agriculute
- Urban-Area- Bareland-Stone
- Urban-Area- Deciduous Forest
- Urban-Area- Evergreen Forest
- Urban-Area- Urban-Area
- Urban-Area- Water-Bodies
- Water-Bodies- Agriculute
- Water-Bodies- Bareland-Stone
- Water-Bodies- Deciduous Forest
- Water-Bodies- Evergreen Forest
- Water-Bodies- Urban-Area
- Water-Bodies- Water-Bodies

Figure 29 Legend of Thematic map of LCCD from 1989-2019

Regarding the research direction, the method to be explained is Post-classification, due to in this section contained the details of the area changing of land cover. I export the classification implemented via GEE, and Arc GIS is used to calculate the areas. Then we able to know the area changed in the study area.

Table 34 Coverage area changing on each class in sq.km 1989-2019

LC- Classes (RF)	**Total Changing Area_sq.km from 1989-2019**						
	Y-1989	Y-1994	Y-1999	Y-2004	Y-2009	Y-2014	Y-2019
Agriculture	373.174	449.578	507.492	579.52	674.737	420.197	527.921
Bareland-Stone	256.905	320.757	258.336	111.803	123.577	45.02	129.168
Urban-Area	9.1188	13.5276	26.7075	43.5003	47.5144	83.1173	105.062
Mixed Deciduous Forest	1958.35	1857.04	880.92	1668.69	1407.47	1729.56	1457.92
Evergreen Forest	888.355	841.081	1704.93	1097.43	1230.92	1199.56	1264.17
Water-Bodies	137.907	141.85	245.467	122.858	139.592	146.396	139.623
Total Area	**3623.8**	**3623.8**	**3623.8**	**3623.8**	**3623.8**	**3623.8**	**3623.8**

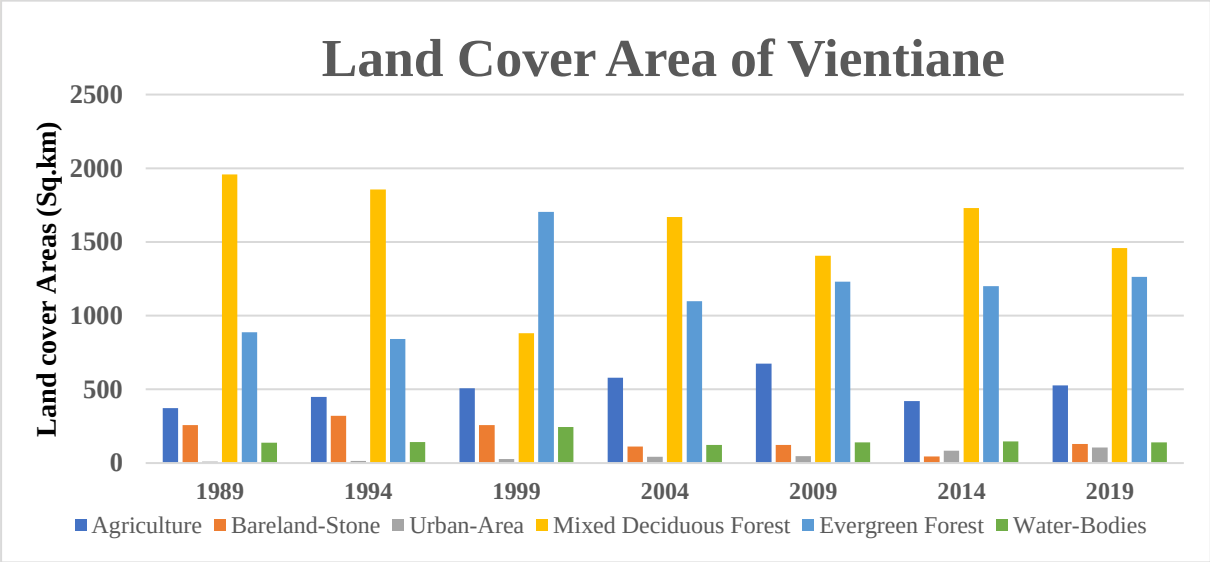

Figure 30 Bar Chart of the coverage area of each land classes by sq.km from 1989-2018

Table 35 Coverage area changed on each class in Percentage (%) 1989-2019

LC-Classes	**Area_Percentage (%)**						
	Y-1989	Y-1994	Y-1999	Y-2004	Y-2009	Y-2014	Y-2019
Agriculture	10.30	12.41	14.00	15.99	18.62	11.60	14.57
Bareland-Stone	7.09	8.85	7.13	3.09	3.41	1.24	3.56
Urban-Area	0.25	0.37	0.74	1.20	1.31	2.29	2.90

Mixed Deciduous	54.04	51.25	24.31	46.05	38.84	47.73	40.23
Evergreen Forest	24.51	23.21	47.05	30.28	33.97	33.10	34.88
Water-Bodies	3.81	3.91	6.77	3.39	3.85	4.04	3.85
Total Area	**100.00**	**100.00**	**100.00**	**100.00**	**100.00**	**100.00**	**100.00**

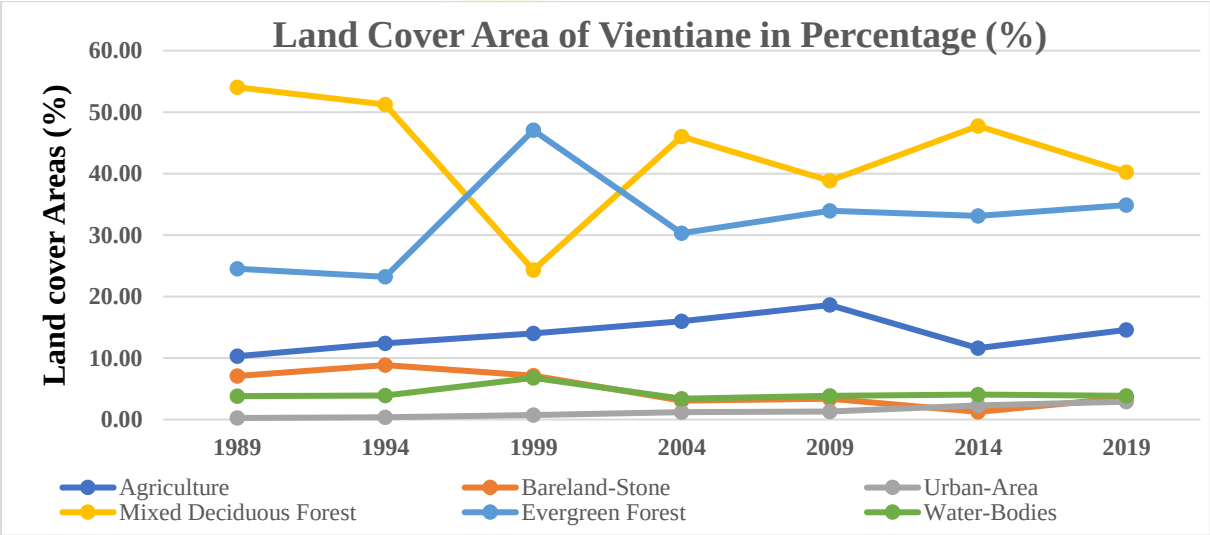

Figure 31 Chart of the average area on each changed class by Percentages (%) 1989-2018

4.5 Summary

The experiment in this chapter is investigated for the Machine Learning Classifiers implemented by GEE. The land cover classification and accuracy assessment are shown for each step of the research, and the changes detection also displayed with a thematic map, bar chart, and line chart, respectively. The expansion of the city plays an essential role in the positive and negative aspects of Urban social development and land-use changes. In this research, the investigation and analysis of land cover change processes took place in Vientiane capital city of Laos during 1989-2019. This accelerated growth leads to most agricultural areas, land for construction for residential, commercial and industrial sectors, and surrounding environment to participate in urban areas. Various factors are affecting the growth of the city. Among them, Vientiane has many changes regarding the shape and form of the town. Different political, economic, social, and environmental factors affect changes. After took over to Lao PDR in 1975, the functionality of the urban has changed the most. Many industrial, commercial, and other activities have started, which in turn encouraged many people to immigrate to the

city for work, education, and resettlement purposes. Thereby, the demand for land housing, construction, and other development purpose has been increased.

Therefore, agricultural land, mixed deciduous forest, evergreen forest areas are used in the creation of cities. The city expansion has been mostly expanded to the North, West, and South direction along the main roads. The city expansion faced with the limitation in the South-West part due to this direction is the Mekong river bank and shared border to the Kingdom of Thailand. The urban area of Vientiane city has increased tenfold during the last three decades. It was 9.11 sq.km in 1989, and it became to 105.06 sq.km in 2019. According to the number of migration rate has caused the population to increase threefold (187,000 in 1975 to 673,000 in 2019). Land growth in the city is accompanied by population growth, which shows the high population density in Vientiane city and let to the expansion of Vientiane city has fueled a land-use change in urban areas. Managers and city planners should observe practical factors and reasons leading to such uneven urban growth so they can prepare a strategy for the city development of Vientiane. Some policies that may be used for urban control expansion are as follows: Reclamation of urban and regional land of the city to achieve a regional balance of buildings and for balanced population distribution. To avoid unauthorized construction and being marginalized on the outskirts, the development of the surrounding areas to prevent further migration building a suburban city and transfer factories and industrial zones to outside city exclusion.

Multi-source satellite imagery used in this study. We can conclude both advantage and disadvantage as follow:

- Landsat 5 Thematic Mapper (TM) and Landsat 8 Operational Land Imager (OLI), as well as infrared thermal sensors (TIR) with a spatial resolution of 30 m and a 16-day temporal resolution both of these satellites, provided us low spatial and temporal resolution

- While the Sentinel-2 provide high revisit time (10 days at the equator with one satellite, and five days with two satellites under cloud-free conditions which result in 2-3 days at mid-latitudes) and 10 m of spatial resolution, the Sentinel-2 gave us high spatial and temporal with the better result compared to Landsat images.

- The pre-processing of satellite image was used as mean values average imagery through the year with full cloud cleared in the study area with all images from Landsat 5, Landsat 8, and Sentinel-2.

- We recommended after processing results found that the best accuracy is given by Sentinel-2, due to this kind of satellite image is provide a high quality of both spatial and temporal resolution.

Postscript. This study is based on my observation. Although the same method was used, the study is in a different area as well as a result may be changed.

CHAPTER 5
DISCUSSION

Getting the maps for land use classification with accuracy is very crucial in remote sensing. Like accuracies impacted from various factors such as the classifiers selection used, sample data training quality, a variety of landscape, dataset used, and so on. Results of performing from different classifiers we mainly performed with three satellites with Landsat 5 (1989), Landsat 8 (2019), and Sentinel-2 (2019). We found the results from three satellite images gave us most the same level. As 1989 (L5), 2019 (L8), and 2019 (S2), the highest performance is performed by Classification and Regression Trees (CART) following by Random Forest (RF), Continuous Naïve Bayes (CNB), GMO Max Entropy (GMO Max Ent) and Minimum Distance (MD).

5.1 Implementation of GEE Machine Learning

Continuous obtaining the higher accuracy of land use maps always exist. The available and free of access to the high-resolution image as well as GEE and machine learning. There are plenty of chances for interested persons to obtain better existing data. We can achieve the target by using a variety of factors such as samples training, including other input features, using multi-source of high-resolution images, advanced technology of machine learning, and other techniques. In the era of Big Data, the requirement for extensive computation infrastructure platforms and large capacity of storage space for image classification [74].

GEE provides petabyte-scale of size by cloud-based computation platform, data catalogue service for whole geospatial planetary scale[75]. The computation is running automatically on the cloud. Dataset for public use store in different types of format and range from United States Geological Survey (USGS) Landsat services, from Landsat Surface Reflectance datasets to Sentinel datasets, various of datasets for global scale of land cover data, climate datasets and so on. GEE provides a multi-scale of methods to help access and simply pre-processing of images. Additional. It has storage of many functions such as cloaking, logical operators, sampling data, etc., which can be used to perform various operations on images and vectors [76].

Global mapping of land cover is a crucial work in remote sensing. Improvement a 30m of the global land cover map by developing a variety of Google Earth Engine software that use cloud computing [77]. Urbanization is another global issue, and they required in-depth analysis of change detection on a large scale, the extensive range of area classification that possible to perform is only on a cloud computing platform environment. GEE is a powerful tool that can run 10-100 times faster than desktop workstation[78].

5.2 Comparison of Difference Machine Learning

The classifiers of machine learning results influenced by many surrounding factors; the one that has the most changed elements such as the features used training samples. Some classifiers gave good results, and some of them gave not so good due to the resolution of satellite imagery and the quality of Machine learning classifiers, as well as the amount and size of the sample taken. The difference in overall Accuracy is observed in the years, such as results from (1)1989 by Landsat 5, (2) 2019 by Landsat 8, and (3) 2019 by Sentinel-2 see below:

1. In 1989 performed with Landsat 5: best performance results started from the CART, following by RF, CNB, MD, and GMO with Overall Accuracies of 94.15%, 93.08%, 87.26%, 76.96%, and 75.43% while Kappa coefficient of 0.87, 0.90, 0.91, 0.71, and 0.66.
2. In 2019 performed with Landsat8: best performance results started from the CART, following by RF, CNB, GMO, and MD with Overall Accuracies of 95.61%, 89.31%, 78.63%, 62.32%, and 48.42% while Kappa coefficient of 0.93, 0.85, 0.71, 0.42, and 0.33.
3. In 2019 performed with Sentinel-2: best performance results started from the CART, following by RF, CNB, GMO, and MD with Overall Accuracies of 96.34%, 95.08%, 90.59%, 81.49%, and 73.95% while Kappa coefficient of 0.95, 0.93, 0.88, 0.74, and 0.66.

I confirmed that by three satellites performed in 1989 (L5), 2019 (L8), and 2019 (S2), the best classifier gave us a high Accuracy, and Kappa coefficient is CART came up with rank number one and along with other classifiers such RF, CNB, GMO, and MD respectively.

Rapidly changing land cover in the study area require quantitative measurement and monitoring for land resource management. I substantiate that the GEE machine learning classifiers can produce high accuracy of land cover classification in Vientiane. Most of the area in Vientiane is a rural area that depends mainly on agricultural activities. The analysis results of land cover changes have performed well and found that the land cover changed from traditional agriculture to plantation and urbanization in recent decades, with rapid economic development and population growth in past years.

Factors caused to land cover changes and being driving forces for urban expansion due to the results demonstrate socio-economic development activities such as urbanization and city expansion reflecting on the dynamics of the land-use changes. Vientiane Capital City, in past decades, has seen a rapid development that consisted of various activities contributing to the evolution of land use. The economy has continuously grown in the last 20 years, from 2000 to 2020. the economic growth in Laos is expected to remain stable, supported by expanding agriculture, energy, industry, and services sector [79], particularly from the investment sector, converted forested land to agricultural and residential by both private companies and local communities. The census data of PopulationStat [80] pointed out that the population has dramatically increased in a few decades from 283,000 in 1990 to 673,000 in 2019 in Vientiane. Vientiane, in past years, many activities have implemented. The numbers of economic have been grown, particularly for investment, changed nature land to agricultural and residential, both commercial and local. The urban area increased from 9.11 sq.km in 1989 to 105.06 sq.km during 1989-2019 is enlarged ten times while agricultural land is also increased at 373.17 sq.km to 527.92 sq.km. The increasing of the urban area came mainly from activities of the plot of arable land for economic development and changing property for agricultural purposes. And this is because of the high demand for plantation such as agriculture for production, agricultural land for business, Infrastructure and commercial of megaproject (Special Economic Development Zone), housing estate, and residential due to population growth.

Urbanization and land development are caused by many natural, economic, technological, demographic, institutional, and cultural factors. [81]. Vice versa, a large number of developing countries gained experiences from the changing of forests that

area designates as a shift from “a shrinking to an expanding forest area” [82]. Nevertheless, Urbanization remains one of the main in driving forces of deforestation, the loss of land resources by urban growth is the lack of land use planning integration in regional scale in many developing countries[26].

CHAPTER 6
CONCLUSION AND FUTURE STUDIES

6.1 Conclusion

The land cover maps are essential from different perspective, and pulling the information from satellite images have been used for long time to detect and derive information via remote sensing techniques and it was utilized over four decades. Among many image classification techniques represent in recent years, machine learning classifiers are reported for high accuracy classification results. Various factors

impact the accuracy of those classifiers, and an understanding of such its features to help improve the classification results. This research is aimed to analyze variety of machine learning classifiers such as Random Forest, Classification and Regression Trees, Continuous Naïve Bayes, GMO Max Entropy and Minimum Distance via GEE platform, under the influence of certain factors such as sample pixel size, dimension and provide a comparison of sensitivity to other factors. The research also focuses mainly on sampling techniques for training data, which requires pay attention, according to the literature review.

In conclusion, Satellite images analysis time-series can help us to know its changes detection and acknowledge the changes in the earth's surface. Therefore, the utilization of cloud-based platform and machine learning classifiers is the best solution for understanding the urban differences, change detection, and environment around us. Using GEE become an essential role in remote sensing with a short time, high speed, and save cost that many people can access the data on a cloud computing platform and highly effective in solving the problem. According to answer the question on the research question, we have proposed the answers as following:

- I strived changes in land use and land coverage for 30 years using GEE and machine learning classifiers. The difference in land use occurred from comparing the land area of each type in 1989-1994, 1994-1999, 1999-2004, 2004-2009, 2009-2014, 2014-2019, and 1989-2019. The surface area of each land cover type was evaluated by the projection of the land cover layer into WGS_84 Universal Transverse Mercator (UTM), Zone 48N, and then using Arc GIS software calculate the classified areas after exported from GEE. At the starting of the study period (1989), the mixed deciduous forest was the major of land use type making up 54.04%, followed by evergreen forest (24.51%), Agriculture (10.30%), Bare-land and stone (7.09%), water-bodies (3.81%), and Urban (0.25%). In 2019 after 30 years later, the mixed deciduous forest area size has decreased from 1958.35sq.km in 1989 to 1457.92sq.km in 2019 (from 54.04% to 40.23%) equal to 13.81% of mixed deciduous forest area loss. Whereas the Agriculture land, evergreen forest, and urban area size had increased by 373.174 sq.km, 888.35 sq.km, and 9.11 sq.km in 1989 to 527.92 sq.km, 1264.17 sq.km, and 105.06 sq.km in 2019 equal to 4.27%, 10.37%, and 2.65% increased Changes covering most areas occur in a mixed

deciduous forest (Figure 1). The prominent land-use change is the conversion of other land use and land coverage into agricultural regions (Table 3).

- I have found that the results illustrate socio-economic development activities such as urban expansion and urbanization that reflect the dynamics of changes in Vientiane land use in the past decade during 2004-2019. Saw rapid development consisting of businesses, land use, economic growth continuously in 2019 and 2020, economic growth in Laos is expected to remain stable, has been driven by expanding agriculture, energy, industry, and services.
- Regarding introductory analysis conducted using GEE, we have found that this platform is a powerful tool for analyzing a variety of data at the same time in a single unified system. However, GEE can support both spatial and temporal analysis and proceed within a matter of minutes, both regional and global scale imagery. The investigation was carried out using the GEE conducted the urban growth took place in Vientiane, Lao PDR for years 1989-2019 using multi-sources visual representations from Landsat5, Landsat 8, and Sentinel-2 data. The primary input of this study is to understand the involvement of the large scale of the dataset, time performance, effectiveness, accuracy, and multi-source of optical images applied for urban expansion and land cover classification. The main point highlight is “research friendliness cost” when compared with using different web services for conducting and processing remote sensing data. Time series analysis provides a vital and robust foundation for detecting trends and long-term changes in land use and land cover. This GEE platforms not only have an advantage of managing large datasets and creating powerful data visualization as well as the friendliness to the users, but it has also created a strong appeal among non-expert users of satellite imagery.

6.2 Future Recommendation

The studying land cover changes detection by using remote sensing method is most famous for Earth Observation and Monitoring and also benefits for Urban planning, with practical and high accuracy, is based on the quality of classifiers and training sample taken with a high-resolution image as well. Even this study gave us high efficiency, but sometimes there are some limitations of applying in an actual urban planning environment. In this study, we classified into six classes, and this research is

focused on urban extension and land cover change only that performed with many different machine learning classifiers and applied to the medium and high resolution of imagery.

From the machine learning perspective, adjusting the machine learning parameters can improve the efficiency and accuracy of the classifier. Moreover, land cover analysis from high resolution images provide better results and can be conducted by using machine learning classifiers. The dataset of land use covers using machine learning can study for large regional and global areas as GEE is enabling for free to access and open us to explore freely. For a large scale of the region need to deep learning and carefully with parameter use and sample training pixel size. Land use cannot be directly detected to standardize Remote Sensing imagery, and the land cover classification method depends on the number of sampling, type, and spatial complexity of cover classes.

Anyway, this research has some limitation due to the author used only remotely sensed data and that the author provided the limitation as below:

- This research has no ground-truth for field observation
- The analyzing of imagery needs a certain skill level
- Data from various sources may create confusion
- Objects can be misclassified or confused
- Distortions may found in an image as they are the relative motion of sensors and sources

มหาวิทยาลัยบูรพา
BURAPHA UNIVERSITY

REFERENCES

[1] B. Catalan, D. Saur ´ ´ı, and P. Serra, “Urban sprawl in the Mediterranean? Patterns of growth and change in the Barcelona Metropolitan Region 1993–2000,” *Landscape and Urban Planning*, vol. 85, no. 3-4, pp. 174–184, 2008. https://www.sciencedirect.com/science/article/pii/S0169204607002848

[2] J. Cheng and I. Masser, “Urban growth pattern modelling: a case study of Wuhan city, PR China,” *Landscape and Urban Planning*, vol. 62, no. 4, pp. 199–217, 2003.

[3] K. M. Lata, C. H. Sankar Rao, V. Krishna Prasad, K. V. S. Badrinath, and V. Raghavaswamy, “Measuring urban sprawl: a case study of Hyderabad,” *GIS Development*, vol. 5, no. 12, pp. 1–4, 2001.

[4] Rubiera Morollón, F., González Marroquin, V. M., & Pérez Rivero, J. L. (2016). Urban sprawl in Spain: differences among cities and causes. *European Planning Studies*, *24*(1), 207–226. https://doi.org/10.1080/09654313.2015.1080230.

[5] E. Simon, A. Vidic, M. Braun, I. Fabi ´ an, and B. T ´ othm ´ er ´ esz, ´ “Trace element concentrations in soils along urbanization gradients in the city of Wien, Austria,” *Environmental Science and Pollution Research*, vol. 20, pp. 917–924, 2013.

[6] T. Magura, G. L. Lovei, and B. T ¨ othm ´ er ´ esz, “Does urbanization ´ decrease diversity in ground beetle (Carabidae) assemblages?” *Global Ecology and Biogeography*, vol. 19, no. 1, pp. 16–26, 2010.

[7] Land Use and Food Security in 2050: A Narrow Road from Agrimonde-Terra Access date 12 Dec 2019. https://agritrop.cirad.fr/588816/1/ID588816.pdf

[8] Hu, Y., Dong, Y., & Batunacun. (2018). An automatic approach for land-change detection and land updates based on integrated NDVI timing analysis and the CVAPS method with GEE support. *ISPRS Journal of Photogrammetry and Remote Sensing*, *146*, 347–359. https://doi.org/10.1016/j.isprsjprs.2018.10.008

[9] Liu, Y.; Liu, X.; Gao, S.; Gong, L.; Kang, C.G.; Zhi, Y.; Chi, G.H.; Shi, L. Social Sensing: A New Approach to Understanding Our Socioeconomic Environments. *Ann. Assoc. Am. Geogr.* 2015, *105*, 512–530. [CrossRef] https://www.tandfonline.com/doi/abs/10.1080/00045608.2015.1018773

[10] Hu, T., Yang, J., Li, X., & Gong, P. (2016). Mapping urban land use by using Landsat images and open social data. *Remote Sensing*, *8*(2). https://doi.org/10.3390/rs8020151

[11] Wei, Y.H.D.; Li, H.; Yue, W.Z. Urban land expansion and regional inequality in transitional China. *Landsc. Urban Plan.* 2017, *163*, 17–31. [CrossRef]

[12] Shalaby, A., & Tateishi, R. (2007). Remote sensing and GIS for mapping and monitoring land cover and land-use changes in the Northwestern coastal zone of Egypt. *Applied Geography*, *27*(1), 28–41. https://doi.org/10.1016/J.APGEOG.2006.09.004

[13] Foody, G., Pal, M., Rocchini, D., Garzon-Lopez, C., Bastin, L., Foody, G. M., … Bastin, L. (2016). The Sensitivity of Mapping Methods to Reference Data Quality: Training Supervised Image Classifications with Imperfect Reference Data. *ISPRS International Journal of Geo-Information*, *5*(11),

[14] Pavlov, Y. L. (2019). *Random forests*. *Random Forests* (pp. 1–122). De Gruyter Mouton. https://doi.org/10.1201/9780429469275-8 https://link.springer.com/content/pdf/10.1023%2FA%3A1010933404324.pdf

[15] Gislason, P. O., Benediktsson, J. A., & Sveinsson, J. R. (2006). Random Forests for land cover classification. *Pattern Recognition Letters*, *27*(4), 294–300. https://doi.org/10.1016/j.patrec.2005.08.011

[16] Dong, J., Xiao, X., Menarguez, M. A., Zhang, G., Qin, Y., Thau, D., … Moore, B. (2016) Mapping paddy rice planting area in northeastern Asia with Landsat 8 images, phenology-based algorithm and Google Earth Engine. *Remote Sensing of Environment*, *185*, 142–154. https://doi.org/10.1016/J.RSE.2016.02.016

[17]. Liu, F., Zhang, Z., & Wang, X. (2016). Forms of urban expansion of Chinese municipalities and provincial capitals, 1970s-2013. *Remote Sensing*, *8*(11). https://doi.org/10.3390/rs8110930

[18] Buhaug, H., & Urdal, H. (2013). An urbanization bomb? Population growth and social disorder in cities. *Global Environmental Change*, *23*(1), 1–10. https://doi.org/10.1016/j.gloenvcha.2012.10.016

[19] Cohen, J. (2006). Social, emotional, ethical, and academic education: Creating a climate for learning, participation in democracy, and well-being. *Harvard Educational Review*. Harvard University. https://doi.org/10.17763/haer.76.2.j44854x1524644vn

[20] Dewan, A. M., & Yamaguchi, Y. (2009). Land use and land cover change in Greater Dhaka, Bangladesh: Using remote sensing to promote sustainable urbanization. *Applied Geography*, *29*(3), 390–401. https://doi.org/10.1016/j.apgeog.2008.12.005

[21] Herzog-Evans, Martine, Judicial Rehabilitation in France: Helping with the Desisting Process and Acknowledging Achieved Desistance (January 1, 2011). European Journal of Probation, Vol. 3, No. 1, pp. 4-19, 2011. Available at SSRN: https://ssrn.com/abstract=2024854

[22] Miller, E. A., Beilharz, T. H., Malkus, P. N., Lee, M. C. S., Hamamoto, S., Orci, L., & Schekman, R. (2003). Multiple cargo binding sites on the COPII subunit Sec24p ensure capture of diverse membrane proteins into transport vesicles. *Cell*, *114*(4), 497–509. https://doi.org/10.1016/S0092-8674(03)00609-3

[23] Qie, L., Chen, W. M., Wang, Z. H., Shao, Q. G., Li, X., Yuan, L. X., … Huang, Y. H. (2012). Nitrogen-doped porous carbon nanofiber webs as anodes for lithium ion batteries with a superhigh capacity and rate capability. *Advanced Materials*, *24*(15), 2047–2050. https://doi.org/10.1002/adma.201104634

[24] Shieh, E., Sharifi, A., & Rafieian, M. (2011). Identification of factors that assure quality of residential environments , using environmental assessment indices : a comparative study of Two of Tehran ’ s neighborhoods (Zafaranieh

& Khaniabad). *International Journal of Architectural Engineering & Urban Planning*, *21*(2), 119–132.

[25] Sun, M., Guo, X., Qian, X., Wang, H., Yang, C., Brinkman, K. L., … Xu, B. (2012). Activation of the ATM-Snail pathway promotes breast cancer metastasis. *Journal of Molecular Cell Biology*, *4*(5), 304–315. https://doi.org/10.1093/jmcb/mjs048

[26] Seto, K. C., Sánchez-Rodríguez, R., & Fragkias, M. (2010). The New Geography of Contemporary Urbanization and the Environment. *Annual Review of Environment and Resources*, *35*(1), 167–194. https://doi.org/10.1146/annurev-environ-100809-125336

[27] Cohen, B. (2006). Urbanization in developing countries: Current trends, future projections, and key challenges for sustainability. Technology in Society, 28, 63–80. http://dx.doi.org/10.1016/j.techsoc.2005.10.005

[28] UNDESA. (2012). World urbanization prospects: The 2011 revision. New York: United Nations Department of Economic and Social Affairs/Population Division.

[29] Parnwell, M., & Bryant, R. L. (1996). Environmental change in South-East Asia: People, politics and sustainable development. London/New York: Routledge.

[30] Sheng, Y. K., & Thuzar, Y. (2012). Urbanization in Southeast Asia: Issues and impacts. Singapore: Institute of Southeast Asian Studies.

[31] Severino, R. (2012). Message from Head, ASEAN Studies Centre. In Urbanization in Southeast Asia: Issues and Impacts (pp. Ix-X). ISEAS–Yusof Ishak Institute.

[32] Urbanization process in the Lao PDR https://www.shareweb.ch/site/Poverty-Wellbeing/currentpovertyissues/Documents/Lao_Urbanization_Study_CDE_final.pdf Accessed date: 27 March 2020.

[33] Askew, M., Logan, W. S., & Long, C. (2007). Vientiane: Transformations of a Lao landscape. London/New York: Routledge.

[34] Okamoto, K., Sharifi, A., & Chiba, Y. (2014). The impact of urbanization on land use and the changing role of forests in Vientiane. In S. Yokoyama, https://link.springer.com/chapter/10.1007/978-4-431-54956-7_2#citeas

[35] Rafiqui, P. S., & Gentile, M. (2009). Vientiane. Cities, 26(1), 38–48. https://www.deepdyve.com/lp/elsevier/vientiane-zJsodwm1hz

[36] Nolintha, V. (2011). Cities, SEZs and connectivity in major provinces of Laos. In M. Ishida (Ed.), Intra – aninter-citycity connectivity in the Mekong Region (pp. 176–240). Bangkok, Thailand: Bangkok Research Center, IDE-JETRO. https://www.ide.go.jp/library/English/Publish/Download/Brc/pdf/06_chapter4.pdf

[37] Laos-Urban Population (% of Total) [OnlineAvailablele at https://tradingeconomics.com/laos/urban-population-percent-of-total-wb-data.html Accessed date: 04 April 2020.

[38] Laos -Urban Population growth (annual %) https://tradingeconomics.com/laos/urban-population-growth-annual-percent-wb-data.html Accessed date: 08 April 2020.

[39] Urban Sustainable cities and Communities available at http://www.la.one.un.org/sdgs/sdg-11-cities Accessed date: 04 April 2020.

[40] Vientiane Capital Urban Development Master Plan available at https://www.mendeley.com/catalogue/025b2c15-5153-33a8-8356-a1adfc02e0f9/ Accessed date: 04 April 2020.

[41] World Dometers Report available at https://www.worldometers.info/world-population/laos-population/ Accessed date: 04 April 2020.

[42] Economic indicators for Lao PDR available at https://www.adb.org/countries/lao-pdr/economy Accessed date: 04 April 2020.

[43] Y. H. Tsai, D. Stow, H. L. Chen, R. Lewison, L. An, L. Shi, “Mapping Vegetation and Land Use Types in Fanjingshan National Nature Reserve Using Google Earth Engine,” Remote Sens. 2018, 10, 927DOIoi:10.3390/rs10060927, https://www.mdpi.com/2072-4292/10/6/927 12 Jun 2018.

[44] A. Shelestov, M. Lavreniuk, N. Kussul, A. Novikov, S. Skakun, " Exploring Google Earth Engine Platform for Big Data Processing: Classification of Multi-Temporal Satellite Imagery for Crop Mapping," Front. Earth Sci. 5:17, 24 Feb 2017, https://www.frontiersin.org/articles/10.3389/feart.2017.00017/full

[45] A. Midekisa, F. Holl, D. J. Savory, R. A. Pacheco, P. W. Gething, A. Bennett, H. J. W. Sturrock, "Mapping land cover change over continental Africa using Landsat and Google Earth Engine cloud computing," PLoS ONE 12 (9): e0184926, 27 Sep 2017, https://doi.org/10.1371/journal.pone.0184926

[46] Tumer, K., & Ghosh, J. (1996). Analysis of decision boundaries in linearly combined neural classifiers. *Pattern Recognition*, *29*(2), 341–348. https://doi.org/10.1016/0031-3203(95)00085-2

[47] Breiman, L. (1996). *Bagging Predictors* (Vol. 24). Berkeley: Kluwer Academic Publishers. Retrieved from https://link.springer.com/content/pdf/10.1023%2FA%3A1018054314350.pdf

[48] Pal, M., & Mather, P. M. (2003). An assessment of the effectiveness of decision tree methods for land cover classification. *Remote Sensing of Environment*, *86*(4), 554–565. https://doi.org/10.1016/S0034- 4257(03)00132-9

[50] Pal, M., & Mather, P. M. (2005). Support vector machines for classification in remote sensing. *International Journal of Remote Sensing*, *26*(5), 1007–1011. https://doi.org/10.1080/01431160512331314083

[51] Nathan, A. J., & Scobell, A. (2012, September). How China sees America. *Foreign Affairs*. https://doi.org/10.1017/CBO9781107415324.004.

[52] H., L., & Feller, W. (1959). An Introduction to Probability Theory and Its Applications. *Population (French Edition)*, *14*(2), 359. https://doi.org/10.2307/1526422. https://my.eng.utah.edu/~cs5961/lec_Notes/feller.chap2.pdf

[53] Guan, H., Li, J., Chapman, M., Deng, F., Ji, Z., & Yang, X. (2013). Integratio image and lidar data for object-based urban thematic mapping using random forests. *International Journal of Remote Sensing*, *34*(14), 5166–5186.

[54] Belgiu, M., & Drăguţ, L. (2016). Random forest in remote sensing: A review of applications and future directions. *ISPRS Journal of Photogrammetry and Remote Sensing*, *114*, 24–31. https://doi.org/10.1016/j.isprsjprs.2016.01.011

[55] Ghosh, A., Sharma, R., & Joshi, P. K. (2014). Random forest classification of urban landscape using Landsat archive and ancillary data: Combining seasonal maps with decision level fusion. *Applied Geography*, *48*, 31–41. https://doi.org/10.1016/j.apgeog.2014.01.003

[56] Rodriguez-Galiano, V. F., Ghimire, B., Rogan, J., Chica-Olmo, M., & Rigol-Sanchez, J. P. (2012). An assessment of the effectiveness of a random forest classifier for land-cover classification. *ISPRS Journal of Photogrammetry and Remote Sensing*, *67*, 93–104. https://doi.org/10.1016/J.ISPRSJPRS.2011.11.002

[57] Ghimire, B., Rogan, J., Galiano, V. R., Panday, P., & Neeti, N. (2012). An Evaluation of Bagging, Boosting, and Random Forests for Land-Cover Classification in Cape Cod, Massachusetts, USA. *GIScience & Remote Sensing*, *49*(5), 623–643. https://doi.org/10.2747/1548-1603.49.5.623

[58] Ghosh A, et al. (2014) Rps5-Rps16 communication is essential for efficient translation initiation in yeast S. cerevisiae. *Nucleic Acids Res* 42(13):8537-55

[59] Waske, B., & Braun, M. (2009). Classifier ensembles for land cover mapping using multitemporal SAR imagery. *ISPRS Journal of Photogrammetry and Remote Sensing*, *64*(5), 450–457. https://doi.org/10.1016/j.isprsjprs.2009.01.003

[60] Loh, W. Y. (2011). Classification and regression trees. *Wiley Interdisciplinary Reviews: Data Mining and Knowledge Discovery*, *1*(1), 14–23. https://doi.org/10.1002/widm.8

[61] Kohavi, R. (1995). A Study of Cross-Validation and Bootstrap for Accuracy Estimation and Model Selection. *International Joint Conference on Artificial Intelligence*, *14*(2), 1137–1145. Retrieved from http://robotics.stanford.edu/~ronnyk

[62] J. Brownlee. (2016): Master Machine Learning Algorithms: Discover How They Work and Implement Them from Scratch. [Online]. Available at. https://machinelearningmastery.com/master-machine-learning-algorithms/. Accessed date: 24 Feb 2020.

[63] S. Haykin. (2008): Neural Networks and Learning Machines, 3rd edition. Upper Saddle River: NJ: Prentice Hall, Brownlee, J. (1393). Master Machine Learning Algorithms - Jason Brownlee. http://repository.fue.edu.eg/xmlui/bitstream/handle/123456789/3421/5618.pdf?sequence=1

[64] Abramson, N., Braverman, D., & Sebestyen, G. (1963). Pattern recognition and machine learning. *IEEE Transactions on Information Theory*, *9*(4), 257–261. https://doi.org/10.1109/TIT.1963.1057854. Google Scholar, http://sar.kangwon.ac.kr/etc/rs_note/rsnote/cp11/cp11-6.htm

[65] A Brief Introduction to Supervised Learning (2019): https://towardsdatascience.com/a-brief-introduction-to-supervised-learning-54a3e3932590 Accessed date: 15 April 2020.

[66] Spectral Indices from harrisgeospatial : https://www.harrisgeospatial.com/docs/SpectralIndices.html Accessed date: 15 April 2020.

[67] Earth Observatory, NASA blogs [Online]. Available at. https://earthobservatory.nasa.gov/features/MeasuringVegetation/measuring_vegetation_1.php Accessed date: 15 December 2019.

[68] Canada Centre of Remote Sensing. (2007): Fundamentals of Remote Sensing. [Online]. Available at.

https://www.nrcan.gc.ca/sites/www.nrcan.gc.ca/files/earthsciences/pdf/resource/tutor/fundam/pdf/fundamentals_e.pdf. Accessed date: 16 December 2019.

[69] United States Geological Survey (USGS). Landsat 5. [Online]. Available at https://www.usgs.gov/land-resources/nli/landsat/landsat-5?qt-science_support_page_related_con=0#qt-science_support_page_related_con Accessed date: 11 December 2019.

[70] United States Geological Survey (USGS). Landsat 8. [Online]. Available at https://www.usgs.gov/land-resources/nli/landsat/landsat-8?qt-science_supp=&qt-science_support_page_related_con=0#qt-science_support_page_related_con Accessed date: 11 December 2019.

[71] Sentinel-2 Mission Sentinel Online [Online] Available at https://sentinel.esa.int/web/sentinel/missions/sentinel-2 Accessed date: 15 December 2019.

[72] Li, X., Zhou, Y., Zhu, Z., & Cao, W. (2019). A national dataset of 30-m annual urban extent dynamics (1985–2015) in the conterminous United States. *Earth System Science Data Discussions*. https://doi.org/10.5194/essd-2019-107

[73] Mohammady, S., & Delavar, M. R. (2016). Urban sprawl assessment tingling using Landsat images and GIS. *Modeling Earth Systems and Environment*, *2*(3). https://doi.org/10.1007/s40808-016-0209-4

[74] Azzari, G., & Lobell, D. B. (2017). Landsat-based classification in the cloud: An opportunity for a paradigm shift in land cover monitoring. *Remote Sensing of Environment*, *202*, 64–74. https://doi.org/10.1016/j.rse.2017.05.025

[75] Giri, C., Pengra, B., Long, J., & Loveland, T. R. (201Next-generation of global land cover characterization, mapping, and monitoring. *International Journal of Applied Earth Observation and Geoinformation*, *25*, 30–37. https://doi.org/10.1016/J.JAG.2013.03.005

[76] Gong, P., Wang, J., Yu, L., Zhao, Y., Zhao, Y., Liang, L., … Chen, J. (2013). Finer resolution observation and monitoring of global land cover: first mapping results with Landsat TM and ETM+ data. *International Journal of Remote Sensing*, *34*(7), 2607–2654. https://doi.org/10.1080/01431161.2012.748992

[77] Padarian, J., Minasny, B., & McBratney, A. B. (2015). Using Google's cloud-based platform for digital soil mapping. *Computers & Geosciences*, *83*, 80–88. https://doi.org/10.1016/j.cageo.2015.06.023

[78] Gorelick, N., Hancher, M., Dixon, M., Ilyushchenko, S., Thau, D., & Moore, R. (2017). Google Earth Engine: Planetary-scale geospatial analysis for everyone. *Remote Sensing of Environment*, *202*, 18–27. https://doi.org/10.1016/j.rse.2017.06.031

[79] Laos' economic growth outlook stable 2019, 2020: ADB http://www.xinhuanet.com/english/2019-04/04/c_137949373.htm Accessed date: 09 April 2020.

[80] Vientiane, Laos Population, https://populationstat.com/laos/vientiane Accessed date: 09 April 2020.

[81] Lambin, Eric F Geist, Helmut J Lepers, Erika D YNAMICS OF L AND -U SE AND L AND -C OVER C HANGE IN T ROPICAL R EGIONS, https://doi.org/10.1146/annurev.energy.28.050302.105459

[82] Sharifi, A., Chiba, Y., Okamoto, K., Yokoyama, S., & Murayama, A. (2014). Can master planning control and regulate urban growth in Vientiane, Laos? *Landscape and Urban Planning*, *131*, 1–13. https://doi.org/10.1016/j.landurbplan.2014.07.014 CrossRef from (Meyfroidt & Lambin, 2011, p.344)

APPENDIX

In this section, we have shown some samples of GEE coding that applied for land cover classification by combining with two primary machine learning classifiers, like Random Forest (RF) and classification and regression tree (CART), the GEE users are free of charge when performing correctly with its platforms.

1. Random Forest applied with Landsat 5 in 1989

```
var table: Table users/vjfrash77/L5SPII_1989
var roi: Table users/vjfrash77/Export_VTE_Area
var start_date = '1989-07-01';
var end_date = '1989-09-30';
//landsat 5
var l5Col = ee.ImageCollection('LANDSAT/LT5_L1T_TOA')
    .filterBounds(roi)
    .filterDate(start_date,end_date)
//remove Cloud in landsat
//--- Cloud Function ---
var cloud_thresh = 40;
var cloudFunction = function(image){
    //use add the cloud likelihood band to the image
    var CloudScore = ee.Algorithms.Landsat.simpleCloudScore(image);
    //isolate the cloud likelihood band
    var quality = CloudScore.select('cloud');
    //get pixels above the threshold
    var cloud01 = quality.gt(cloud_thresh);
    //create a mask from high likelihood pixels
    var cloudmask = image.mask().and(cloud01.not());
    //mask those pixels from the image
    return image.mask(cloudmask);
}
var l5_NoCloud = l5Col.map(cloudFunction);
//reduce to median value per pixel
var l5 = l5_NoCloud.median().clip(roi)
var bands = l5.bandNames()
// Make training data by 'overlaying' the points on the image.
var training = l5.sampleRegions({
  collection: table,
  properties: ['Type'],
  scale: 100
});
print(training)
// Get a Random Forest classifier and train it.
var classifier = ee.Classifier.randomForest(1).train({
  features: training,
  classProperty: 'Type',
  inputProperties: bands});
// Classify the image.
var classified = l5.select(bands).classify(classifier);
// Define a palette for the IGBP classification.
var igbp = [
  'f1e00c',
  'f4f10e',
  'f1440c',
  '0b6615',
  '08d2ea',
  '1b216c'];
Map.centerObject(roi, 10);
Map.addLayer(classified, {palette: igbp, min: 0, max: 17}, 'classification');
// accuracy assessement
var confMat = classifier.confusionMatrix();
print('Confusion matrix: ', confMat);
print('Overall accuracy: ', confMat.accuracy());
print('Producer Accuracy: ', confMat.producersAccuracy());
print('Consumer Accuracy: ', confMat.consumersAccuracy());
  Export.image.toDrive({
  image: classified,
  folder: 'GEE_EXPORTS',
  description: 'RF_L5_LC_SP-II_1989_JulToSept',
  scale: 30,
  region: roi
});
```

2. Random Forest applied with Landsat 8 in 2019

```
var table: Table users/vjfrash77/L8SPII-2_2019
var roi: Table users/vjfrash77/Export_VTE_Area
var start_date = '2019-01-01';
var end_date = '2019-12-31';
//landsat 8
var l8Col = ee.ImageCollection('LANDSAT/LC08/C01/T1_TOA')
    .filterBounds(roi)
    .filterDate(start_date,end_date)
//remove Cloud in landsat
//--- Cloud Function ---
var cloud_thresh = 40;
var cloudFunction = function(image){
    //use add the cloud likelihood band to the image
    var CloudScore = ee.Algorithms.Landsat.simpleCloudScore(image);
    //isolate the cloud likelihood band
    var quality = CloudScore.select('cloud');
    //get pixels above the threshold
    var cloud01 = quality.gt(cloud_thresh);
    //create a mask from high likelihood pixels
    var cloudmask = image.mask().and(cloud01.not());
    //mask those pixels from the image
    return image.mask(cloudmask);
}
var l8_NoCloud = l8Col.map(cloudFunction);
//reduce to median value per pixel
var l8 = l8_NoCloud.median().clip(roi)
var bands = l8.bandNames()
// Make training data by 'overlaying' the points on the image.
var training = l8.sampleRegions({
  collection: table,
  properties: ['Type'],
  scale: 100
});
print(training)
// Get a Random Forest classifier and train it.
var classifier = ee.Classifier.randomForest().train({
  features: training,
  classProperty: 'Type',
  inputProperties: bands});
// Classify the image.
var classified = l8.select(bands).classify(classifier);
// Define a palette for the IGBP classification.
var igbp = [
  'f1e00c',
  'f4f10e',
  'f1440c',
  '0b6615',
  '08d2ea',
  '1b216c'];
Map.centerObject(roi, 10);
Map.addLayer(classified, {palette: igbp, min: 0, max: 17}, 'classification');

// accuracy assessement
var confMat = classifier.confusionMatrix();
print('Confusion matrix: ', confMat);
print('Overall accuracy: ', confMat.accuracy());
print('Producer Accuracy: ', confMat.producersAccuracy());
print('Consumer Accuracy: ', confMat.consumersAccuracy());
  Export.image.toDrive({
  image: classified,
  folder: 'GEE_EXPORTS',
  description: 'RF_L8_LC_SP-II_2019',
  scale: 30,
  region: roi
});
```

3. Random Forest applied with Sentinel-2 in 2019

```
Imports (2 entries)
  var table: Table users/vjfrash77/S2SPII_2019
  var roi: Table users/vjfrash77/Export_VTE_Area
var start_date = '2019-01-01';
var end_date = '2019-12-31';
//sentinel 2
var senCol = ee.ImageCollection('COPERNICUS/S2')
    .filterBounds(roi)
    .filterDate(start_date,end_date);
//Remove Cloud for sentinel2
// Bits 10 and 11 are clouds and cirrus, respectively.
var cloudBitMask = ee.Number(2).pow(10).int();
var cirrusBitMask = ee.Number(2).pow(11).int();
var qa = senCol.select('QA60');
function maskS2clouds(image) {
  var qa = image.select('QA60');
  // Both flags should be set to zero, indicating clear conditions.
  var mask = qa.bitwiseAnd(cloudBitMask).eq(0).and(
                qa.bitwiseAnd(cirrusBitMask).eq(0));
  return image.updateMask(mask);
}
var sen_NoCloud = senCol.map(maskS2clouds);
//reduce to median value per pixel
var sen2= sen_NoCloud.median().clip(roi)
var bands = sen2.bandNames()
// Make training data by 'overlaying' the points on the image.
var training = sen2.sampleRegions({
  collection: table,
  properties: ['Type'],
  scale: 100
});
print(training)
// Get a Random Forest classifier and train it.
var classifier = ee.Classifier.randomForest().train({
  features: training,
  classProperty: 'Type',
  inputProperties: bands});
// Classify the image.
var classified = sen2.select(bands).classify(classifier);
// Define a palette for the IGBP classification.
var igbp = [
  'f1e00c',
  'f4f10e',
  'f1440c',
  '0b6615',
  '08d2ea',
  '1b216c'];
Map.centerObject(roi, 10);
Map.addLayer(classified, {palette: igbp, min: 0, max: 17}, 'classification');
// accuracy assessement
var confMat = classifier.confusionMatrix();
print('Confusion matrix: ', confMat);
print('Overall accuracy: ', confMat.accuracy());
print('Producer Accuracy: ', confMat.producersAccuracy());
print('Consumer Accuracy: ', confMat.consumersAccuracy());
  Export.image.toDrive({
  image: classified,
  folder: 'GEE_EXPORTS',
  description: 'RF_S2_LC_SP-II_2019',
  scale: 10,
  region: roi
});
```

4. CART applied with Landsat 5 in 1989

```
Imports (2 entries)
  var table: Table users/vjfrash77/L5SPII_1989-CART
  var roi: Table users/vjfrash77/Export_VTE_Area
var start_date = '1989-01-01';
var end_date = '1989-12-31';
//landsat 5
var l5Col = ee.ImageCollection('LANDSAT/LT5_L1T_TOA')
    .filterBounds(roi)
    .filterDate(start_date,end_date)
//remove Cloud in landsat //--- Cloud Function ---
var cloud_thresh = 40;
var cloudFunction = function(image){
    //use add the cloud likelihood band to the image
    var CloudScore = ee.Algorithms.Landsat.simpleCloudScore(image);
    //isolate the cloud likelihood band
    var quality = CloudScore.select('cloud');
    //get pixels above the threshold
    var cloud01 = quality.gt(cloud_thresh);
    //create a mask from high likelihood pixels
    var cloudmask = image.mask().and(cloud01.not());
    //mask those pixels from the image
    return image.mask(cloudmask);}
var l5_NoCloud = l5Col.map(cloudFunction);
//reduce to median value per pixel
var l5 = l5_NoCloud.median().clip(roi)
var bands = l5.bandNames()
// Make training data by 'overlaying' the points on the image.
var training = l5.sampleRegions({
  collection: table,
  properties: ['Type'],
  scale: 100});
print(training)
// Get a Random Forest classifier and train it.
var classifier = ee.Classifier.cart().train({
  features: training,
  classProperty: 'Type',
  inputProperties: bands});
// Classify the image.
var classified = l5.select(bands).classify(classifier);
// Define a palette for the IGBP classification.
var igbp = [
  'f1e00c',   'f4f10e',   'f1440c',   '0b6615',   '08d2ea', '1b216c'];
Map.centerObject(roi, 10);
Map.addLayer(classified, {palette: igbp, min: 0, max: 17}, 'classification');
// accuracy assessement
var confMat = classifier.confusionMatrix();
print('Confusion matrix: ', confMat);
print('Overall accuracy: ', confMat.accuracy());
print('Producer Accuracy: ', confMat.producersAccuracy());
print('Consumer Accuracy: ', confMat.consumersAccuracy());
  Export.image.toDrive({
  image: classified,
  folder: 'GEE_EXPORTS',
  description: 'CART_L5_LC_SP-II_1989',
  scale: 30,
  region: roi });
```

5. CART applied with Landsat 8 in 2019

```
Imports (2 entries)
  var table: Table users/vjfrash77/L8SPII-2_2019
  var roi: Table users/vjfrash77/Export_VTE_Area
var start_date = '2019-01-01';
var end_date = '2019-12-31';
//landsat 8
var l8Col = ee.ImageCollection('LANDSAT/LC08/C01/T1_TOA')
    .filterBounds(roi)
    .filterDate(start_date,end_date)
//remove Cloud in landsat //--- Cloud Function ---
var cloud_thresh = 40;
var cloudFunction = function(image){
    //use add the cloud likelihood band to the image
    var CloudScore = ee.Algorithms.Landsat.simpleCloudScore(image);
    //isolate the cloud likelihood band
    var quality = CloudScore.select('cloud');
    //get pixels above the threshold
    var cloud01 = quality.gt(cloud_thresh);
    //create a mask from high likelihood pixels
    var cloudmask = image.mask().and(cloud01.not());
    //mask those pixels from the image
    return image.mask(cloudmask);}
var l8_NoCloud = l8Col.map(cloudFunction);
//reduce to median value per pixel
var l8 = l8_NoCloud.median().clip(roi)
var bands = l8.bandNames()
// Make training data by 'overlaying' the points on the image.
var training = l8.sampleRegions({
  collection: table,
  properties: ['Type'],
  scale: 100});
print(training)
// Get a Random Forest classifier and train it.
var classifier = ee.Classifier.cart().train({
  features: training,
  classProperty: 'Type',
  inputProperties: bands});
// Classify the image.
var classified = l8.select(bands).classify(classifier);
// Define a palette for the IGBP classification.
var igbp = [  'f1e00c',   'f4f10e',   'f1440c',   '0b6615',   '08d2ea',  '1b216c'];
Map.centerObject(roi, 10);
Map.addLayer(classified, {palette: igbp, min: 0, max: 17}, 'classification');
// accuracy assessement
var confMat = classifier.confusionMatrix();
print('Confusion matrix: ', confMat);
print('Overall accuracy: ', confMat.accuracy());
print('Producer Accuracy: ', confMat.producersAccuracy());
print('Consumer Accuracy: ', confMat.consumersAccuracy());
  Export.image.toDrive({
  image: classified,
  folder: 'GEE_EXPORTS',
  description: 'CART_L8_LC_SP-II_2019',
  scale: 30,
  region: roi });
```

6. CART applied with Sentinel-2 in 2019

```
Imports (2 entries)
  var table: Table users/vjfrash77/S2SPII-2_2019
  var roi: Table users/vjfrash77/Export_VTE_Area
var start_date = '2019-01-01';
var end_date = '2019-12-31';
//sentinel 2
var senCol = ee.ImageCollection('COPERNICUS/S2')
    .filterBounds(roi)
    .filterDate(start_date,end_date);
//Remove Cloud for sentinel2
// Bits 10 and 11 are clouds and cirrus, respectively.
var cloudBitMask = ee.Number(2).pow(10).int();
var cirrusBitMask = ee.Number(2).pow(11).int();
var qa = senCol.select('QA60');
function maskS2clouds(image) {
  var qa = image.select('QA60');
  // Both flags should be set to zero, indicating clear conditions.
  var mask = qa.bitwiseAnd(cloudBitMask).eq(0).and(
                qa.bitwiseAnd(cirrusBitMask).eq(0));
  return image.updateMask(mask);}
var sen_NoCloud = senCol.map(maskS2clouds);
//reduce to median value per pixel
var sen2= sen_NoCloud.median().clip(roi)
var bands = sen2.bandNames()
// Make training data by 'overlaying' the points on the image.
var training = sen2.sampleRegions({
  collection: table,
  properties: ['Type'],
  scale: 100
});
print(training)
// Get a Random Forest classifier and train it.
var classifier = ee.Classifier.cart().train({
  features: training,
  classProperty: 'Type',
  inputProperties: bands});
// Classify the image.
var classified = sen2.select(bands).classify(classifier);
// Define a palette for the IGBP classification.
var igbp = [
  'f1e00c',
  'f4f10e',
  'f1440c',
  '0b6615',
  '08d2ea',
  '1b216c'];
Map.centerObject(roi, 10);
Map.addLayer(classified, {palette: igbp, min: 0, max: 17}, 'classification');

// accuracy assessement
var confMat = classifier.confusionMatrix();
print('Confusion matrix: ', confMat);
print('Overall accuracy: ', confMat.accuracy());
print('Producer Accuracy: ', confMat.producersAccuracy());
print('Consumer Accuracy: ', confMat.consumersAccuracy());
  Export.image.toDrive({
  image: classified,
  folder: 'GEE_EXPORTS',
  description: 'CART_S2_LC_SP-II_2019',
  scale: 30,
  region: roi
});
```

Figure A1. JavaScript code used in GEE APIs to explore the handing classified raster and sample training with GEE.

7. NDVI applied with Landsat 8 in 2019

Note: add a variable entry as geometry (study area in shapefile), this NDVI provided in ANNUAL, 32DAY, and 8DAY.

```
Imports (1 entry)
  var geometry: Table users/vjfrash77/Export_VTE_Area
var dataset = ee.ImageCollection('LANDSAT/LC08/C01/T1_ANNUAL_NDVI')
                    .filterDate('2019-01-01', '2019-12-31');
var colorized = dataset.select('NDVI');
var colorizedVis = {
  min: 0.0,
  max: 1.0,
  palette: [
    'FFFFFF', 'CE7E45', 'DF923D', 'F1B555', 'FCD163', '99B718', '74A901',
    '66A000', '529400', '3E8601', '207401', '056201', '004C00', '023B01',
    '012E01', '011D01', '011301'
  ],
};
var colorized = dataset.median().clip(geometry); // here we are taking the median at each pixel in the collection
Map.addLayer(colorized)
Map.centerObject(geometry)
//// If you want to export any, edit this:
Export.image.toDrive({
  image: colorized, /// To choose which imagery to export change the number (e.g. L5, L7 or L8)
  description: 'VTE_ANNUAL_L8_NDVI_2019',  //give correct name
  scale: 30,
  maxPixels: 1e13,
  region: geometry
});
```

```
var dataset = ee.ImageCollection('LANDSAT/LC08/C01/T1_32DAY_NDVI')
                    .filterDate('2019-01-01', '2019-12-31');
var colorized = dataset.select('NDVI');
var colorizedVis = {
  min: 0.0,
  max: 1.0,
  palette: [
    'FFFFFF', 'CE7E45', 'DF923D', 'F1B555', 'FCD163', '99B718', '74A901',
    '66A000', '529400', '3E8601', '207401', '056201', '004C00', '023B01',
    '012E01', '011D01', '011301'
  ],
};
var colorized = dataset.median().clip(geometry); // here we are taking the median at each pixel in the collection
Map.addLayer(colorized)

Map.centerObject(geometry)

//// If you want to export any, edit this:
Export.image.toDrive({
  image: colorized, /// To choose which imagery to export change the number (e.g. L5, L7 or L8)
  description: 'VTE_32DAY_L8_NDVI_2019',  //give correct name
  scale: 30,
  maxPixels: 1e13,
  region: geometry
});
/////////////////////////////////////////////////////////////////////////
```

```
var dataset = ee.ImageCollection('LANDSAT/LC08/C01/T1_8DAY_NDVI')
                    .filterDate('2019-01-01', '2019-12-31');
var colorized = dataset.select('NDVI');
var colorizedVis = {
  min: 0.0,
  max: 1.0,
  palette: [
    'FFFFFF', 'CE7E45', 'DF923D', 'F1B555', 'FCD163', '99B718', '74A901',
    '66A000', '529400', '3E8601', '207401', '056201', '004C00', '023B01',
    '012E01', '011D01', '011301'
  ],
};
var colorized = dataset.median().clip(geometry); // here we are taking the median at each pixel in the collection
Map.addLayer(colorized)
Map.centerObject(geometry)
//// If you want to export any, edit this:
Export.image.toDrive({
  image: colorized, /// To choose which imagery to export change the number (e.g. L5, L7 or L8)
  description: 'VTE_8DAY_L8_NDVI_2019',  //give correct name
  scale: 30,
  maxPixels: 1e13,
  region: geometry
});
```

8. NDBI applied with Landsat 8 in 2019

Note: add a variable entry as geometry (study area in shapefile), this NDBI provided for Landsat 5, 7, and 8.

Figure A2. JavaScript code used in GEE APIs to explore the handing classified raster with NDVI and DNBI in GEE.

```
Imports (1 entry)
  var roi: Table users/vjfrash77/Export_VTE_Area
var start_date = '2015-01-01';
var end_date = '2015-12-31';
//landsat 5
var l5Col = ee.ImageCollection('LANDSAT/LT5_L1T_TOA')
    .filterBounds(roi)
    .filterDate(start_date,end_date)
//landsat 7
var l7Col = ee.ImageCollection('LANDSAT/LE7_L1T_TOA')
    .filterBounds(roi)
    .filterDate(start_date,end_date)
//landsat 8
var l8Col = ee.ImageCollection('LANDSAT/LC8_L1T_TOA')
    .filterBounds(roi)
    .filterDate(start_date,end_date)
//remove Cloud in landsat
//--- Cloud Function ---
var cloud_thresh = 40;
var cloudFunction = function(image){
    //use add the cloud likelihood band to the image
    var CloudScore = ee.Algorithms.Landsat.simpleCloudScore(image);
    //isolate the cloud likelihood band
    var quality = CloudScore.select('cloud');
    //get pixels above the threshold
    var cloud01 = quality.gt(cloud_thresh);
    //create a mask from high likelihood pixels
    var cloudmask = image.mask().and(cloud01.not());
    //mask those pixels from the image
    return image.mask(cloudmask);
}
//var l5_NoCloud = l5Col.map(cloudFunction);
var l7_NoCloud = l7Col.map(cloudFunction);
//var l8_NoCloud = l8Col.map(cloudFunction);
//reduce to median value per pixel
//var l5 = l5_NoCloud.mosaic().clip(roi);
var l7 = l7_NoCloud.mosaic().clip(roi);
//var l8 = l8_NoCloud.mosaic().clip(roi);
//NDBI Calculation (SWIR and NIR)
//var ndbi_l5 = l5.normalizedDifference(['B5','B4']);
var ndbi_l7 = l7.normalizedDifference(['B5','B4']);
//var ndbi_l8 = l8.normalizedDifference(['B6','B5']);
Map.centerObject(roi, 10);
Map.addLayer(ndbi_l7, {palette: ["000055","0000FF","FF9999","00FF00"]}, 'NDBI');
//If you want to export landsat 5 and 8, change image: ndbi_l7 to l5 n l8
Export.image.toDrive({image:ndbi_l7,
                      description:"NDBI",
                      region:roi,
                      scale:30,
                      maxPixels:1e13});
```

BIOGRAPHY

NAME	Vorlajuck KHANTIVONG
DATE OF BIRTH	02 Feb 1984
PLACE OF BIRTH	Champasak Province, Lao PDR
PRESENT ADDRESS	007 Unit 01, Rd: 20A Salavan เขต/อำเภอ Salavan Foreign 01 โทร: 008562091164448, 02077717701
POSITION HELD	Assistant Manager at MLC Project, Ministry of Post and Tellecommunication, Lao PDR
EDUCATION	MSc in Geoinformatics M.Eng in Photogrammetry and Remote Sensing

BURAPHA UNIVERSITY